Master Thesis, Department of Geosciences

Landslide Hazard Mapping in Norddal, Møre og Romsdal

A case study and review of landslide hazard mapping according to current requirements of the Norwegian Water Resources and Energy Directorate (NVE)

Nils Arne Kavli Walberg

UNIVERSITY OF OSLO

FACULTY OF MATHEMATICS AND NATURAL SCIENCES

Landslide Hazard Mapping in Norddal, Møre og Romsdal

A case study and review of landslide hazard mapping according to current requirements of the Norwegian Water Resources and Energy Directorate (NVE)

Nils Arne Kavli Walberg

Master Thesis in Geosciences

Discipline: Environmental Geology and Geohazards

Department of Geosciences

Faculty of Mathematics and Natural Sciences

University of Oslo

[30 ECTS]

June 1st 2013

Supervisors: Andrea Taurisano (NVE) and Valerie Mauphin (UiO)

This work is published digitally through DUO – Digitale Utgivelser ved UiO

http://www.duo.uio.no

It is also catalogued in BIBSYS (http://www.bibsys.no/english)

Front page photo: Outer part of the Norddal village, taken from SE (photo: M. Lund)

Abstract

Landslide hazard mapping in Norway today is usually performed by external consulting companies on behalf of the Norwegian Water Resources and Energy Directorate (NVE), resulting in varying level of mapped details and interpretation of guidelines. The focus of this study has been existing methodology within landslide hazard mapping, and the aim of the project is to evaluate its appropriateness within current landslide hazard mapping. To do this, a complete landslide hazard mapping assessment is conducted for *Norddal* in *Møre og Romsdal*, and the methodology used are thoroughly explained and discussed. *Norddal* was chosen as it was assigned 1st priority regarding rock fall and snow avalanche hazard, and 2nd priority regarding debris slide and debris flow hazard in an initial national mapping of landslide prone areas conducted by NVE.

The methodology includes determination of a landslide inventory map, meteorological investigations related to landslide and snow avalanche initiation, topographical studies and run out modeling, where the later is emphasized. Six different models were performed to determine run out; the α,β-model for both snow avalanches and rock falls, RocFall and Rockyfor3D for rock falls, and AVAL-1D and RAMMS for snow avalanches. They range from simple empirical models based on the height of a cliff, to more complex numerical simulations that require extensive input.

All methods used were found suitable and provided important information to the mapping project, where the main challenge was considered the adaption of the obtained information to the recurrence intervals stated in the regulations. Four hazard maps were produced from the available information, calculations and field work for each of the mass movement types: rock falls, snow avalanches and debris slides, and one for the total hazard which should be used in land use planning. The rating of the different methods used in the preparation of the extent of the hazard zones are thoroughly explained, together with advantages and disadvantages of the different methods. The kind of methods which could be applied under different conditions and how their results can be interpreted regarding different hazard zones is considered the main focus of this project. This information may be applied to future guidelines for landslide hazard mapping in Norway.

Sammendrag

Skredfarekartlegging i Norge blir i dag i stor grad utført av eksterne selskaper på oppdrag fra Norges vassdrags- og energidirektorat (NVE), noe som fører til varierende tolkning av retningslinjer og detaljnivå. Målet med denne oppgaven er å evaluere de mest vanlige metodene innen skredfarekartlegging i Norge i dag, og å diskutere fordeler, ulemper og utfordringer knyttet til disse metodene. Dette er gjort gjennom en detaljert farekartlegging i *Norddal*, *Møre og Romsdal*, hvor områder utsatt for snøskred, steinsprang, jord- og flomskred er kartlagt. *Norddal* er valgt som studielokalitet på grunn av at området ble rangert som 1.prioritet for kartlegging av snøskred- og steinsprangfare, samt 2. prioritet i forhold til jordskred og flomskredfare i innledende skredfarekartleggingsundersøkelser utført av NVE.

Metodene som er brukt inkluderer utarbeidelsen av et hendelseskart basert på tidligere skred i området, undersøkelser av lokale meteorologiske forhold som kan påvirke utløsning av skred, topografiske studier og modellering av utløpslengder for ulike skredtyper. Spesielt sistnevnte er vektlagt stor betydning og seks ulike modeller er benyttet til simuleringer av utløpsdistanse; α,β-modellen for snøskred og steinsprang, RocFall og Rockyfor3D for steinsprang, samt AVAL-1D og RAMMS for snøskred. Modellene strekker seg fra enkle, empiriske modeller som tar utgangspunkt i høyden til fjellsiden, til mer kompliserte dynamiske modeller som krever mer og detaljert bakgrunnsinformasjon.

Alle metodene har vist seg nyttige og tilført viktig informasjon i kartleggingsarbeidet, hvor hovedutfordringen har vært å koble sammen resultater fra metodene til gjentaksintervallet som faresonene bygger på. Fire ulike skredfarekart er utarbeidet, ett for hver av de tre ulike skredtypene og ett for den totale faren, hvor sistnevnte skal brukes innen arealplanlegging. Grunnlaget for utstrekningen til de ulike faresonene er grundig forklart, det samme gjelder utfordringer knyttet til de ulike metodene. Hvilke metoder som kan anvendes og hvordan resultatene fra disse kan settes i sammenheng med de ulike faresonene vurderes som det viktigste resultatet i denne oppgaven, noe som kan brukes i et kommende arbeid angående retningslinjer innen skredfarekartlegging i Norge.

Acknowledgments

This work is made possible by the collaboration of the University of Oslo (UiO) and the Norwegian Water Resources and Energy Directorate (NVE). Several people deserve to be thanked.

First, I would like to express my gratitude to my supervisor, Andrea Taurisano (NVE). Thank you for introducing me to the field of landslide hazard mapping, for all rewarding meetings at NVE and your encouraging advices in an otherwise busy schedule. I would also thank my co-supervisor, Valerie Mauphin (UiO) for useful contribution to the final outline of the thesis.

I would also like to thank all the people within the Norwegian scientific environment which have helped me out with the different issues I have questioned – thank you! An extra thanks goes to Luzia Fischer at the Geological Survey of Norway (NGU) for valuable insight in and discussions about their ongoing project about debris flow susceptibility mapping.

Judith Wells-Walberg, I am incredible grateful for you proofreading my thesis! I am very glad you did not back down when my thesis inexplicably doubled in size from the aforementioned 60 pages. You have really learned me a lot about grammar!

Thanks to my family which always has been there for me and my fellow students for interesting discussions and nice friendship the last five years! I hope we will stay in touch after the graduation as well!

The biggest thank goes to my girlfriend Monika. Despite writing your own thesis, you have always answered my questions and provided me new approaches during discussions. I am very grateful for knowing you!

Nils Arne

Blindern, 01.06.2012

Table of contents

1 Introduction

1.1 Background

Norway's topography and climate make the country very prone to natural hazards such as landslides and snow avalanches. During historical time, evidence was found of 3500 events that occurred throughout Norway causing several thousand deaths (Furseth, 2006). Lately, there has been considerable attention focused on accidents related to snow avalanches caused by skiers skiing off-piste in steep mountain terrain where the skiers often cause the release of the avalanches themselves and then become caught by the moving snow mass. One such tragedy occurred in March 2012 where 5 skiers from abroad were on ski vacation in Norway and were caught and killed by a massive snow avalanche during off-piste skiing in Lyngen, Troms (Brattlien, 2012). From the year 1900, it is believed that approximately 1100 people have been killed in more than 500 registered landslide related accidents (Figure 1-1). Of these, there are close to 500 registered accidents involving settlements, 200 when performing outdoor activities, approximately 70 along roads and roughly 250 during other outdoor situations including military services (St. Meld., 2012).

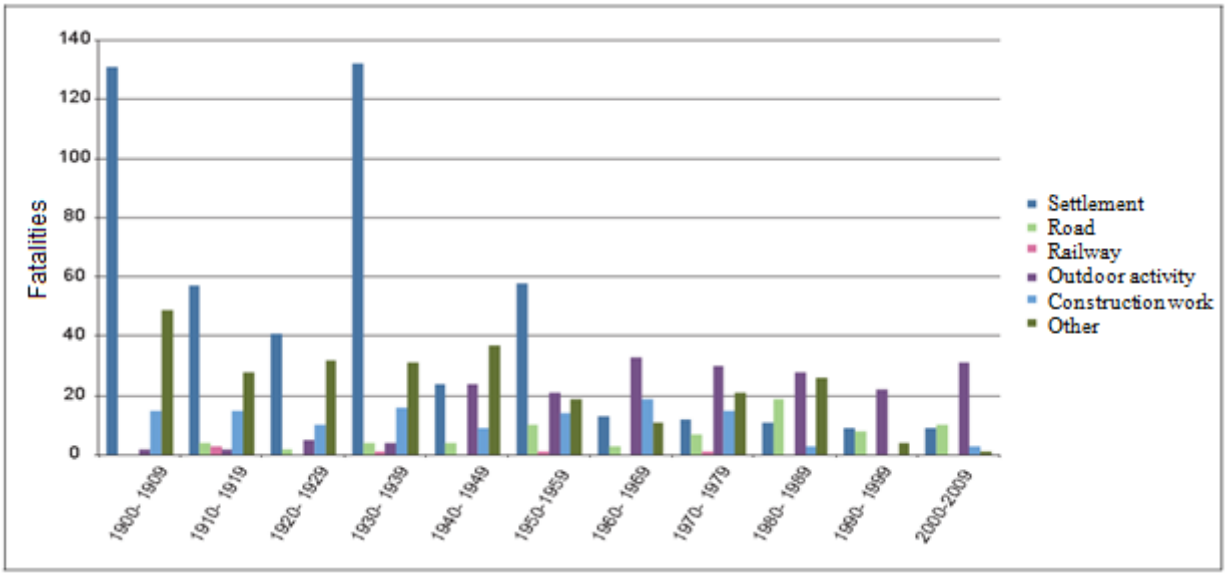

Figure 1-1: Registered fatalities the last century due to landslides in Norway, distributed by activities (St. Meld., 2012) Data from www.skrednett.no

Governmental landslide hazard mapping in Norway has been done sporadically since the *Tafjord* accident in 1934, where 40 people were killed by a tsunami after a rock avalanche

plummeted into the fjord (Furseth, 2006; NVE, 2011e). After the large quick clay slide of *Rissa* in 1978, the Norwegian Geotechnical Institute (NGI) and Geological Survey of Norway (NGU) conducted an extensive mapping of potentially prone areas for quick clay slides that identified a series of quick clay zones, specifically in eastern Norway and *Trøndelag*. Mapping related to hazards from snow avalanches, rock falls and rock avalanches has been performed by NGI for some decades mainly focusing on the western, north-western and northern parts of Norway. Some mapping of large unstable mountain sides within roughly the same areas has been performed by NGU since 1990 (NVE, 2011e). Over the years, the contractor from the State has varied from Statens Naturskadefond (before 1995), Norwegian Mapping Authority (1996-2003), NGU (2004-2008), and eventually to the Norwegian Water Resources and Energy directorate (NVE) since January 1st 2009 (NVE, 2011e). NVE's tasks and responsibilities are outlined in the St. Meld. (2008) where it is said that NVE was assigned the overall governmental management responsibility for the prevention of landslides including regional landslide hazard mapping. It was determined in St.prp. (2009) that a comprehensive model for NVE's responsibilities within landslide management should include landslide hazard mapping; provision of professional assistance and guidelines related to development and land use planning in landslide prone areas; planning and implementing measures for monitoring and warning, and the provision of technical- and expert assistance in emergency response planning during emergency situations.

Because of their designation as national landslide authority, NVE started a national project of landslide mapping. As a part of the project, they developed a plan for governmental landslide hazard mapping. The plan, see NVE (2011e), is intended as a framework for the landslide hazard mapping in the coming years and includes a priority list of areas to be investigated first. The priorities can be changed as new information and knowledge are obtained, while the mapping progress is determined by the allocation of grant monies in the yearly national budget. Separate plans are developed for the different landslide processes present in Norway: earth- and debris flows (NVE, 2011a), quick clay slides (NVE, 2011b), snow avalanches and slush avalanches (NVE, 2011c) and rock fall, rock avalanches and rockslides (NVE, 2011d). Based on the current priority list, the first two communities, Odda and Årdal, received their new landslide hazard maps in spring 2013. The work was conducted by NGI on behalf of NVE, and can be found in NVE (2013a) and NVE (2013b).

For all these process types, a hazard mapping methodology is to be developed to make it easier for other firms to conduct hazard mapping, and thereby, increasing the rate and quality of landslide hazard mapping in Norway. Such work is essential for land use planning and construction approvals in the municipalities. The project that follows is intended to contribute to this work.

1.2 Purpose of study

By using the village of *Norddal*, *Møre og Romsdal*, this project will provide an example of landslide hazard mapping according to Norwegian regulations. A variety of possible methods will be applied to determine the present hazards from landslides and snow avalanches in the area. The project will compare different models that can help specialists to assess run out of events and discuss challenges they meet while carrying out this type of assessment. The goal is to perform a complete landslide hazard analysis for the valley and to make an assessment of the methods used to evaluate their usability within landslide hazard mapping in Norway.

The thesis will focus on the hazards related to rock falls, snow avalanches, debris slides and debris flows as these processes are present in *Norddal*. Hazards and methods related to quick clay slides will, therefore, not be included as they are not present in the valley. The hazard map will also not take into account the hazards related to large rock slides, since their appearance and frequency are very hard to predict. This exclusion also includes the threat from rock slide induced tsunamis in the nearby fjords.

To assure no misunderstandings related to the different use of terms, a terminology will be established in accordance with the definitions of Varnes (1978). An English – Norwegian glossary from NVE and a map of the most used place names and their localization in *Norddal* are enclosed. These names can differ from local use as they are based on maps from The Norwegian Mapping Authority, which provide all background maps used in this project.

2 Terminology and process types

2.1 Terminology

To prevent misunderstandings due to various meanings of terms in Norwegian and English, this section will define the main differences between various terms and identify the terminology on which this project will focus. There are two major misunderstandings that may occur related to 1) the English term "landslide" versus the Norwegian term "skred" and 2) the differences between "debris" and the associated translation "løsmasser". The Norwegian term "skred" includes all types of mass movement such as rock falls, slides and snow avalanches; while in English and international literature, the term "landslide" corresponds to mass movement related to geological material such as bedrock and soil and, therefore, does not include snow avalanches. The same applies to the next example, while the Norwegian term "løsmasser" includes clay, silt, mud, sand, gravel, loose rocks, soil, peat etc., the English term "debris" is much more specific. In the classification of Varnes (1978), debris is denoted as "an engineering soil, generally surficial, that contains a significant amount of coarse material; 20 to 80 percent of the fragments are greater than 20 mm in size and the remainder of the fragments less than 2 mm".

Several classification schemes exist among academics and around the globe due to the great variability of these processes and the aim of this investigation for which it is adapted**.** Varnes (1958, 1978) proposed a classification of slope movements which continues to be accepted and widely used among specialists. From this classification, the landslide type can be distinguished by two main variables that include the type of movement and the type of material involved. The movement of a mass can be separated into five different principal types: falls, slides, topples, spreads and flows. The material involved includes rock and engineering soil where the latter is divided into earth and debris. This definition implies that the classification does not include snow avalanches (Varnes, 1978). Snow avalanches show less variability than slope movements related to geological material, and while a variety of different types exist, the focus tends to be on slab, loose snow and slush avalanches, or dry snow, wet snow and slush avalanches if one chooses to name them based on their water content.

TYPE OF MOVEMENT		TYPE OF MATERIAL		
		BEDROCK	ENGINEERING SOILS	
			Predominantly coarse	Predominantly fine
FALLS		Rock fall	Debris fall	Earth fall
TOPPLES		Rock topple	Debris topple	Earth topple
SLIDES	ROTATIONAL	Rock slide	Debris slide	Earth slide
	TRANSLATIONAL			
LATERAL SPREADS		Rock spread	Debris spread	Earth spread
FLOWS		Rock flow (deep creep)	Debris flow (soil creep)	Earth flow
COMPLEX		Combination of two or more principal types of movement		

Figure 2-1: Abbreviated landslide classification based on Varnes (1978). From USGS (2012).

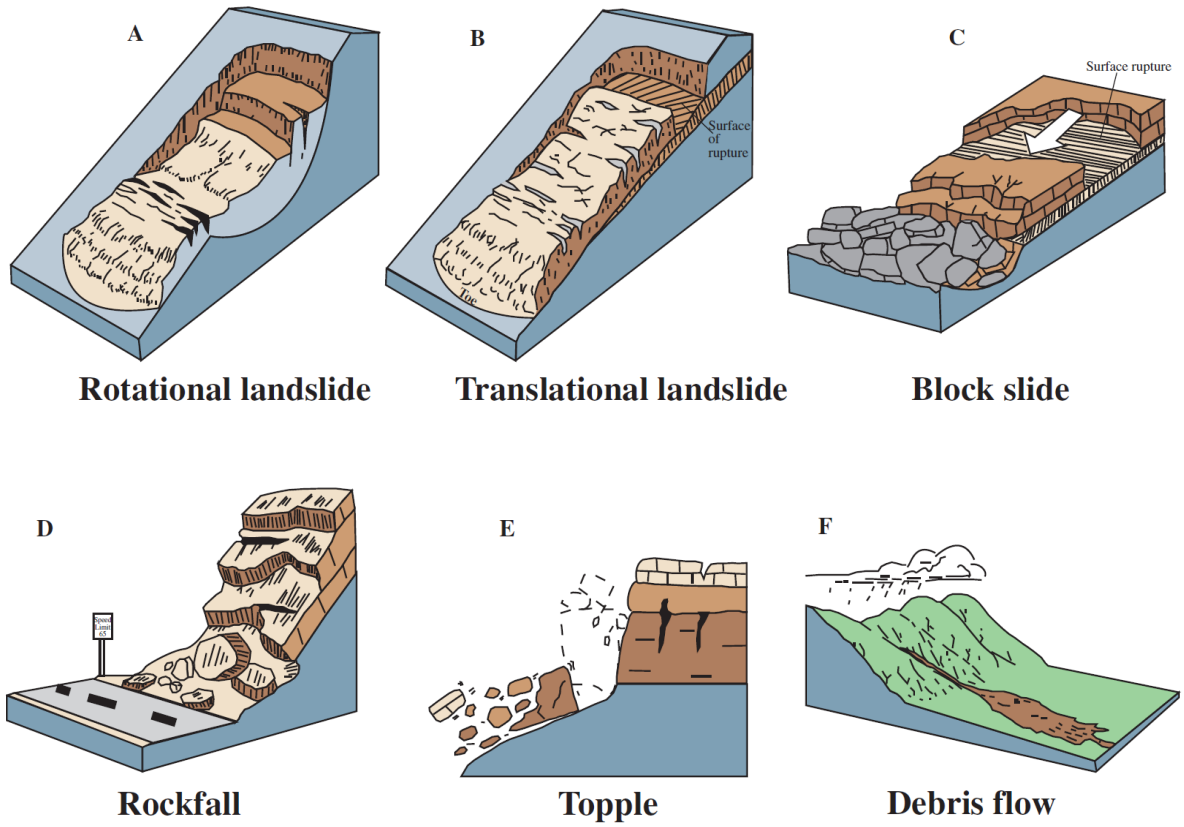

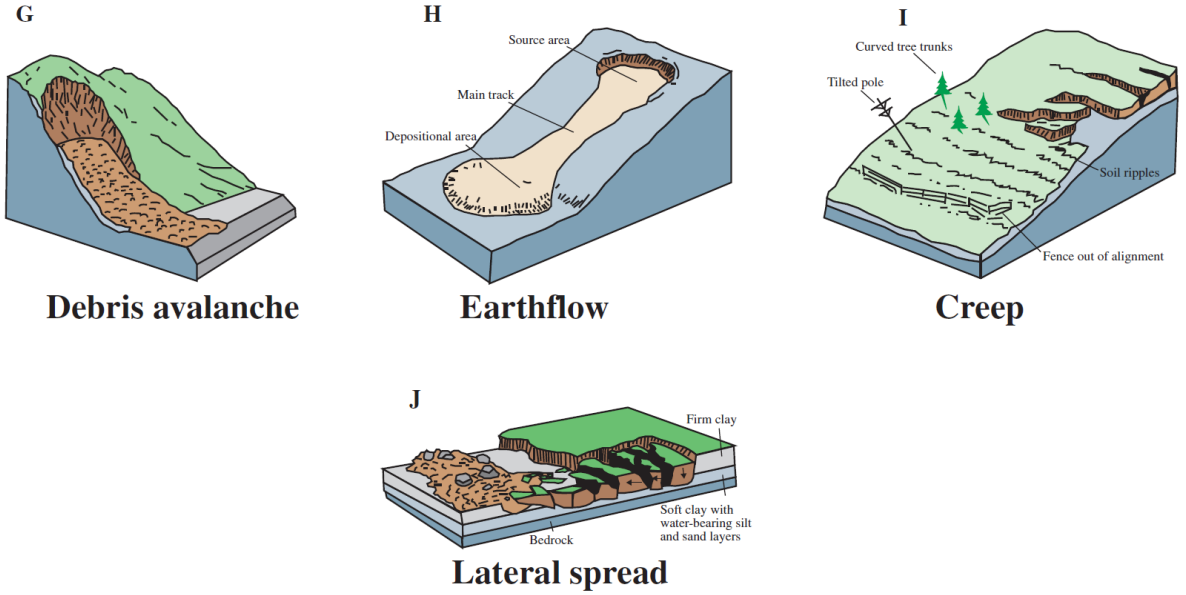

Figure 2-2: Schematic illustrations of the main landslide types (USGS, 2012).

2.2 Process types

Landslides and snow avalanches are naturally occurring processes driven by gravity that cause materials such as rock, snow and soil to move downward. These processes act as an important part of a continuous process of erosion (Ramberg et al., 2007). The type of movement depends on the material and topography, but typically, a falling, bouncing, gliding or flowing movement occurs. One landslide may often contain several types of movements (NVE, 2011e). In the following sections, all of the main types of events related to bedrock, loose soil (debris) and snow will be explained as well as their most frequent release mechanisms and causes. The focus will be on the types of movements that may cause a severe and unpredictable threat to people and infrastructure; hence, the rapid mass movements, while slow movements referred to as creep will be excluded.

2.2.1 Rock falls and rock avalanches

Landslides in bedrock can theoretically occur in all places where a steep mountain side or cliff exists. The type and property of bedrock very much decides the amount of landslide activity. Rocks will move downward when gravity exceeds friction (Lied, 1992). The most common type is rock fall where single blocks fall, bounce and roll down the mountain side due to

gravity. The volume is normally small; however, the rock fall can cause considerable damage if people or infrastructure are involved (NVE, 2011d). To predict rock falls is very problematic as there are no distinct release mechanisms or deformation that occurs in advance (NVE, 2011d). However, freeze-thaw mechanisms (Bjerrum and Jørstad, 1968) and water pressure in joint systems (Sandersen et al., 1997) are known to participate as well as chemical decomposition, root pressure, temperature variations and the influence of snow cover (Bjerrum and Jørstad, 1968). The activity depends on the type of rock with highly weathered and fractured rocks in steep slopes being clear indicators of rock fall hazard, while strong, non-fractured rock as granite may stay stable without apparent activity in steep slopes (NVE, 2011d). This suggests that slopes of weak bedrock may exhibit large frequency rock falls with small consequences, while usually stable rock such as granite infrequently may cause larger rock falls with possible higher consequences. This suggestion is confirmed by Bjerrum and Jørstad (1968) who reported that most of the unstable slopes along glaciated valleys in Norway likely failed a short time after the last glaciations, and thus, today can be found as stable slopes, possibly covered by scree. The resistant rocks which then showed stability in steep slopes have been exposed by weathering and changing conditions for several thousands of years and can today cause rock falls.

It is typical to distinguish between small events of volume less than 100 m^3 which are called rock falls and events with larger volume which are denoted as rock avalanches (Lied, 1992). The process is the same with rocks falling independent from each other. When an entire mountain side is unstable and it appears as though it will detach from the base, it is defined as a rock slide. These are rare events, but may cause severe damage especially when they occur along a fjord, coast or lake as a tsunami may result (Bjerrum and Jørstad, 1968; Furseth, 2006). Such catastrophic events happened in *Loen* (1905 and 1936) and *Tafjord* (1934) where respectively 61, 73 and 40 people died. During the *Tafjord* rock slide, it was estimated that 2-3 million m^3 of rock plunged into the fjord causing runup heights up to 63.5 m (Furseth, 2009). Rock slides, before their catastrophic release, are characterized by a more or less constant rate of movement normally from millimeters to centimeters per year. Several such slides are under continuous monitoring in Norway, such as the *Åknes* rock slide in *Møre og Romsdal*. Monitoring is meant to provide information needed for early warning and evacuation which is regarded as the only protective measure regarding the size of these events (Åknes/Tafjord Beredskap IKS).

2.2.2 Flows and slides in soil

As mentioned in Chapter 2.1 regarding terminology, there are a great variety of landslide types which can occur in loose soils depending on the soil properties and type of movement involved. The most common types of mass movement are slides and flows which differ in the type of releasing conditions and mechanisms, including the type of movement and deposition, see Table 2-1 (NVE, 2011a). The kind of soil involved is often included in the name of the slide such as mud slide, earth slide and debris slide. Debris slide will be used as an example in the review of properties for loose soil slides, since debris is a very common type of soil in Norway with the presence of moraine and scree deposits. Slides in loose soil, often called shallow landslides, are movements of soil in planar mountain sides. Typically, large slides often start at a point and spread downward making a triangle in the mountain side. Glacier excavated valleys covered by moraine are especially vulnerable to debris slides as the till often is deposited within the limit of their stability range. In such a case, only a releasing factor is needed for the debris slide to occur, which often is water related. Heavy precipitation, snowmelt or artificial constrains including erosion due to blocked culverts is often enough for release. Small shallow landslides are also common in small slopes and fillings, especially during thawing in spring when frost in the ground acts as a gliding layer (NVE, 2011a).

Old debris slide scars often become concentration zones for water along a slope, and such gullies eroded by water or debris slides often become the location for another type of landslide called debris flows. A debris flow can be defined as a very rapid to an extremely rapid flow of saturated non-plastic debris in a steep channel (Jakob and Hungr, 2005). In this context, debris refers to loose, unsorted material of low plasticity which can originate from deposition of other mass movement processes, weathering and glacial erosion, volcanism or deposits from human activity (Hungr et al., 2001). Debris flows differ from the debris slide by their occurrence in previous existing gullies and ravines, something which also affects their release mechanisms. Debris flows often occur in river gullies during high discharge due to erosion along the flanks. Another type of release mechanism results when small shallow landslides from the sides cause a temporary damming of a stream, resulting in a wave of water and debris rapidly flowing downward, possibly exceeding existing levees and the normal path of the stream (NVE, 2011a). For more details about the distinction between debris slides and flows, see *Table 2-1*

Figure 2-3: Debris flows near Kvam in Gudbrandsdalen. Several debris slides and flows occurred in the area during three days of heavy rain in June 2011 (Photo: A.T. Hamarsland, NVE).

Table 2-1: A comparison of the two most common mass movement types occurring in loose soil; flows and slides. Edited from NVE (2011a).

	Release area characteristics	Release mechanisms	Movement and runout distance	Depositional characteristics
Slides	Steep, soil covered slopes (>25-30°) Beyond steams and gullies Presence of fine grained material mixed with sand, gravel, rocks and vegetation Fluctuating water content	Intense/prolonged precipitation and/ or snow melt Fracture as point or crack in saturated soil	Slippage of water saturated material which can increase length and width May develop into flow like behavior increasing the runout	Depositional lobes and parallel levees of coarse grained soil along the path and in the path where the terrain flattens Forms a fan existing of coarse material in the upper part and gradually finer material down slope. Often steeper than debris flow fans
Flows	Steep streams and rivers erode in surrounding soil cover during high discharge periods Occurs in previous developed gullies and ravines which not necessarily contains permanent water flows High water content	Flooding due to intense/ prolonged precipitation and/or snowmelt, breach of temporarily dams from small landslide deposits, wet snow or vegetation Intensive erosion due to very high discharge can cause water saturated flow of sediments Supply of masses from adjacent slides	Rapid wave of water, sediments and organic material High velocity and density Large volume Very long runout The flood water itself can have much longer runout than the sediments	Levees deposited parallel along the path and as lobes at the front The coarsest material is deposited at the top of the fan, and size decreases downward. Very fine sediments can be deposited longer by the water

2.2.3 Snow avalanches

Snow avalanches differ from the other types of gravity mass movements, because they are temporary hazards as they depend on the presence of snow. They occur as snow slips along a gliding surface which can involve a lower snow layer or the ground, and result in a downward gliding movement. Snow avalanches are the major natural hazard regarding mass movement processes in Norway since they cause most damage to houses, infrastructure and human fatalities (Furseth, 2006; NVE, 2011c). Snow avalanche accidents can roughly be divided into two groups relatively to their triggering factors. The first group involves accidents where people performing sport or outdoor activities are caught by an avalanche released by the activity. The other occurs when naturally triggered avalanches affect settlements and infrastructures.

There are mainly three types of snow avalanches which are considered: loose snow, slab and slush avalanches. Loose snow avalanches occur in loose snow, often fresh fallen, when the bonds between the snow grains haven't established yet or when old snow looses cohesion due to warming from the sun or from rain. This type of avalanche begins at one point and spreads downward as it entrains more snow forming a kind of lobe. They often occur on steep slopes when the snow has settled on a gradient steeper than the snows natural angle of repose and the grains, therefore, quite easily begin to flow downhill. Loose snow avalanches are normally small and harmless, but if they happen in very large slopes, they can spread laterally and involve large snow masses and high speeds that can become dangerous. If the snow avalanche is especially dry, large and fast, it can cause an avalanche cloud which may travel faster and further than the avalanche itself, causing harm to houses and roads. Wet loose snow avalanches, although slower, may be more destructive than dry ones since the density and pressure involved are higher (Norem, 2011; NVE, 2011c).

Slab avalanches occur when a part of the snowpack, a slab, starts to glide along a plane. This is often a weak layer in the snow pack between two layers of different properties of hardness or density. Slab avalanches occur as the stress increases above the strength of the weak layer, and if the gradient exceeds 30°, the slab will begin to move. Releasing factors may include additional loads from snowfall, wind drifted snow, cornice falls or the added weight of skiers and hikers (Landrø, 2007). As the slab begins to move, it will break up and move as a granular flow downhill increasing in size as it entrains snow until it stops when the terrain

becomes level. Most accidents with snow avalanches involve release of slab avalanches during outdoor activities such as skiing in mountainous terrain and they do not need to be vast to cause harm or become deadly. On the other hand, slab avalanches can propagate over an entire mountainside and form very large avalanches threatening whole villages as observed in Ørsta, where, during bad winters and unfavorable conditions, it is sometimes necessary to evacuate large parts of the settlement due to avalanche danger (Sandersen, 2012).

Slab avalanches are characterized by a crown with heights ranging from a few centimeters to several meters. If an avalanche is several hundred meters wide with a crown of 2-3 m, the involved snow mass will be enormous, registering several hundred thousands of cubic meters. The velocities may exceed 55 m s^{-1} and the density of the solid part of the avalanche may be in the range of 150-300 kg m^{-3}. This affects the impact pressures reaching values of up to 600 kPa, enough to destroy anything in its way (NVE, 2011c).

Slush avalanches occur when parts of the snow are totally saturated by water. This occurs most commonly in spring or during heavy rain along small creeks or depressions in the terrain. Water builds up within the snow behind a kind of impermeable barrier or in ponds, and as it releases, the water and snow mixture will flow downward. The mixture has a high density that depending on the speed may cause severe damage. Another special feature of this type of avalanche is its ability to move in very gentle terrain due to the high water content with inclines down to 5° having been measured and recorded. (Hestnes, 1985; NVE, 2011c).

Figure 2-4: Slab avalanche from Tamokdalen, northern Norway (Photo: Kristin N. Heggland).

3 Governmental regulations

The following section is a summary of the regulations according to the Planning and Building Act for developing and building in landslide prone areas. The full description may be found in (TEK10, 2012). The guidebook specifies safety regulations that protect against natural hazards such as landslides, floods and storm surges. It also suggests that global change may affect the frequency and magnitude of natural hazards, which is important when considering the location of buildings and the amount of load the construction is built to withstand.

Paragraph §7-3 deals with safety against landslides, and states that in locations where consequences of a landslide are expected to be large, buildings should be avoided; therefore, all buildings in landslide prone areas should have a safety class determination. Constructions within landslide prone areas should be located, dimensioned or secured against landslides, with the result that the annual probabilities do not exceed values that are typical of each of the three safety classes; S1 - S3. In other words, constructions for which consequences of a landslide would be catastrophic and unacceptable for the community should not be located in vulnerable areas. Such buildings could be regional or national hospitals and emergency institutions or manufacturing plants where toxic substances are located, and could have constituted a fourth safety class; "S4".

The nominal annual probability is defined as the inverse of the return period of a landslide of a certain magnitude against the object of interest (note the safety classes in Table 3-1)**.** The nominal probability is considered because it is impossible to compute the exact annual probability, and therefore, computational models and professional judgment are necessary. If the path of the probable landslide cannot be predicted to follow a certain track in the terrain, such as along a gully or a ravine, then the nominal probability may be computed for a 30 m width perpendicular to the landslide direction. An example might be a steep rock cliff being prone to rock falls (TEK10, 2012). Assigning safety classes helps ensure the safety of both human lives and property values; the higher the consequence, the lower the accepted nominal probability of an event. If an area is vulnerable against more than one landslide type, it is the total probability that should be assumed, although it during normal practice often is the probability of the most frequent or destructive event which is considered.

Table 3-1: Safety classes regarding construction within landslide prone areas (TEK10, 2012).

Safety class	Consequence	Maximum nominal annual probability
S1	Small	1 / 100
S2	Medium	1 / 1000
S3	Large	1 / 5000

Safety class S1 includes constructions where a landslide will have small consequences. These constitute buildings where people normally do not reside or where the economic or social consequences are small, such as garages, storage rooms, boat houses or small piers.

Safety class S2 includes constructions where the consequences of a landslide will be intermediate. This represents buildings where a maximum of 10 people reside at a time, and the economic and social consequences are on an intermediate level. These constructions include detached houses, holiday houses, and small commercial buildings, piers and port facilities.

Safety class S3 includes constructions where a landslide will have considerable consequences involving large economic or social damages or buildings where more than 10 people reside. These include housing and apartment blocks, schools, kindergartens, commercial buildings, places that provide accommodations and local emergency institutions.

If these landslide prone areas are not avoidable, constructions may be built in these areas with a higher nominal annual probability than its safety class recommends requiring that structural measures are incorporated to reduce the risk to the specified level (TEK10, 2012).

4 Study area

4.1 Geography

Norddal, or *Dalsbygda* as it also is called, is a small settlement in Møre og Romsdal, Western Norway. It is located in the *Norddal* municipality and is considered a World Heritage municipality recognizing the natural wilderness of Norwegian fjords surrounded by high mountains. It also recognizes the cultural history of agriculture and dairy farming in the area (Stranda kommune, 2012). The municipality of *Norddal* is located around the fjords *Storfjorden* and *Tafjorden*, with *Sylte*, *Eidsdal*, *Norddal/Dalsbygda*, *Tafjord* and *Fjørå* as the main settlements for the roughly 1700 (per 1st Jan 2012) inhabitants (SSB, 2012). Approximately 150 people live in the small settlement of *Norddal*.

The settlement in *Norddal* is spread over the two-kilometer long valley with some mountain farms on the western side (see Figure 4-2). The valley terminates into the *Storfjorden* in the North and is divided by *Daurmålsfjellet* (831 m.a.s.l.) into two valleys in the South, *Herdalen* and *Dyrdalen*. The eastern valley side rises steeply up to *Kyrkjefjellet* (1270 m.a.s.l.) while the more vegetated western side gently rises up toward *Middagshesten* (1382 m.a.s.l.).

Figure 4-1: Location of Norddal, Møre og Romsdal, western Norway.

Figure 4-2: Overview of Norddal taken from North-West. Daurmålsfjellet (831m.a.s.l.) is the steep mountain face located in the middle of the picture, and the road continues into Herdalen to the left of this mountain. Picture from www.norgei3d.no

4.2 Climatology

Norddal is located in the inner part of *Norddalsfjorden* which is part of a larger fjord system, approximately 50 km inland from the main Norwegian coast. The climate is strongly influenced by location near the western coast with the Gulf Stream leading to mild temperatures, especially in winter, where all monthly temperature normal's lay above 0 °C, as can be seen in Figure 4-3. *Tafjord* has one of the highest measured winter temperatures in Norway with 17.9 °C in January. Due to *Norddal's* relatively long distance from the sea, with several mountainous areas above 1000 m.a.s.l. in between, the precipitation is relatively low compared to the settlements of *Molde* and *Ålesund* which are located further west near the coast. The decline in precipitation inland is due to orographic precipitation occurring nearer the coast as moist air is lifted and cooled on its way across the outermost mountains. This phenomenon also applies to the wind which often declines inland (Tafjord, 1977). As seen in Figure 4-3, the normal monthly precipitation in *Norddal* varies from 35 mm in May to 127 mm in December, with the accumulation to a yearly normal precipitation

of 965 mm. This yearly accumulation of precipitation more closely compares to the amount of precipitation in *Oslo* (763 mm), which is considered a continental climate, than for *Ålesund* (1531 mm) (eklima.no, 2013). It is important to remember that the large topographic variations in the area cause large local variations in temperature and precipitation; as the temperature normally decreases with 0.6 °C/100 m, the precipitation increases with increasing height above sea level. Another important consideration is the large variations in weather conditions with local weather differing substantially from that which was expected due to the local climate regime. Further information about the climate in *Norddal* can be found in Chapter 5.5.

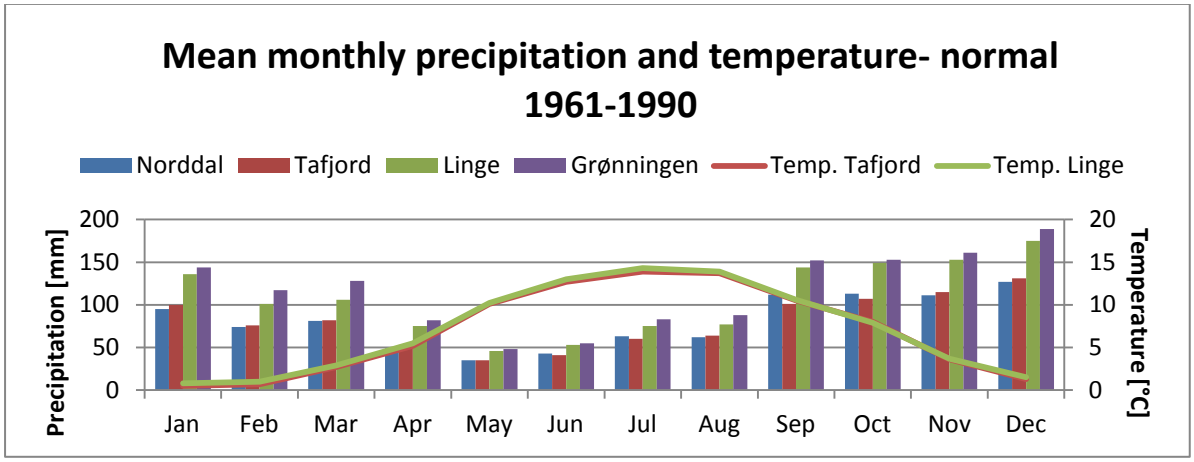

Figure 4-3: Monthly normal values for precipitation and temperature in Norddal and some stations located nearby (eklima.no, 2013).

4.3 Geology

4.3.1 Bedrock geology

The rocks in the area belong to the western gneiss region, a region of rocks from the Precambrian age which were heavily deformed and altered during the Caledonian orogeny 4-500 million years ago (Ramberg et al., 2007). Coarse-grained, granodioritic gneisses characterize the area with inclusions of amphibolites, dunite, and serpentine – all metamorphic rocks (Gjelsvik, 1951). The mineral content of the rocks in the area shows a large variation, and the gneisses are mostly grey or grey-white in color with established layering depending on the feldspar and hornblende/biotite content which defines the metamorphic foliation (Henderson et al., 2006). The areas of dunite are easy to recognize

since they weather into brownish sand, while some areas are transformed into serpentine. A map of the bedrock geology can be seen in Figure 4-4.

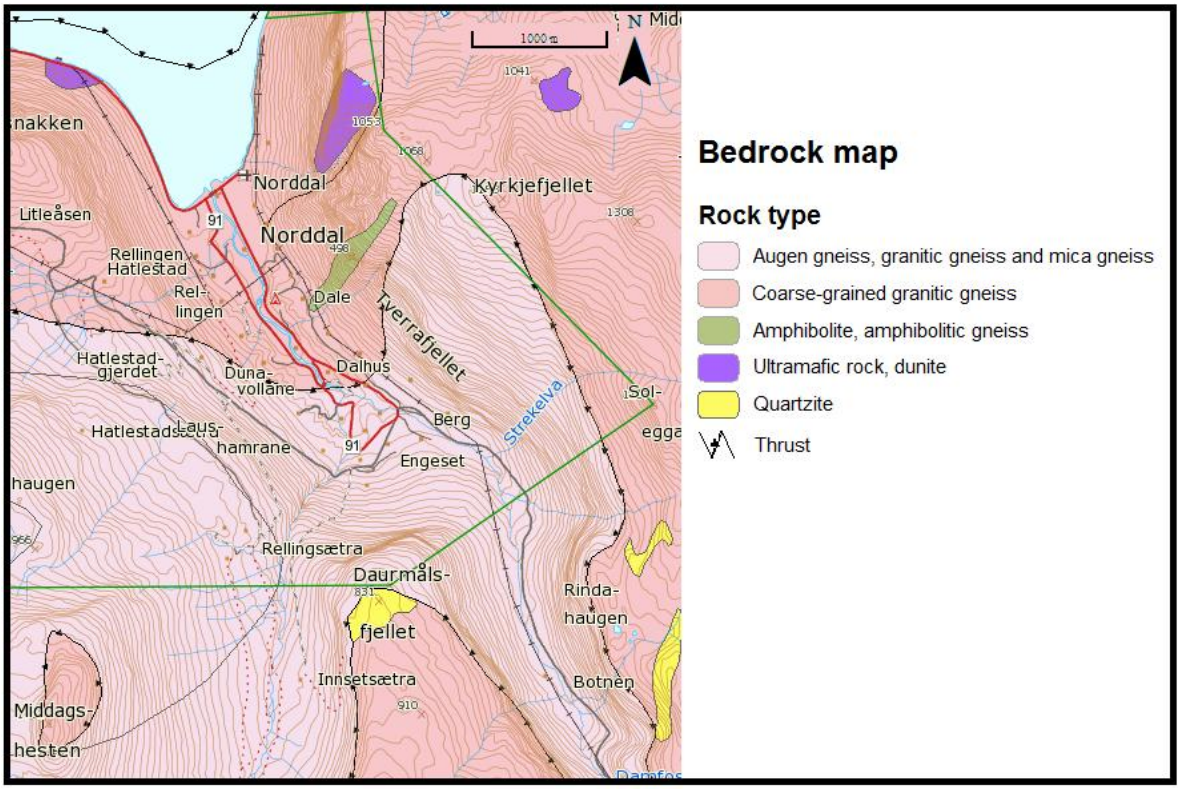

Figure 4-4: Different kinds of gneisses dominate the bedrock geology in Norddal. The data is based on a 1:250 000 map. Data from NGU (2012).

Olivine is an important mineral within the industry, and mining of olivine rich bedrock has a long history in *Norddal*. From around 1920 until 1979, olivine was mined from *Svarthammaren* along the road between *Norddal* and *Eidsdal*. Several hundred thousand tons where extracted, and at most 600 tons were mined daily by 25-30 workers (Furseth, 1987). Today there is one operational olivine mine in the area located in *Robbervika* further out in the fjord.

4.3.2 Quaternary geology

As we can see from the Quaternary map in Figure 4-5, *Norddal* shows a large variety of glacial and post-glacial sedimentary deposits. The western valley flank side is covered by till, while the eastern is almost continuously covered by a massive talus formed by rock fall processes. Beneath the valley sides are several zones of glacio-fluvial material present in the form of terraces, while the central valley floor is dominated by recent fluvial processes from

the river *Storelva*, see Figure 4-6. The eastern valley side is densely covered with ravines and drainage paths formed by water erosion, and debris slide deposits are also present. These geomorphologic features were created during or after the retreat of the last ice cap that covered the area. Reite (1966) suggests that the ice cap stretched all the way to the fjords in the inner part of the *Storfjorden* area during the climatic detoriation in the Younger Dryas time, and the glacio-fluvial deposits in *Norddal* are thought to have originated from this period (Stokke, 1983). More information about the Quaternary geology deposits in *Norddal* can be found in the Chapter 7.

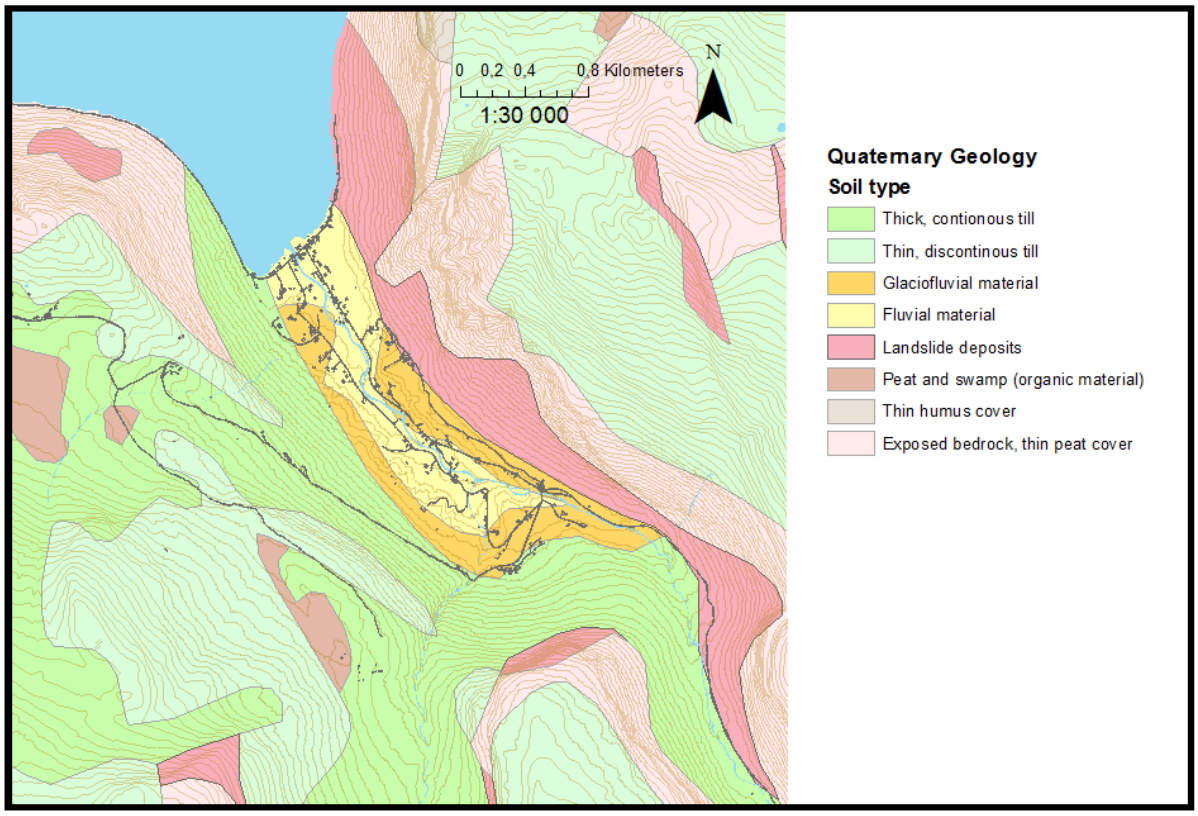

Figure 4-5: Quaternary geology map of the Norddal municipality. Data is based on a 1:250 000 map. Data from NGU (2012)

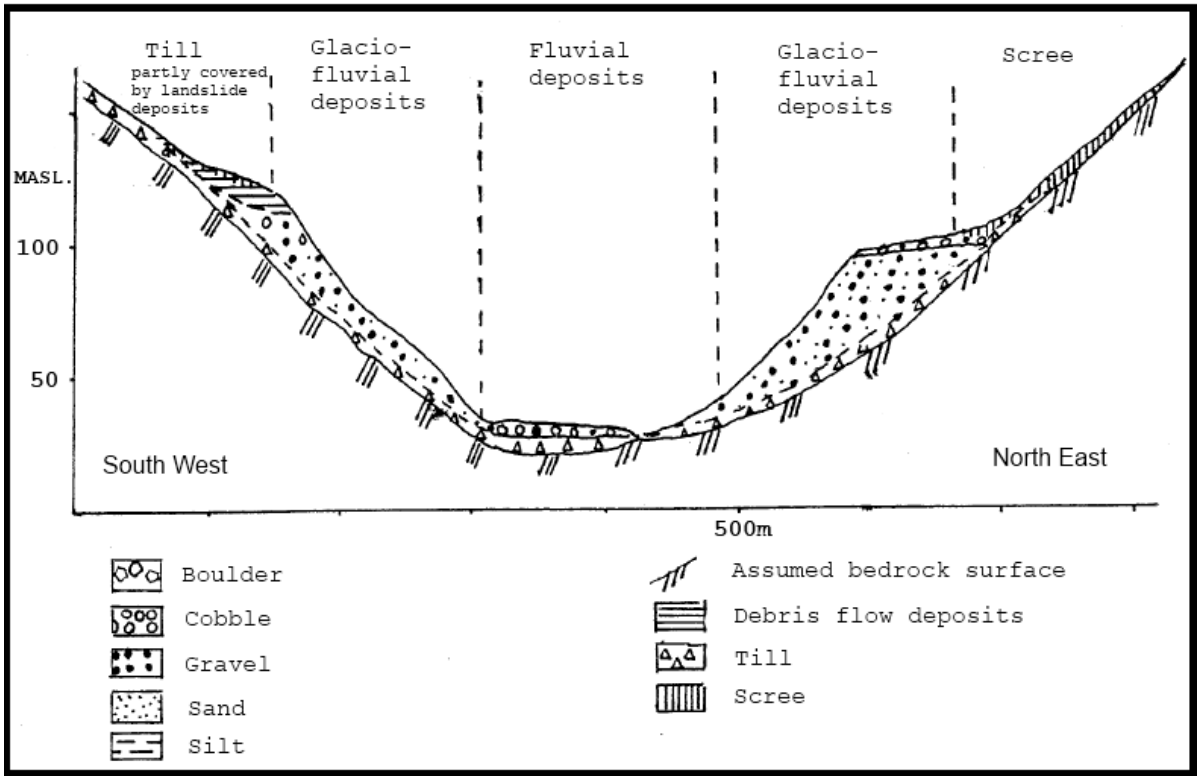

Figure 4-6: Cross section of the Norddal valley. Edited from Stokke (1983).

4.4 Vegetation

Large topographic variations and a climate with mild winters and warm summers are important factors for the flora in the area, allowing species which need warm conditions. The geology also plays an important role as most of the ground consists of hard, acidic gneisses poor in nutrients. Most of the valley floor in *Norddal* is cultivated land while the valley sides are more or less covered by forest. The vegetation on the eastern side covered by rock fall debris changes from no vegetation to dense young deciduous forest with some areas spread with old birches. The southern and western sides are covered by rich deciduous forests of birch, elms, hazel, alder and ash trees with some distinct polygons of spruce, which according to the local residents were planted in the first half of the 1900's. It is reasonable to assume that timber was removed for heating in earlier times which is not necessary these days, and therefore, allows denser vegetation today. Grazing was likely more commonly seen in the past, also. Some animals are observed grazing today which especially affects the low vegetation.

5 Methodology

The most thorough landslide hazard assessment involves combining existing, observed and modeled information (Figure 5-1). The obtainment of assessment information comprehends the gathering and evaluation of existing landslide mapping surveys, historical records, geological maps, climatic information and susceptibility maps. Initial field investigations were performed June 2nd 2012, while field work was performed during 7 days at the beginning of August 2012. Field work involved detection of local conditions which are important for the hazard zone determination, such as terrain features and vegetation. Detecting signs of present and past landslide activity were emphasized together with an information exchange with local inhabitants and the collection of data for modeling. Due to topographic conditions most of the rock face was inaccessible. Only remote investigations using binoculars were performed for the steep areas. Appendix C gives an overview of important observations determined from field work.

A climatic assessment was done to obtain an overview of the factors which could lead to landslide initiation, and run out models were performed to predict the magnitude of landslides and snow avalanches under differing conditions. Six different models were used, three for snow avalanches and three for rock falls. The ranges considered were from simple empirical models based on the height of the slope to dynamic models. For rock falls, the models Rockyfor3D, RocFall and α,β-model for rock falls were used, while modeling for snow avalanches was performed by RAMMS, AVAL-1D and the α,β-model for snow avalanches. No models were performed regarding debris flows, but preliminary results of the ongoing project regarding susceptibility mapping of debris flows on a national scale in Norway, see Fischer et al. (2012), were evaluated.

The results from field observations and modeling can be found in the chapters regarding the respective types of mass movements, see Chapter 6-8, while other information was commonly assessed for the entire mapped area and can be found in this chapter. This includes landslide history, existing susceptibility maps, previous landslide mapping surveys and evaluation of how meteorological parameters influence initiation of landslides and snow avalanches.

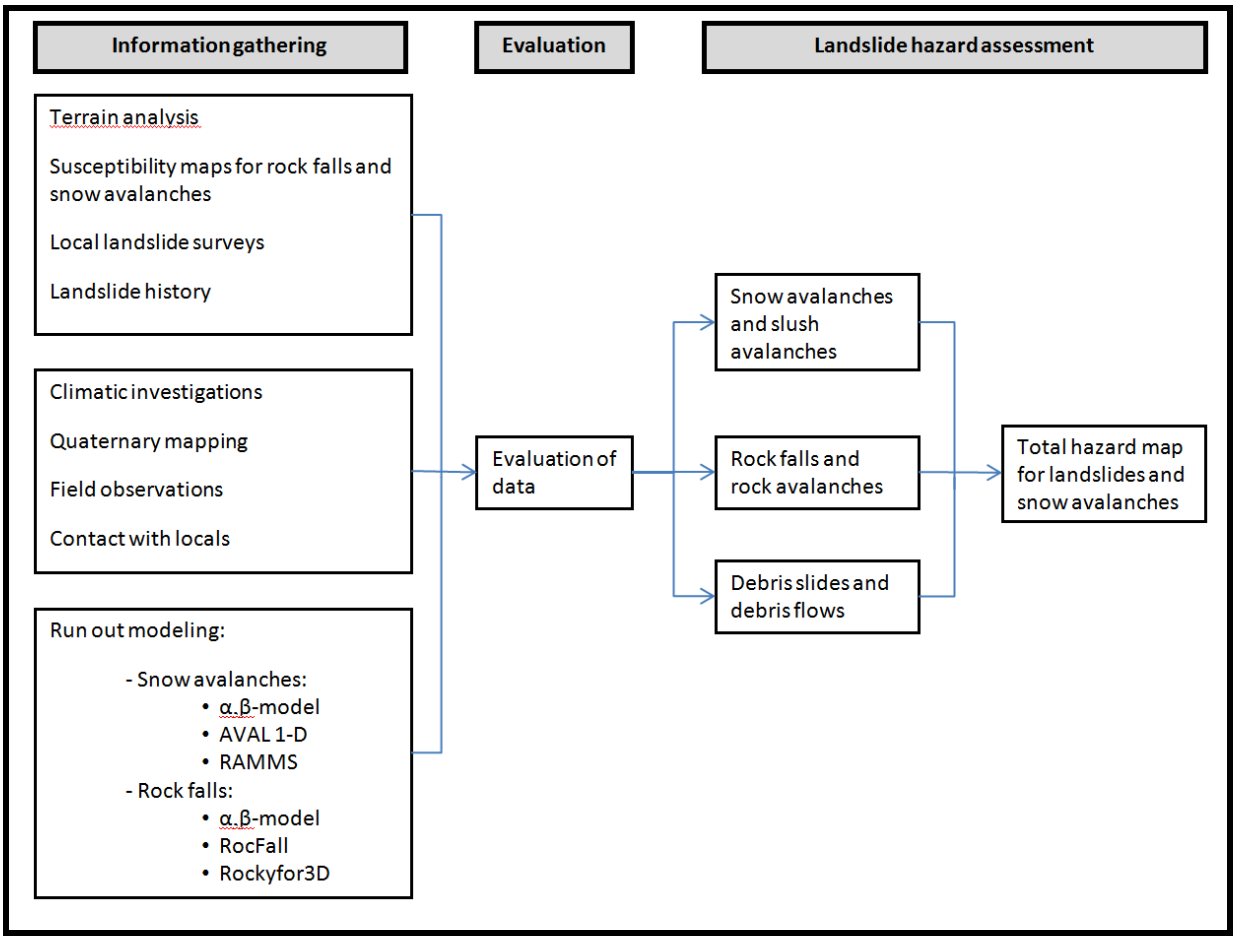

Figure 5-1: Simple schematic sketch of the methodology in this landslide hazard assessment.

5.1 Topography

A digital elevation model (DEM) with 1x1 m resolution, developed from a laser scan, is available for most of the mapped area, while the southernmost part, *Daurmålsfjellet*, is covered by a DEM with 25x25 m resolution. A slope map derived from these can be found in Appendix A (5x5 m). Topographical conditions are continuously described in this project.

5.2 Landslide history

The map in Figure 5-2 shows landslides and snow avalanches which are known to have occurred in Norddal. The numbers refers to the table of events that can be found in Appendix D. The map is based on the national landslide database (NVE Skredatlas), personal observations during field work and information from local inhabitants. There are likely more

events that have not been recorded. The map shows that mass movements related to bedrock, soil and snow have been reported in the area. The eastern mountain side is prone to frequent rock falls that have caused a massive talus to develop over time. This information is confirmed by the inhabitants who every year hear and observe rock falls in the area. The rock falls usually stop within the talus formation and, therefore, do not affect the inhabitants. The exception is in the outer area toward the fjord where rocks fall a distance into the water. The settlement here is sparse and has not reportedly been hit, but rock falls in between of the houses have been reported. Locals shared concern regarding driving their fishing boats along the coast during bad weather because of the long reach of rock falls. The latest major event happened in 1996 when 10 000 m^3 of rock fell from the *Kvitfjellet* mountain centrally located in the eastern valley side (3). Deposits were spread 70-80 m out from the talus side almost reaching the nearest houses (Anda and Flemsætherhaug, 1996). According to local inhabitants, similar deposits had been removed prior to the 1996 event, indicating a similar event had occurred in the past.

Two snow avalanche events are also reported in the eastern valley side. A snow avalanche reportedly came from *Tverrafjellet* mountain in 1690, destroying some houses and a farm while the residents where away (5). According to sources, the inhabitants moved after the event, and the farm was not rebuilt. Conversation with several individuals confirmed that this area (between point 5 and 10) is prone to snow avalanches and rock falls, a point also evidenced by the fact that no settlement is nor has been present in this area. Around 1980, another snow avalanche occurred down the eastern valley side at the inner end of the valley (10). It destroyed several cabins in the area and reached the houses at Berg on the opposite side of the river, here it caused a window to break in a house and left snow deposition in the living room. An attempt to reproduce this event by the use of a snow avalanche model can be found in Chapter 8.2.3.

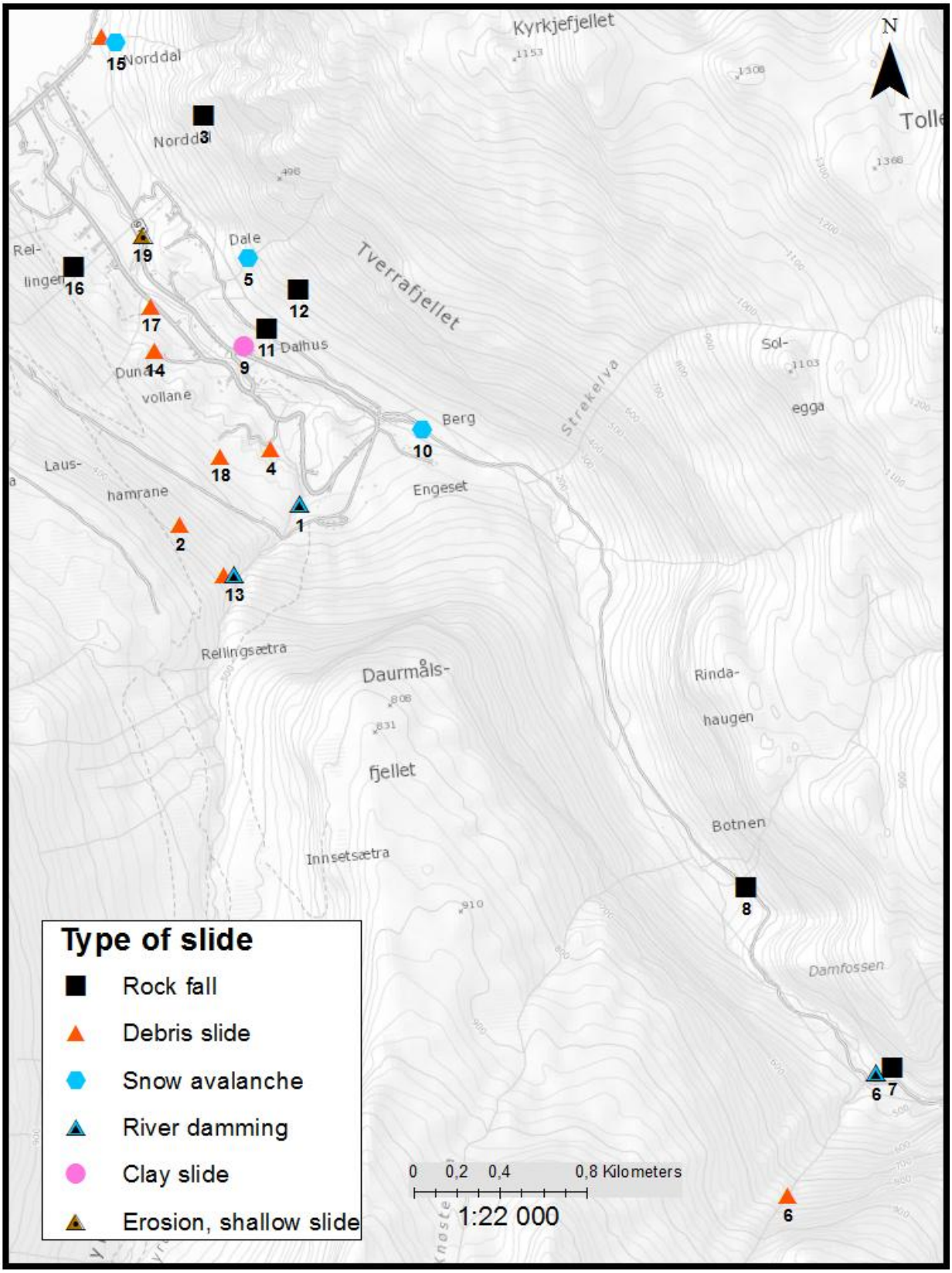

Figure 5-2: The reported hazard related to mass movements around Norddal. The area have experienced hazard related to both rock falls, snow avalanches, debris flows and damming of the river. The numbers refer to events in Appendix D.

On the western valley side, several debris slides and debris flows are reported in the debris rich areas, mostly related to large heavy rainfall and snow melt. On 9th October 1975, two large debris flows, which were related to flooding in the area, began high up on the hillside causing damage to agricultural land and the road (2). A debris slide also occurred around 1980 which caused the damming of the river flowing down *Dyrdalen* (13). While this event was not considered severe, a man died in an 1850 event when the same river was dammed by ice and suddenly flooded down stream (1). Another severe event related to river damming occurred around 1880 when the river *Herdøla* was dammed by a debris slide coming down *Furnesdalen* (6). This resulted in a major flash flood destroying all the bridges downstream in Norddal. The event posed a severe threat for the inhabitants due to its rapid occurrence; however, no fatalities were recorded.

The major concern, noted after interviewing more than 20 residents in *Norddal*, was the slope instability at *Åkneset* further out on the fjord where a rock slide would most probably cause a tsunami. Residents also reported concern for the only road connecting *Norddal* with *Eidsdalen* which is exceptionally prone to rock falls. The national landslide database (NVE Skredatlas) shows more than 20 reported rock falls along this distance of 4 km.

5.3 Existing susceptibility maps

Susceptibility maps of the area, available from NVE Skredatlas (2013), show that most of the settlement is laying within theoretical reach of rock falls (Figure 5-3). Everything east of the river *Storelva* lays within the reach of rock falls from the eastern valley side. Also the mountain *Daurmålsfjellet*, located in the southern end of the valley, may be a susceptible area for rock falls reaching the inner settlement, as well as some small cliffs and the outermost part of the western valley side.

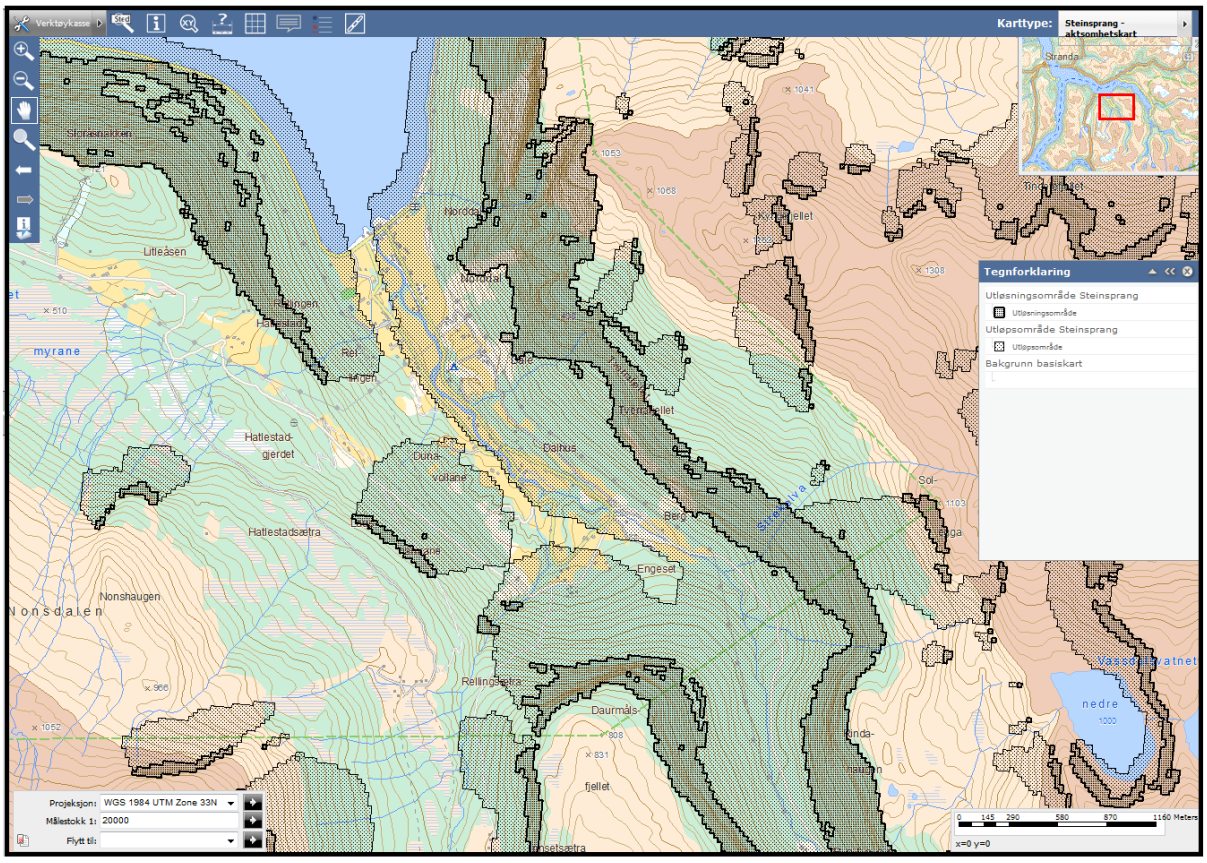

Figure 5-3: The susceptibility map for rock falls indicates that large parts of the settlement lay within the reach for rock falls (NVE Skredatlas, 2013). Dark shaded areas are source areas, while lighter shaded areas are possible run out zones.

The susceptibility map for snow avalanches states that the whole valley floor lays within the reach of snow avalanches, see Figure 5-4. Common for both susceptibility maps is that they are automatically generated for the whole country based on the topographic conditions and do not take local conditions into account. Therefore, the susceptibility map regarding snow avalanches appears erroneous, since snow avalanches seldom occur in dense forests which the western valley side of Norddal is covered by. Such maps are, therefore, only an indication of possible threats in the area.

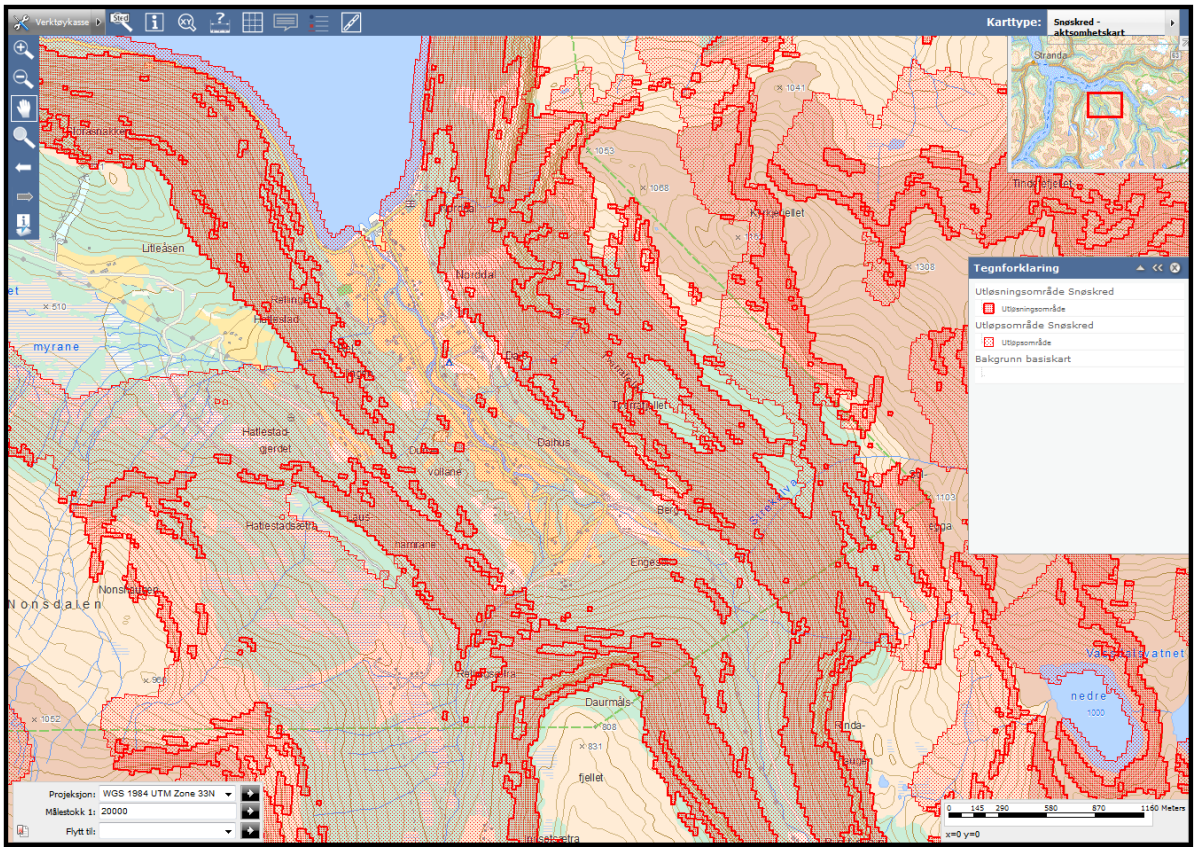

Figure 5-4: The susceptibility map for snow avalanches indicates that most of the settlement lay within the run out from possible snow avalanches. The map do not take forest and vegetation into account (NVE Skredatlas, 2013). Dark shaded areas are source areas, while lighter shaded areas are possible run out zones.

A third susceptibility map available is a common susceptibility map for rock falls and snow avalanches. This map is commissioned by the State and developed by Norwegian Geotechnical Institute (NGI). It differs from the previously mentioned maps by the use of easy field investigation together with computational models. The investigation takes local conditions into consideration such as forests and smaller terrain features which affect the run out distance. This map represents the actual susceptibility area more accurately than the previous mentioned maps and tends to show a less severe extent of the hazards (NVE, 2012a). For Norddal, this is evident by observing most of the settlement outside the susceptibility areas for rock falls and snow avalanches, see Figure 5-5.

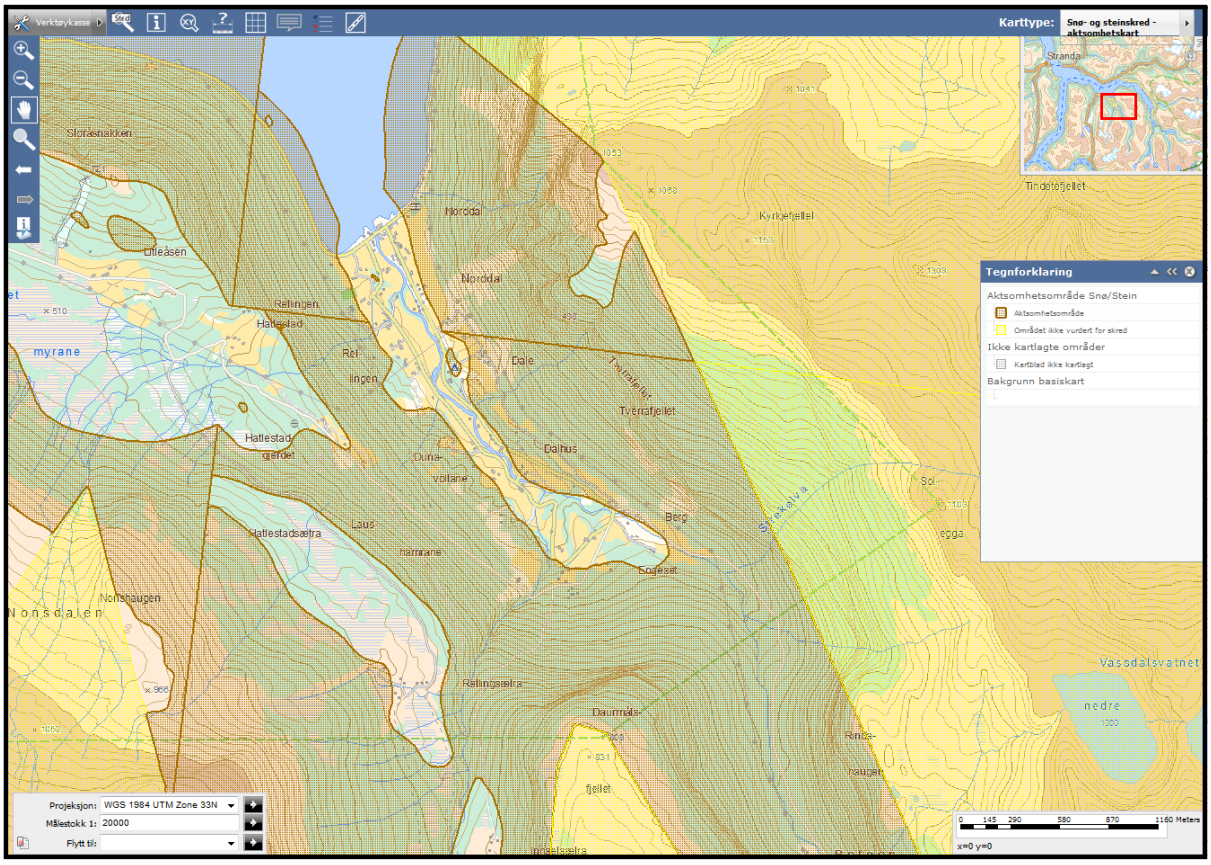

Figure 5-5: This susceptibility map for rock falls and snow avalanches prepared by NGI include field work and thus take local conditions as forest and terrain features into account (NVE Skredatlas, 2013). Brown shaded areas are susceptibility areas for snow avalanches and rock falls, while yellow areas are unmapped areas.

5.4 Previous landslide mapping surveys

No detailed landslide hazard mapping has been performed for Norddal, but the area has been included as a method example in multiple regional and national investigations related to natural hazards, mainly rock falls. This section will review these investigations containing the most relevant information. For more details, please see the specified sources.

During work with the national landslide hazard mapping in Norway, studies were conducted to establish a list of areas to prioritize. Oppikofer et al. (2011) did an investigation to establish which areas needed detailed investigation regarding rock falls. The results of this investigation are based on the national rock fall susceptibility map available from NVE Skredatlas (2013) mentioned in Chapter 5.3. The information was used together with population statistics to establish potential vulnerable areas and the potential risk. Altogether 21 zones were classified as 1st priority regarding rock fall mapping in Norway, and 94 zones

were classified as 2nd priority, mostly within the counties of *Sogn og Fjordane* and *Møre og Romsdal*. More than 55,000 people could be affected by rock falls national-wide within these zones. Norddal was designated 1st priority due to the high rock fall activity in the area together with the number of people exposed, estimated to 472. The results in Figure 5-6**,** show the rock fall zones with respect to the number of people involved in *Norddal*, divided into 250x250 m squares. (Oppikofer et al., 2011).

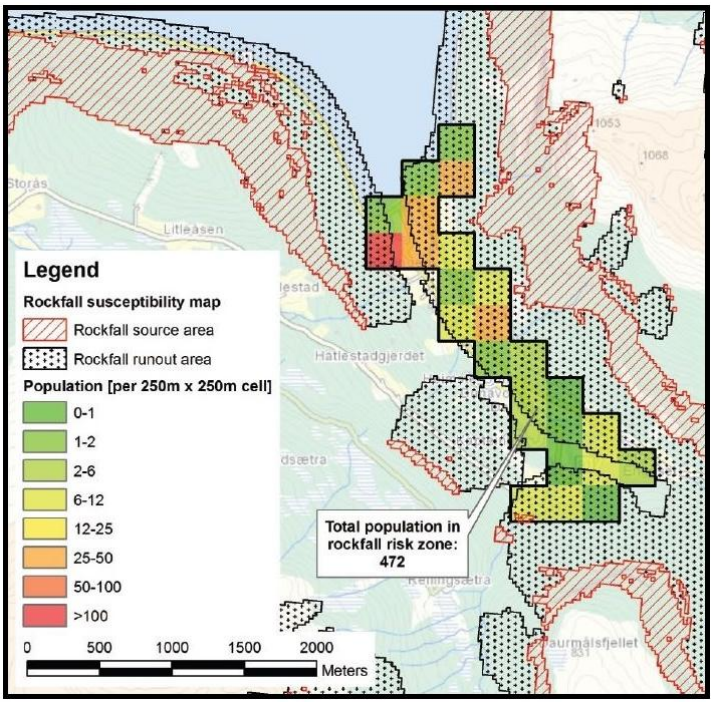

Figure 5-6: Calculated rock fall risk in Norddal (Oppikofer et al., 2011).

In 2005, major field investigations were conducted in the *Storfjorden* area to define how structural geology determines hazardous effects of large rock slides. In advance of the field work, aerial photos, bathymetric data and historical events were reviewed to establish target areas for further investigation. Several geological, geometrical and topographical factors, such as pre-existing lineaments, foliation, joints and development of faults, folds and extensional back fractures were analyzed due to their potential as controlling factors for rock slope failure (Henderson et al., 2006). The investigation revealed the importance of orientation of the foliation in the bedrock in relationship to the fjord orientation, and fall-line toward sea-level with respect to potential landslide sites. An example close to *Norddal*, see Figure 5-7, is a site where 'vertical foliation associated with a set of conjugate near vertical fractures along pre-existing lineaments' cause mass detachment from the slope. The foliation is vertical and trending NW-SE with open joints present along the foliation. The combination of structures and their direction indicates that toppling is the most likely failure mechanism, reducing the chances of a large slope detachment causing a tsunami which immediately could threaten the village.

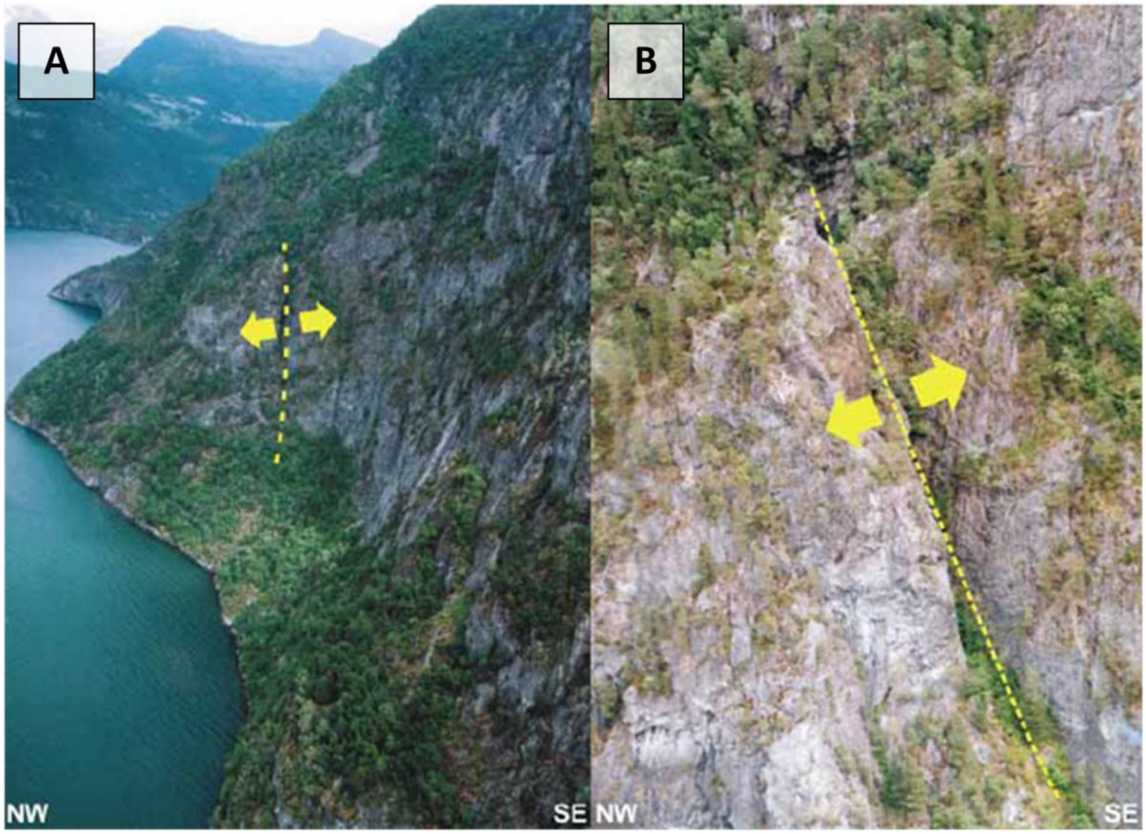

Figure 5-7: A) General view of the mountain side right north for Norddal showing the area prone to toppling. B) Detailed photo of a mass detached from the slope (Henderson et al., 2006).

The report also provides a review of *Kvitfjellet* in *Norddal*. *Kvitfjellet* is of interest because of a well defined wedge structure located in an area experiencing several recent rock falls and rock avalanches. The wedge is defined by two differently oriented basal shear planes, the north-western dipping 45° SE and the south-eastern dipping 45° NW. Additionally, there are one or two secondary fractures present at the back which affects the wedge geometry and the possible rock slide mass. The north-eastern basal shear plane was the only one accessible during the investigation and was, therefore, investigated in more detail. The shear plane was found to be sub-parallel to an amphibolitic foliation orientated 45° to the valley side and located on a lithological contact between an amphibolite (lower) and a dioritic gneiss (above). The gneiss holds steep joint structures forming conjugate extensional sets, which together with signs of what appeared to be brecciated mica, may indicate recent movement activity (Henderson et al., 2006). Two GPS points were set out during this field work in 2005 to determine the possible magnitude of movement, but as will be seen in Oppikofer et al. (2012), no movement has been detected.

Four times between 2006 and 2011, the face of Kvitfjellet was scanned utilizing long-range Terrestrial Laser Scanning (TLS) which is widely used to study rock slope instabilities. The scanning was performed by the Geological Survey of Norway (NGU) which use TLS to measure periodic displacement, orientation of main discontinuities and rock fall activity within rock slopes (Oppikofer et al., 2012). A comparison of the 2006 and 2011 TLS measurements of *Kvitfjellet* revealed no significant displacements of the unstable slope, but did determine 10 rock falls (see Figure 5-8). Four of these rock falls occurred along the basal sliding layer, but others were also noted all over the cliff, both inside and outside the instability. The volumes involved can be seen in Table 5-1, and vary from 0.12 m^3 to 65.0 m^3, where the latter originates from an overhanging wall near the top of the mountain slope (Oppikofer et al., 2012). These results indicate that there is a high rock fall activity rate in this area which coincides with what the people in the area related; several rock fall events occur every year.

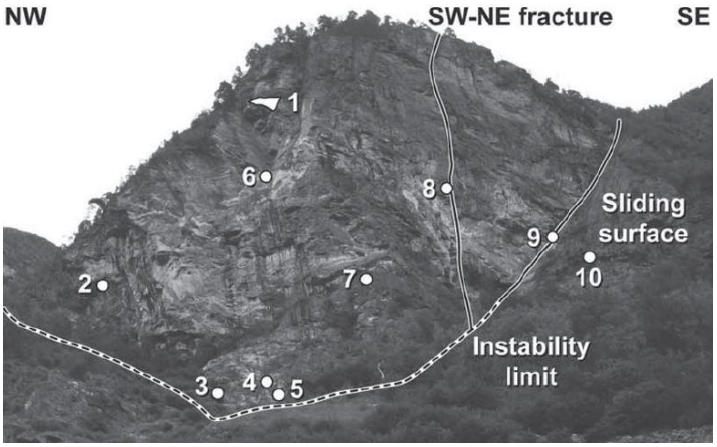

Figure 5-8: Rock falls at Kvitfjellet between 2006 and 2011. Photograph of the rock slope instability, the sliding surface in the SE and the location of rock falls. Numbers refer to Table 1. (Oppikofer et al., 2012)).

Table 5-1: Location and volume of rock falls determined at Kvitfjellet between 2006 and 2011 (Oppikofer et al., 2012).

#	Particular location	Altitude [m]	Volume [m^3]
1	Overhanging wall	516.6	65.0
2	Overhanging wall	455.9	1.24
3	Along sliding surface	352.2	5.78
4	Along sliding surface	352.0	0.56
5	Along sliding surface	348.8	0.12
6	Within the main cliff	478.2	0.26
7	Within the main cliff	420.3	0.33
8	Along SW-NE fracture	472.7	1.93
9	Along sliding surface	474.7	2.08
10	Outside of the instability	448.3	0.53

A regional risk- and vulnerability analysis regarding rock avalanches in Møre og Romsdal (FylkesROS, 2011) was also completed, which among others is based on the previously

mentioned report by Henderson et al. (2006). In this report, *Kvitfjellet* is designated as a low probability and high consequence case, making it a modest risk situation. The results predicted a possible 1 million cubic meter rock slide, although no movements were recorded. Despite the low probability of failure, it was regarded as a modest risk due to the high possible consequences for settlements in the run out area, which included a possible damming of the river, causing additional hazard of dam failure and flooding (FylkesROS, 2011).

In addition to the previously mentioned surveys, several local landslide hazard assessments have been performed, mostly related to events that occurred near the settlement, see Appendix D. Fischer et al. (2012) used *Norddal* as a test site for an ongoing project related to national debris flow susceptibility mapping, a survey which will be discussed in more detail in Chapter 7.3.

5.5 Meteorological parameters and landslides

Meteorological factors may act as important parameters for the inducement of mass movement processes. Regarding snow avalanches, the amount of precipitation as snow, the wind distribution and the maximum measured snow depths are of interest. For debris flows and debris slides, the release is mostly connected to water supply coming from precipitation as rain or from snow melt. The relationship between rock falls and meteorological parameters are not as clear as for snow avalanches and debris flows (Sandersen et al., 1997).

The meteorological stations used are located in *Norddal*, *Linge*, *Tafjord* and *Grønningen* (Figure 5-9), and their operational period can be found in Table 5-2. Please note that values from eklima.no

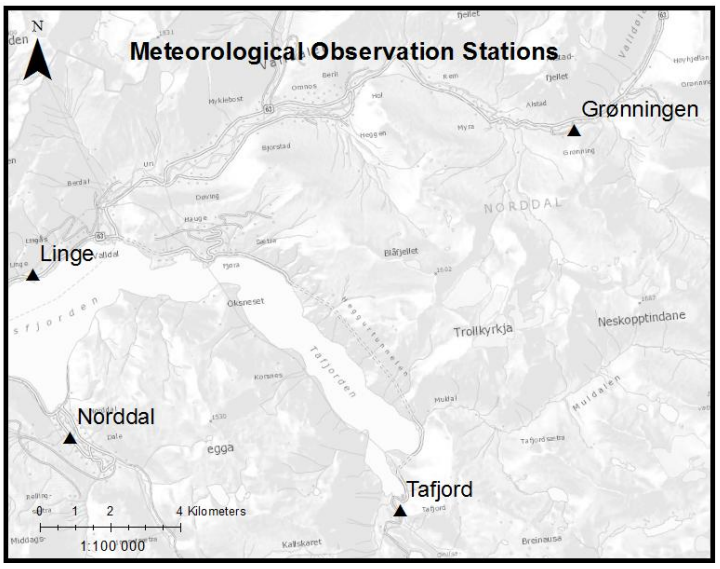

Figure 5-9: Location of meteorological stations that are used in the project.

(2013) might be interpolated when it comes to normal periods outside the operational period of the station. The stations at *Linge* and *Tafjord* are also slightly moved during the period.

Table 5-2: Meteorological stations near Norddal.

Station	Norddal	Tafjord	Linge	Grønningen
Altitude [m.a.s.l.]	28	11	34	312
Operational period	1895 →	1925 →	1961 - 74, 2005→	1972 →

5.5.1 Precipitation and debris flows

Figure 5-10 shows clearly that the precipitation in *Norddal* is lowest in the summer, while the highest values can be found from September to January. The same pattern can be found for the monthly and daily values. The period of heaviest precipitation in *Norddal* correlates with the season of highest probability of debris flow occurrence in marine climate region of Norway, which is in the autumn period from August to December (Sandersen et al., 1997).

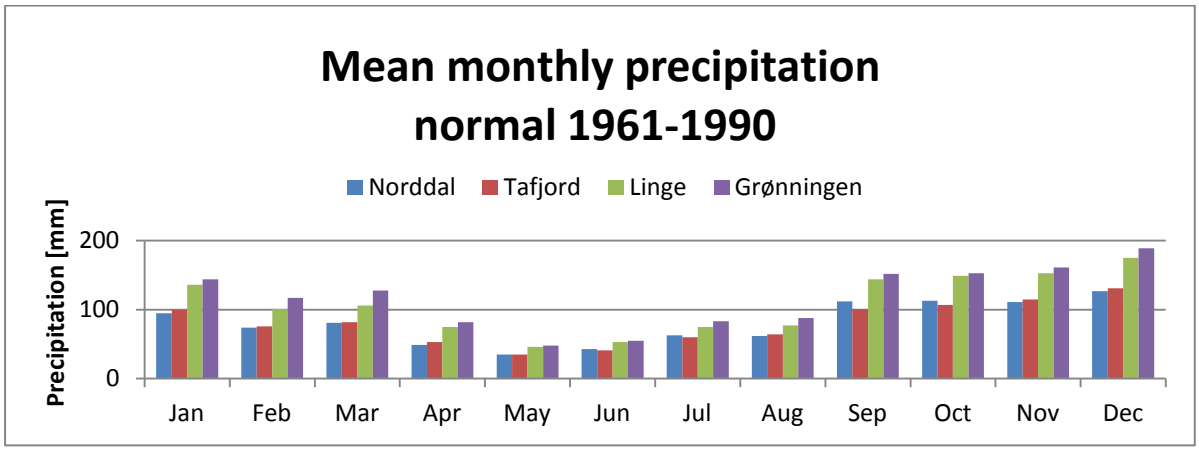

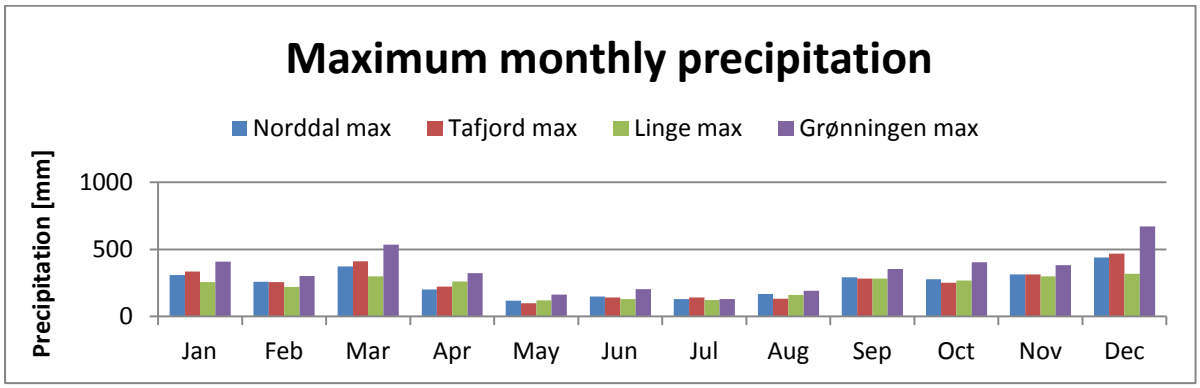

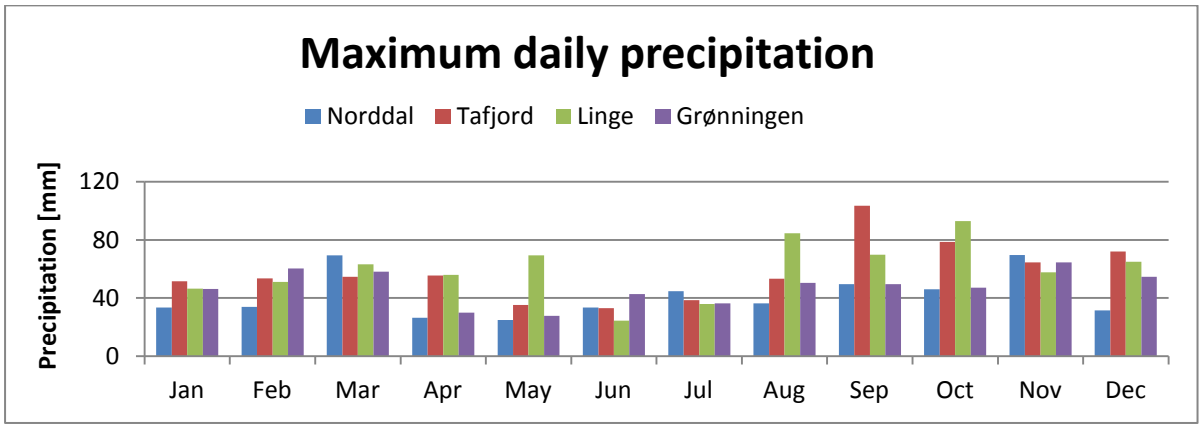

Figure 5-10: Precipitation data for Norddal and nearby stations. From the top; mean monthly precipitation for the normal period 1961-1990, maximum measured monthly precipitation and maximum daily precipitation. Data from eklima.no (2013).

Sandersen et al. (1997) studied the weather conditions prior to 30 debris flows in Norway to investigate the significance of meteorological factors on failure. They established the following relationship between critical water supply expressed as a percentage of mean annual precipitation (P) and duration in hours (D):

$$P = 1.2 * D^{0.6} \qquad \text{Equation 1}$$

Equation 1 is used to calculate the water supply critical for debris flow inducement for 12, 24, 48 and 72 h periods, resulting in the critical values 5.3, 8.0, 12.2 and 15.6 % of the annual precipitation. The converted values in mm valid for *Norddal* with 965 mm yearly normal precipitation can be found in Table 5-3. The table also includes calculated return periods of these threshold values based on 24 h fixed precipitation observations (07-07, also denoted daily values) and the five highest measured values within the operational period of the stations in *Norddal* and *Tafjord*. Important to note is that the calculated return periods only take water supply from precipitation into account, and the return periods will probably be lower as additional water supply from snow melt is taken into consideration (Sandersen et al., 1997).

Table 5-3: Calculated precipitation thresholds for different durations according to Sandersen et al. (1997), and the 5 highest measured precipitation values for the meteorological station in Norddal). Return period is calculated automatically. Data based on daily values (07-07) from eklima.no (2013).

	Station	Tafjord	Norddal		
	Precipitation duration [h]	**12h**	**24h**	**48h**	**72h**
	Critical values of mean annual prec. [%]	5.3	8	12.2	15.6
	Critical precipitation values [mm]	51.1	77.2	117.7	150.5
	Critical intensity [mm/h]	4.3	3.2	2.5	2.1
	Return period [years]:		55	>100	>100
Measured values	**1. highest value [mm]**	62.4	71.1	108	144.7
	Median date	08.10.1992	26.10.1974	08.09.1897	08.09.1897
	2. highest value [mm]	57	70.8	100.5	124.5
	Median date	18.09.1978	18.09.1978	15.11.2005	18.09.1978
	3. highest value [mm]	54.6	69.7	100.4	122.9
	Median date	07.10.1975	15.11.2005	01.02.1896	15.11.2005
	4. highest value [mm]	46.6	69.5	98.2	118.6
	Median date	17.09.1978	22.03.2011	19.09.1978	27.12.1975
	5. highest value [mm]	44.6	68.4	93.4	113.5
	Median date	06.12.1974	07.10.1975	27.12.1975	01.04.1997

Førland (1984) describes a way of determining return period of extreme precipitation based on the precipitation value with average recurrence interval once within 5 years (M5). The method is adapted from empirical studies in Britain ((NERC (1975) in Førland (1984)), and the precipitation with a T year return period can be described as

$$MT = M5 * e^{c*\ln(T-0.5)-1.5} \qquad \textit{Equation 2}$$

where c depends on M5 and can be determined from

$$c = 0.3584 - 0.0473 * \ln(M5) \qquad for\ 25 < M5 < 350\ [mm] \qquad \textit{Equation 3}$$

Return periods from other intervals than 24 h can be determined using ratios based on the M5-value. This method is the same as the one automatically calculated in eklima.no, but eklima.no use point values from the meteorological station in Norddal. Since this station is located at sea level, and thus don't take increased precipitation with altitude in the surrounding mountains into account, an additional calculation is performed using the M5-value representing the catchment draining to the western valley side. The results can be

found in Figure 5-11, which shows the calculated return periods for 24, 48 and 72 h intervals.

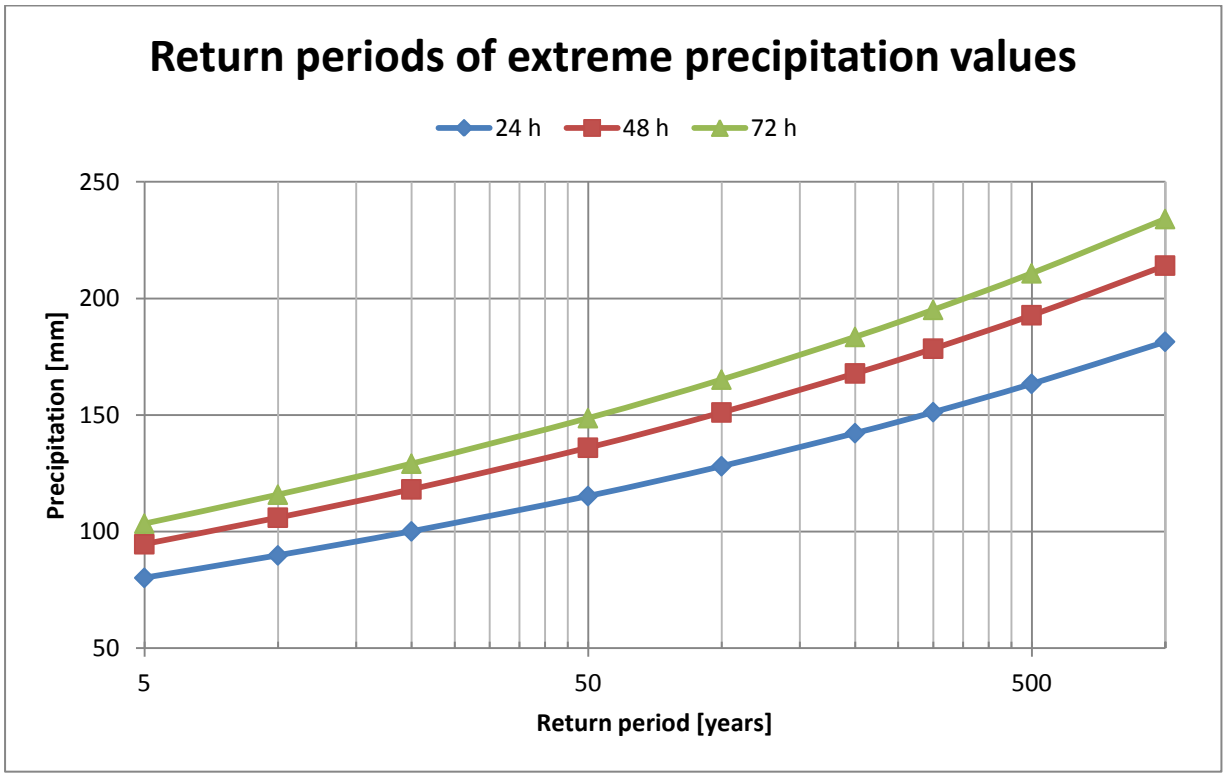

Figure 5-11: Calculated extreme precipitation values for different intervals and return periods based on Førland (1984).

The recurrent intervals calculated are significantly lower than the one calculated directly from eklima.no (Table 5-3), despite using the same calculation method. The reason is apparently different input as a higher value for M5 is used (80.2 mm). This value represents the 11 km^2 catchment centrally located in *Norddal* (Figure 5-12), which includes mountain areas on both valley sides, unlike the station based value determined from precipitation in a point in the valley floor. The higher M5-value for the catchment compared to the station is consistent with Alfnes (2007), which compared grid-based versus station based M5-values in extreme precipitation calculations.

As the thresholds are calculated from the annual normal precipitation at the meteorological station (28 m.a.s.l.), a direct comparison of the calculated recurrent intervals in Table 5-3 and Figure 5-11 is of low value. This is because the annual normal precipitation is higher in the mountains surrounding Norddal than in the valley floor. Interpolated annual normal precipitation values for the western valley side towards *Middagshesten* in *Norddal* indicate a value in the range of 1000-2000 mm/year (seNorge.no, 2013).

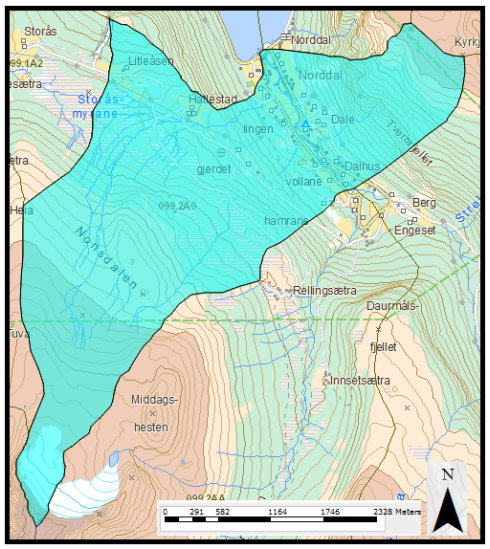

Figure 5-12: Extent of catchment (10.95km^2) used in frequency analysis (NVE Atlas, 2013).

The actual return periods are hard to determine due to large topographic variability and variation in precipitation with altitude. Appendix E contains all daily precipitation observations higher than 30 mm in *Norddal*, where 135 of a total of 220 events are reported as rainfalls. Several of the debris flow events are reported in conjunction with heavy precipitation and flooding, but only one exact date of debris flow initiation is known, October 9th 1975 (Appendix D). Precipitation rates the last 3 days before this event shows 19.9, 68.4 and 17.6 mm/24 hr. This period of heavy precipitation is the 5th highest measured daily value, but also close to the highest measured values for 48 h and 72 h precipitation periods (Table 5-3). These values give an indication of which precipitation values which could cause debris flow initiation in *Norddal*. Precipitation rates above the measured values for the 1975 debris flow have occurred several times after this event, implicating that such intensities are not unusual over longer periods. Since no landslides are reported in conjunction with these precipitation events, debris flows not necessarily have to initiate during high precipitation rates. Additional water supply from snow melt and the ground storage capacity prior to the rainfall do also play an important role in debris flow initiation (Sandersen et al., 1997).

5.5.2 Meteorological parameters and snow avalanches

Jaedicke et al. (2008) did an extensive study of more than 20 000 historical landslides and snow avalanches in Norway including their predictability related to meteorological

conditions. Regarding snow avalanches in the western part of Norway, one-day precipitation was found to be the most important trigger for snow avalanche release, and this cause is therefore emphasized in the following, although, also other intensities and weather conditions are known to cause snow avalanche release. Critical snow fall intensity for snow avalanches in Norway is described as more than 30 cm per day (Sandersen, 2012). Such snow fall intensities are not unusual in western Norway. Precipitation data from *Norddal* (eklima.no) for days in the winter period (November-March) 1930-2012 with temperature beneath 3 °C at sea level (temperature values from Tafjord station) reveals 72 days with more than 30 mm precipitation (water equivalent). Additionally, 234 days show more than 20 mm precipitation, a value which would probably increase with altitude. The threshold value of 3 °C is thought to reflect snow conditions above 400-500 m.a.s.l. The precipitation is measured from fixed 24 h periods, and the actual amount of snow fall intensities exceeding 30 cm/24 h could, therefore, be higher (Alfnes, 2007). Reservation must also be considered as the temperature does not always decrease with altitude, implying that some of the events could occur as rain in the mountains. Appendix E reveals that 14 precipitation events exceeding 30 mm/24 hr are recorded as snow, with additional 66 are reported as rain/snow. The results suggest that critical intensities for snow avalanche release are not unusual in the mountainous areas surrounding *Norddal*.

Figure 5-13 shows the maximum measured snow depth within each month for *Norddal* and surrounding stations independently of the operational period. The station at *Grønningen* shows significantly higher maximum values, which is related to the higher altitude, and 3.25 m was measured on level ground in 1968 (Furseth, 1987). This is also clearly evident in Figure 5-14 that shows the yearly maximum of *Norddal* and *Grønningen* within their operational period with *Grønningen* generally recording higher measured values than *Norddal*. The fact that the measurements from *Norddal* are acquired at sea level makes them undependable for the determination of snow depth related to snow avalanche modeling, but they do give an acceptable indication of minimum values. Figure 5-15 shows interpolated values from seNorge.no (2013) which takes topography into account. The map indicates a maximum normal snow depth of up to 2-4 m in the mountains surrounding *Norddal* for the period 1971 – 2000.

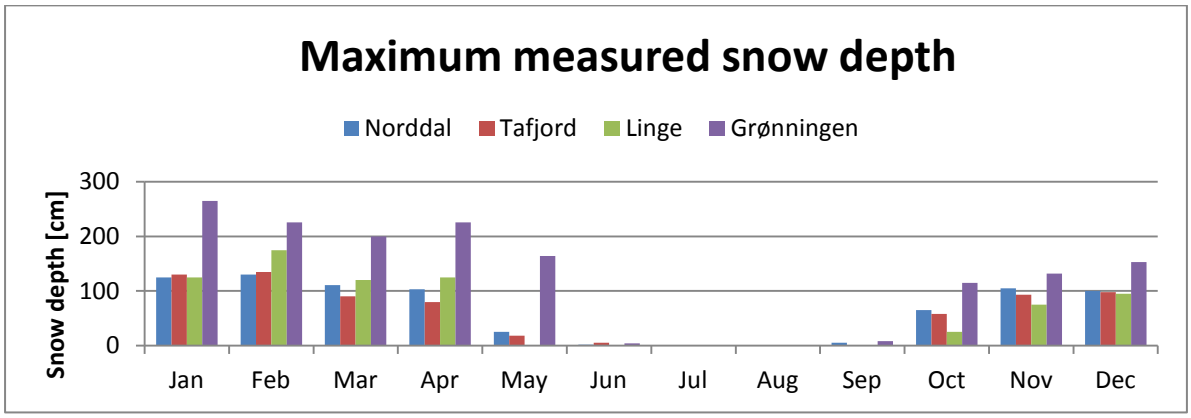

Figure 5-13: Maximum measured snowdepth for Norddal and surrounding stations. Notice the significant higher values for Grønningen, which is located almost 300 m higher. Data from eklima.no (2013).

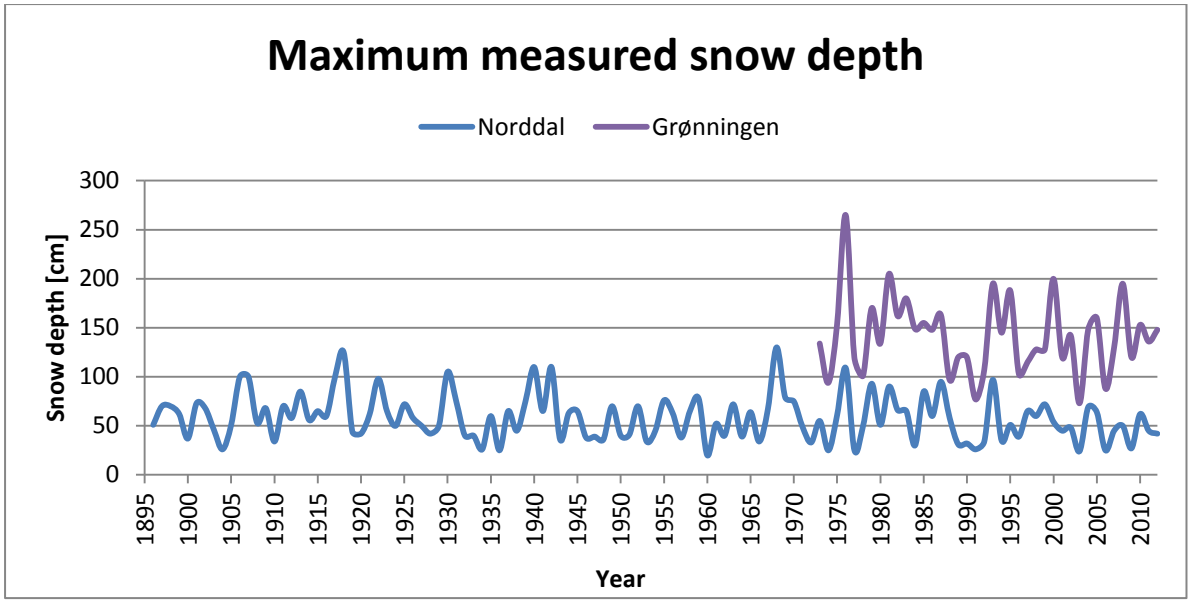

Figure 5-14: Maximum measured snow depth in Norddal every winter since 1896, and Grønningen from 1972. The plot shows how the higher altitude at Grønningen generally increases the maximum measured snow depth. Data from eklima.no (2013).

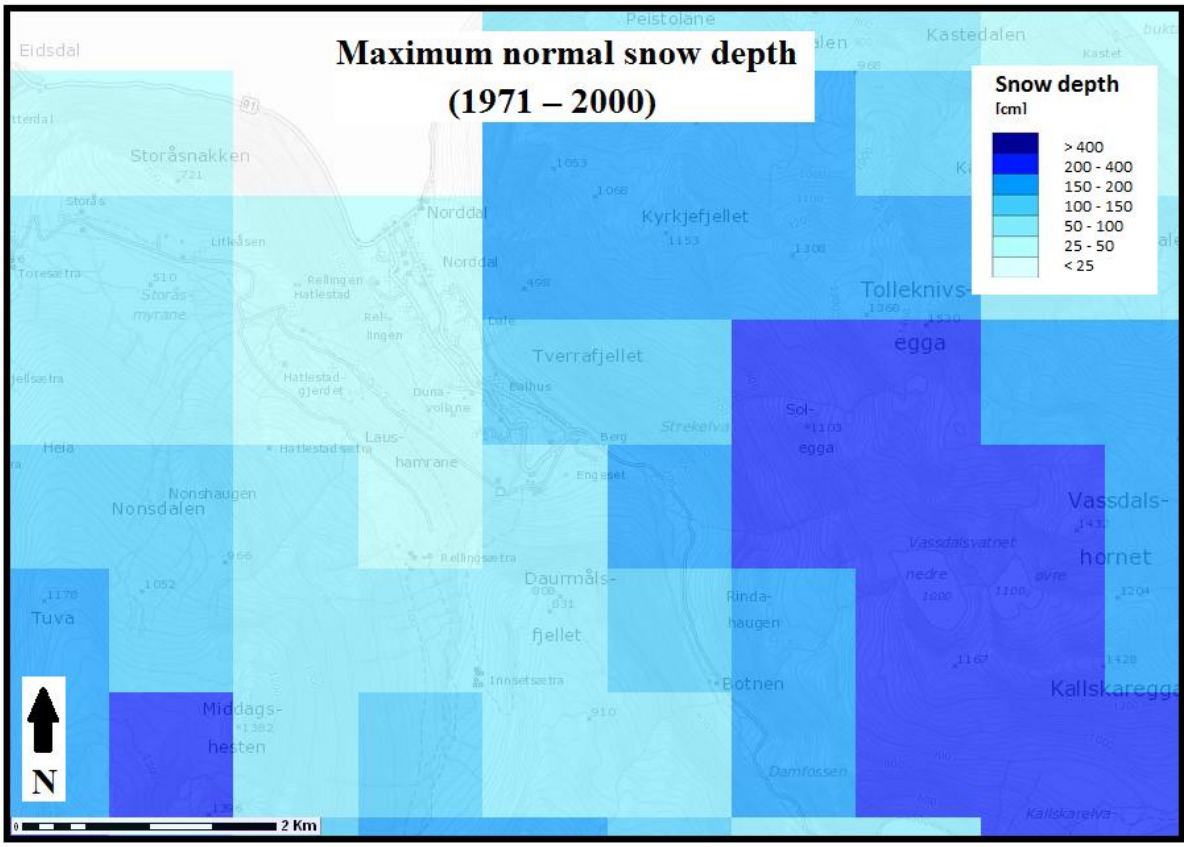

Figure 5-15: Maximum interpreted normal snow depth as a function of elevation. Snow depth generally increases with elevation and Kyrkjefjellet shows a maximum normal snow depth of 150-200 cm. Data from seNorge.no (2013).

Wind drift plays an important role in snow distribution in the mountains by quickly moving large deposits of snow (Landrø, 2007). The prevailing wind direction can, therefore, indicate where the snow will deposit and which areas will experience a higher chance of snow avalanche release. Figure 5-16 shows the wind distribution for *Tafjord* for the whole year in the period 1980 - 2012 (A) and the winter months (B). The prevalent wind direction coming from S-SE is thought to derive from the topographic conditions in the area with wind following the local valleys and fjords. The conditions in *Norddal* are thought to closely coincide with observations from *Tafjord* due to topographic similarities.

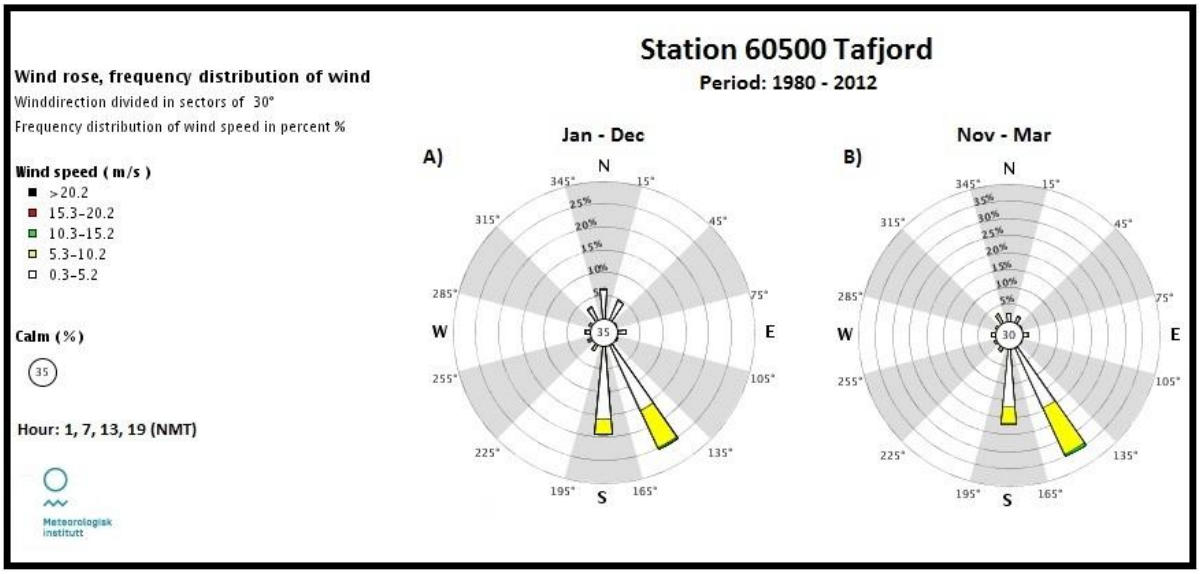

Figure 5-16: Wind distribution for Tafjord. A) Yearly values for the period 1980-2012. B) Values for November – March in the same period. The general pattern shows wind from SE. Data from eklima.no (2013).

The wind direction during snow fall is also important for snow distribution. Figure 5-17 shows the wind distribution during snow fall for *Linge* and *Tafjord*. The data used differs from above as only wind measurements during precipitation and temperatures < 3 °C are used. This is meant to represent *conditions* of snow fall above 400-500 m.a.s.l., a period of high snow drift. The results are affected by topography, but a more NW direction can be observed for Tafjord. This is consistent with inhabitants from *Valldal* (across the fjord from *Norddal* near *Linge* meteorological station) who state that the wind direction related to large snow falls are mainly from W-NW (Taurisano, 2013a), something which is similar to the general conditions along the western coast.

Furseth (1987) described several snow avalanche accidents related to extreme winters in the *Norddal* municipality, and up to 70 people lost their lives during one night of major snow avalanche activity in the region (February 6th 1679). Several winters are reported as specifically snow avalanche winters; 1699, 1700, 1855, 1886, 1880, 1881, 1895 and 1905. Major events are also reported in 1921, 1979 and 1982. This historical record and the conditions revealed from meteorological studies tell about a region where weather conditions favorable to snow avalanches initiation must be expected with irregular intervals.

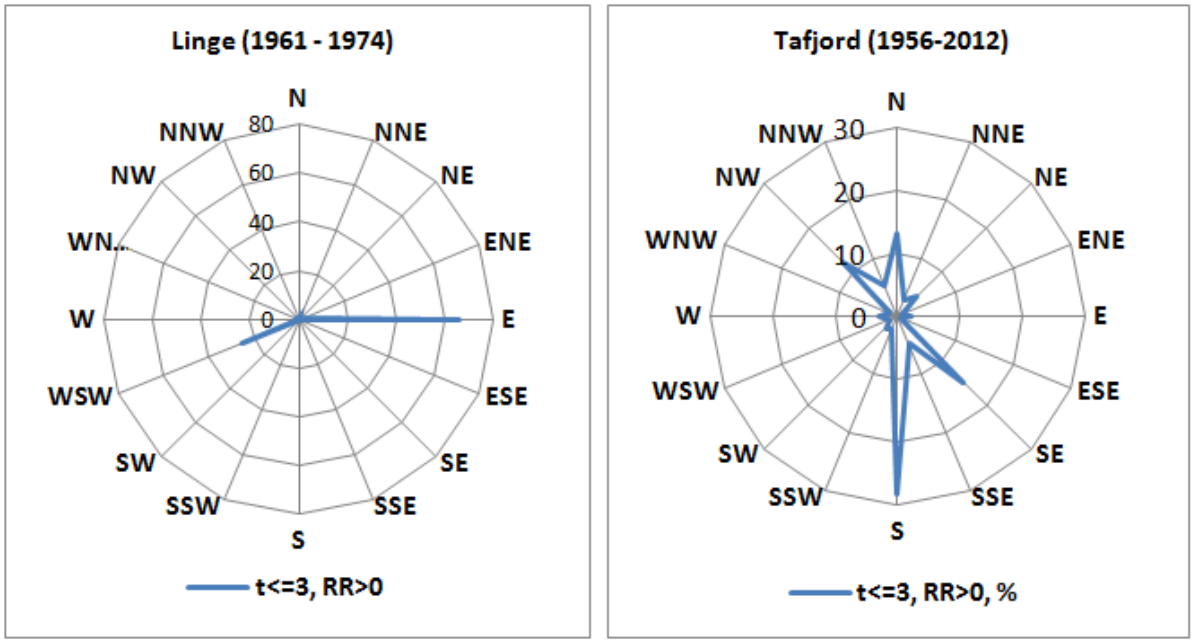

Figure 5-17: Wind distribution during snow fall for Linge (1961-1974) and Tafjord (1956-2012). The wind distribution coincides with local topographic conditions. Data from eklima.no (2013).

5.5.3 Precipitation and rock falls

Occurrence of rock falls, rock avalanches and rock slides do not show the same strong correlation with meteorological conditions as debris flows and snow avalanches (Jaedicke et al., 2008). Bjerrum and Jørstad (1968) stated that the majority of the investigated rock falls in Norway occurred during spring and autumn, seasons where the temperature often fluctuates around 0 °C. Their results are summarized in Figure 5-18, which shows the occurrence of rock falls as a function of season and altitude. Most of the investigated rock falls above 100 m.a.s.l. occurs within the period where temperature is expected to fluctuate around 0 °C. Sandersen et al. (1997) investigated in detail the relationship between 27 rock falls and possible weather influence. It was discovered that the most significant factor was weekly precipitation prior to the rock fall, closely followed by temperature alterations across the freezing point. Six of the investigated rock falls did not show any distinct correlation with meteorological factors. Rock fall and rock slide hazards are, therefore, thought to increase during periods of high water supply or temperature fluctuations around the freezing point. Additional processes such as weathering also play an important part in rock fall, rock avalanche and rock slide release, making them hard to predict.

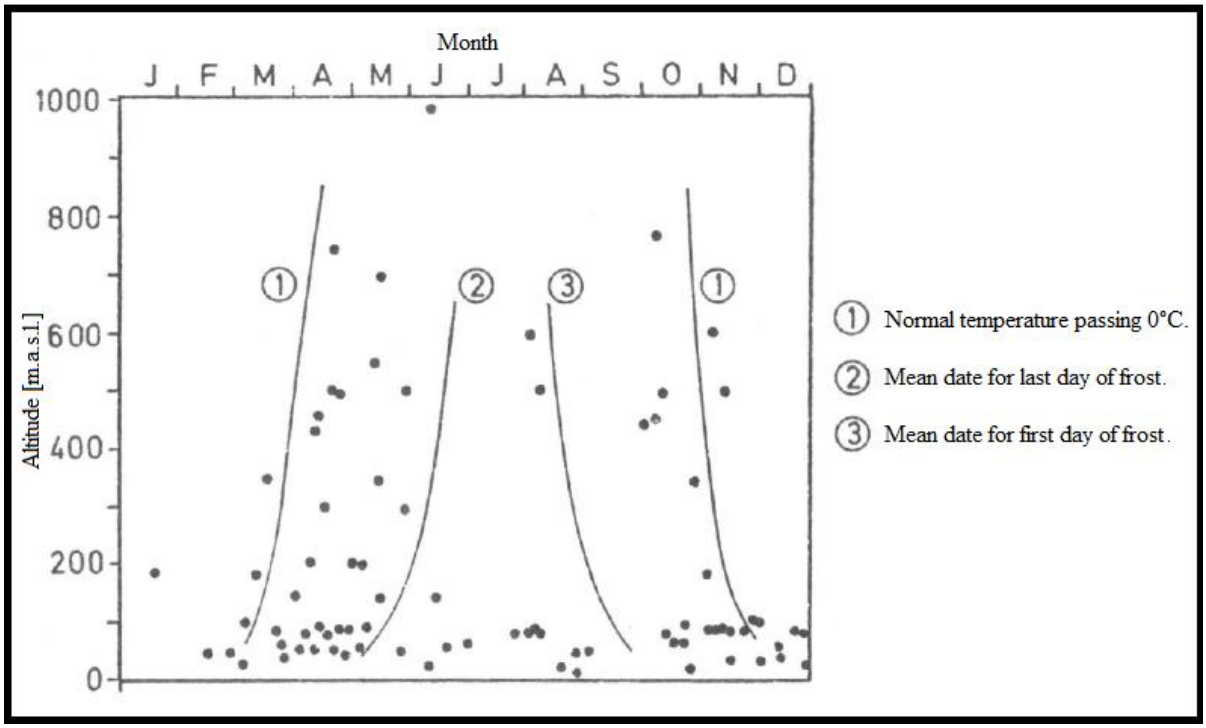

Figure 5-18: Rock falls as a function of season and altitude. The plot shows a strong correlation between rock fall occurrence and temperature alterations around 0°C (Bjerrum and Jørstad, 1968).

The rock avalanche in *Kvitfjellet* happened during heavy rain in November 1996. The precipitation rates the last three days before the event showed 17.3, 32.1 and 17.2 mm of precipitation. Precipitation the last month before this was low. The temperature recorded in *Tafjord* was -0.2 °C on the day of the event, but positive the previous month and the day after. This is not enough information to conclude about something, but high water supply can have been a contributing factor. Another rock fall of known date in the western valley side (February 18th 1998) shows no correlation with temperature alterations around the freezing point or precipitation the last 30 days.

6 Rock falls and rock avalanches

6.1 Field work

An important observation in *Norddal* is the massive talus slope along the eastern valley side. Reaching from sea level to more than 300 m.a.s.l. in places, it is a distinct sign of previous and present rock fall activity. The same applies to the fresh scar of the 1996 *Kvitfjellet* rock avalanche. The rock face is generally steeper than 45° and consists of gneisses with some intrusions of ultramafic rocks, as explained in Chapter 4.3.1. The lower portion of the mountain side contains many examples of loose rock resting on slope and vegetation or rocks with several free faces which some day will fall downward (Figure 6-1). Overhanging rock outcrops are visible several places, especially in the northern area near *Kvitfjellet* and *Raudnakkene*, leading to frequent rock falls. According to local inhabitants, large ice-fields typically build up during winter which may pose a threat when they fall. This is indicative of a present water pressure year round which may increase the rate of weathering and rock fall due to freeze-thaw interactions. During spring, 2-3 streams mainly fed by snowmelt are visible along the eastern mountain side.

The *Kvitfjellet* mountain is a cliff which holds a large and distinct wedge formation, see Figure 6-2A. No detailed measurements were done, but distinct signs of flowing water were observed along the fractures. This may have negative implications due to high water pressure and freeze-thaw interactions. The lower part of the wedge has fallen away leaving a free face. Investigations by Oppikofer et al. (2012) reveal that the face is a source for frequent rock falls, mostly small ones less than 1 m^3, but volumes up to 65 m^3 where measured by terrestrial laser scanning.

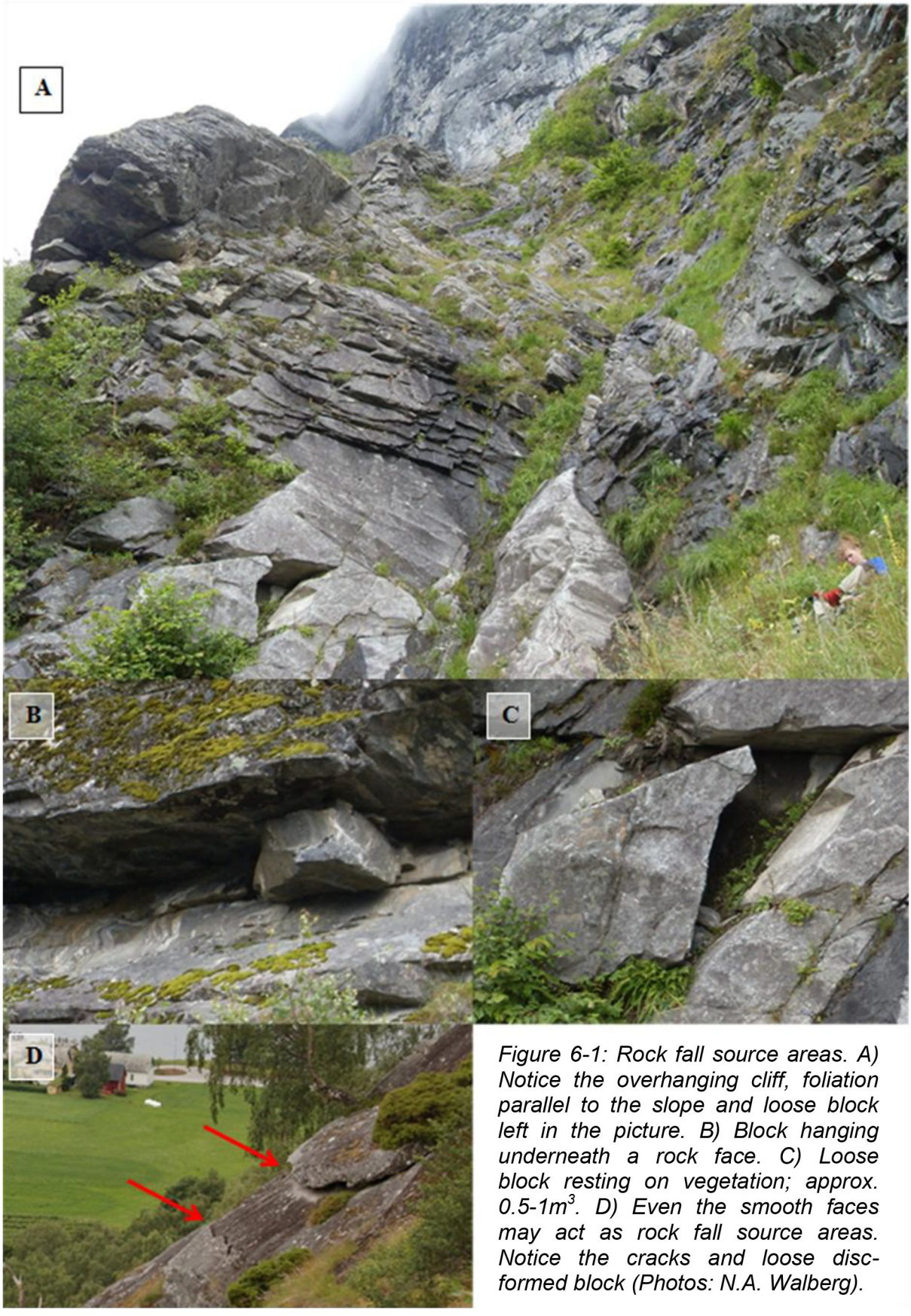

Figure 6-1: Rock fall source areas. A) Notice the overhanging cliff, foliation parallel to the slope and loose block left in the picture. B) Block hanging underneath a rock face. C) Loose block resting on vegetation; approx. 0.5-1m^3. D) Even the smooth faces may act as rock fall source areas. Notice the cracks and loose disc-formed block (Photos: N.A. Walberg).

Figure 6-2: A) Picture of Kvitfjellet. Several rock falls and rock avalanches have occurred from this face. B) Lower part of the steep mountain side shows clear evidence of distinct foliations and bedding planes. C) Loose rocks probably caused by frost shattering in the lower part of the mountain side where I am standing in the next picture. D) Even the lower areas of the mountain side are very steep and hard to access (Photos: A-C: N.A. Walberg, D: M. Lund)

The talus slope exhibits a large variety of block sizes and vegetation cover. Generally, there is a distinct sorting, meaning the rock size increases from the top and downwards. This is typical for talus slopes formed by rock falls. The upper portion consists of sand and pebbles, while in one location there is a distinct lithological change resulting from weathering of the ultramafic rock dunite. The fine-grained upper portions are mostly covered by grassy vegetation. Several scars can be observed where blocks have bounced to the ground, see Figure6-3B. As the terrain descends, the grain size increases dramatically and sight of blocks measuring 1 m^3 are not unusual in the middle of the slope. The vegetation varies widely within the talus. Some areas consist of absolutely no vegetation and some areas are covered by dense forest. Old birches are spread throughout while some areas, especially in the north, are covered by dense vegetation of mosses and young deciduous trees, especially in the lower regions. Remarkable are some vegetation free polygons within otherwise dense vegetation. Examples of such vegetation free polygons can be seen in Figure 6-3 (A, E and F). Also relatively young birch forests with grass cover are present at some locations in the upper areas. The reason for the great variation in vegetation is not determined, but it is possibly due to the rate of rock fall activity, presence of water supply and local climatic conditions. Commonly, the entire talus slope shows clear evidence of creep movement, in some areas more than others.

The lower areas of the talus show fewer signs of recent rock fall depositions, if we omit the deposits from the 1996 *Kvitfjellet* rock avalanche. The rocks are generally large and often partly covered by soil. The vegetation cover is much denser including both mosses and deciduous forest. Some areas are affected by grazing. Near the church, the talus spreads out into a large fan, probably formed by rock falls coming down the above laying ravine and by redistribution from snow avalanches and debris flows down the same ravine. This will be discussed in later sections. Along the entire mountain side individual rock fall blocks are found deposited outside the talus. These are often large, and give an indication of long rock fall run outs valuable for the hazard zone determination. Several boulders have also been removed during clearing of agricultural land. The western valley side and *Daurmålsfjellet* also contain talus formations, but they are not as evident as along the eastern side.

Figure 6-3: A) Large vegetation free area on the talus, picture taken upwards. B) Trace after rock fall on the upper part of the talus. C) Rocks which have stopped toward a three. D) Rock fall scar on a three. E, F) Fresh rock fall deposits (Photos: N. A. Walberg).

6.2 Rock fall modeling

6.2.1 α,β-model for rock falls

The α-β-model for rock falls determines the run out of a rock fall by an angle of propagation from the release area. The model is adapted from the α-β-model for snow avalanches (Lied and Bakkehøi, 1980; Bakkehøi et al., 1983) and follows the same main principles. A release point (A) is determined at the top of the possible rock fall source area. Point B is determined where the slope angle is 23°, and an angle β is determined. Then the run out is determined by the angle α, where the relationship with β is revealed by analysis of 122 rock falls with known release and run out points (U. Domaas (NGI) in Derron, 2010). Higher α-values refer to shorter propagation lengths. The relationship is

$$\alpha = 0.77\beta + 3.9° \qquad \text{Equation 4}$$

The relationship is a linear regression with standard deviation of 2.16° and a coefficient of determination = 0.80.

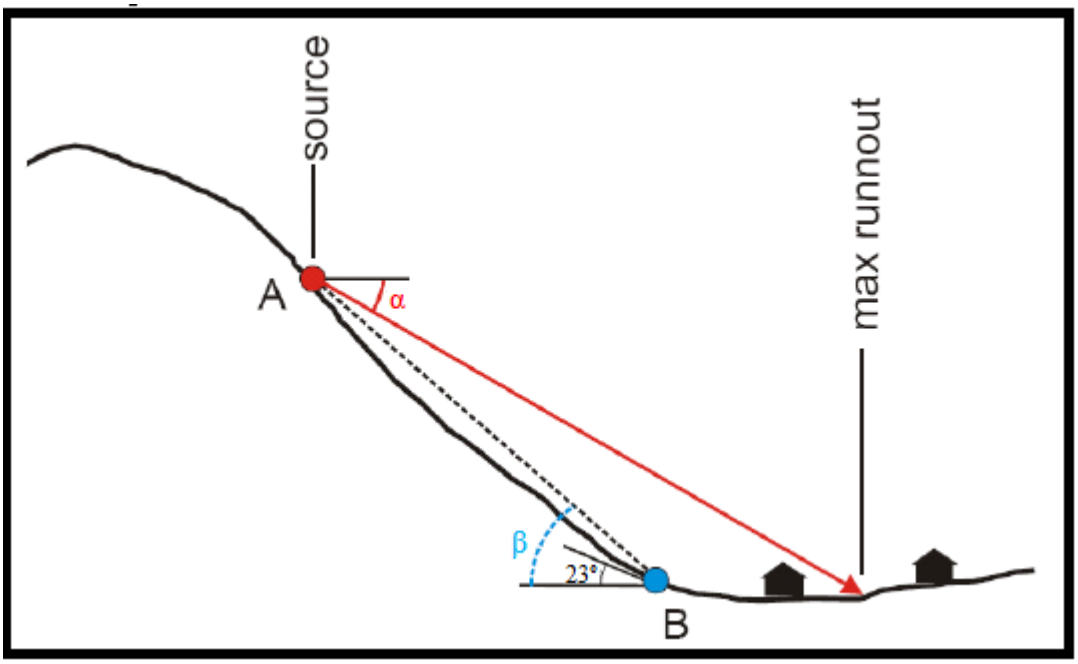

Figure 6-4: Principles of the α-β-model adapted to rock falls (Derron, 2010).

The α-β-model is applied along 7 transects in Norddal, four in the eastern valley side, one toward the settlement beneath *Daurmålsfjelle*t, and the last two near the developed talus deposits in the western valley side above *Rellingen*. These areas were chosen as locations with the most relevant rock fall paths regarding settlement.

The release point was selected at the upper end of the transect, and the 23°-point was determined from a slope map of the area as the point were the mean slope of the terrain drops under 23°. In the case of tortuous topography, a long distance could be traveled before reaching a location with a mean slope ≤ 23°. In such cases, β-angles could be very low, and the associated α-angle are, therefore, limited to a minimum of 30°, as in the rock fall susceptibility maps determined for Norway (Derron, 2010). This problem occurred for transect #6, and a run out determined from α = 30° was found (424 m). The final run out was determined from Equation 4 with the results found in Table 6-1 and visualized in Figure 6-5. The calculated run out is generally longer than observed rock fall blocks.

Table 6-1: Results from α-β-method calculations along the 7 transects in Norddal. The values for slopes 6 are invalid due to low β-angles.

α,β-method rock falls	Slope 1	Slope 2	Slope 3	Slope 4	Slope 5	Slope 6	Slope 7
Height top [m.a.s.l.]	555	560	600	440	749	502	358
Height 23°-point [m.a.s.l.]	20	79	146	150	190	257	55
Length 23°-point - top [m]	543	430	565	321	580	400	370
β-top [°]	44,6	48,2	38,8	42,1	43,9	31,5	39,3
α-top [°]	38,2	41,0	33,8	36,3	37,7	~~28,1~~	34,2
α-top + 1 std [°]	40,4	43,2	35,9	38,5	39,9	~~30,3~~	36,3
α-top - 1 std [°]	36,1	38,9	31,6	34,2	35,6	~~26,0~~	32,0
Length α-top [m]	679	553	679	395	722	~~458~~	446
Length α top + 1 std [m]	629	513	627	365	669	~~419~~	412
Length α top - 1 std [m]	735	597	738	427	781	~~503~~	485

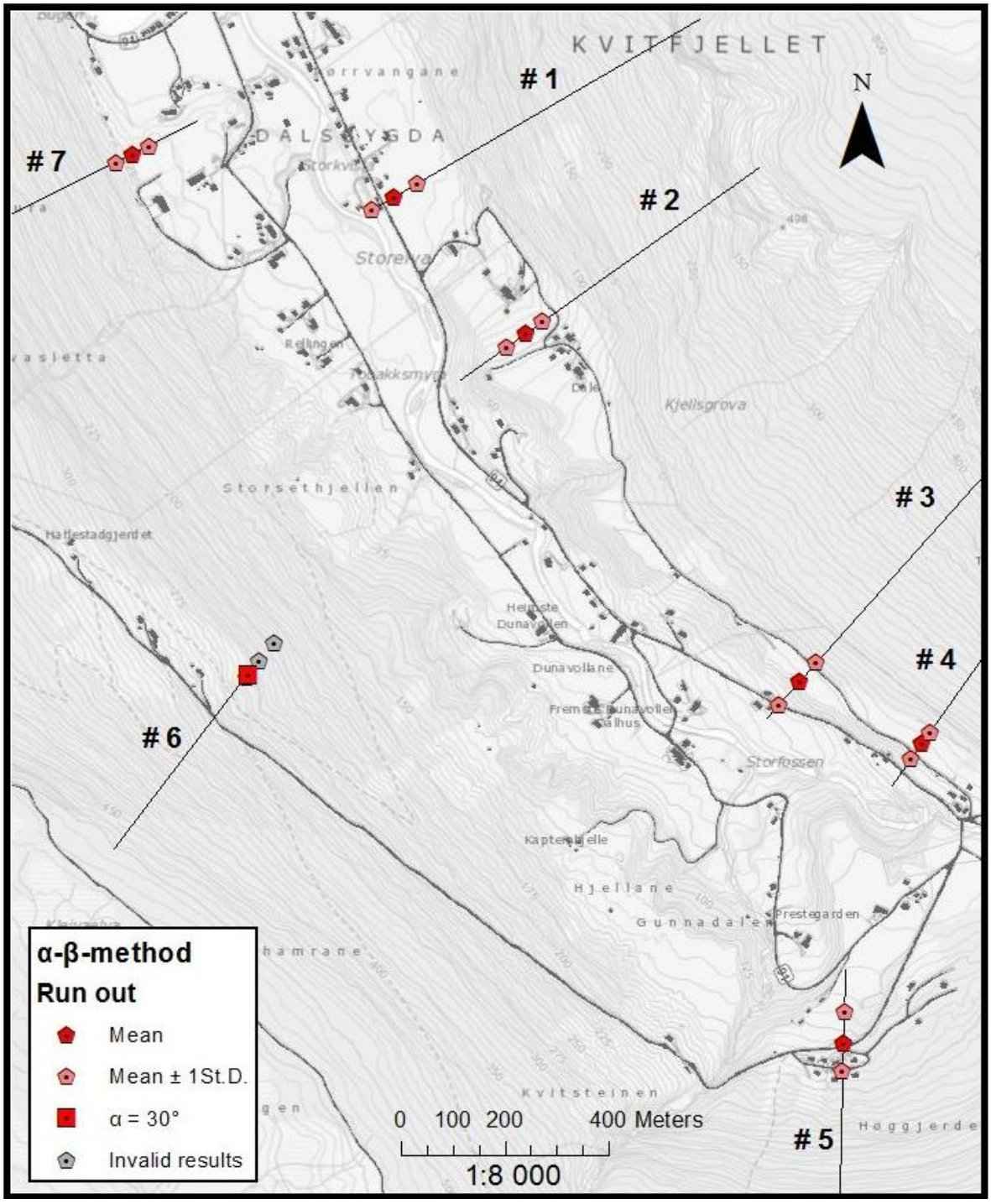

Figure 6-5: The results from α-β-model calculations in Norddal, showing the mean and mean ± one standard deviation. The results for transect #6 gave α-values outside the defined range (α>30°), and only the run out from α = 30° is shown (square). Some of the modeled transects start outside the picture frame.

6.2.2 RocFall

RocFall is a statistical analysis program developed as a tool for probabilistic analysis, design of remedial measures and prediction of rock falls (Stevens, 1998). Today, it is a commercial product provided by RocScience (www.rocscience.com) who develops software tools for soil and rock civil engineering. The version used is RocFall 4.0. RocFall is a lumped mass model, meaning that the mass of each rock is concentrated in a small circle. This means that shape and size adjustments must be accounted for by other parameters. Important parameters in RocFall are angular velocity, coefficients of restitution, friction angle and slope roughness.

The RocFall model is assigned for the same slope transects as the α-β-model. RocFall analysis consist of three parts; definition of the slope, definition and assignment of slope material properties for each slope segment, and definition of the rock fall source positions and block properties (RocScience, 2002).

The slopes were defined by height values extracted from the digital elevation model every 30^{th} horizontal meter. The final slope, therefore, consists of several sections of 30 m length with varying steepness. Each slope segment is assigned as a material with the associated parameter values. Several default materials are predefined in the program, e.g. talus, bedrock and soil. Several values for friction angle and coefficients for normal and tangential restitution were tested to fit with local observations in *Norddal*, but pre-defined values were found to be the most suitable. These are presented in Table 6-2.

Source areas are determined as two point seeders in the steep upper sequence(s) of the slope. The mass is determined from field observations of large rock fall deposited blocks, where volume is calculated from the measured length, width and height of the blocks. An initial mass of 10 000 kg with a standard deviation of 1500 kg is used for all the seeders. Angular velocity is taken into account in the calculations, and the initial horizontal, vertical and angular velocity is set as zero. Density is 2700 kg m^{-3} and 1000 calculations are performed for each slope.

RocFall offers several different calculation settings. One of them is scaling of the coefficient of normal restitution by velocity, which is activated during the calculations. This choice is available because then the coefficient of normal restitution is represented by 'a transition

from nearly elastic conditions at low velocities to highly inelastic conditions caused by increased fracturing of the rock and cratering of the slope surface at higher impact velocities' (Pfeiffer and Bowen (1989) as stated in RocScience (2003)). This implies that the restitution coefficient takes the velocity into account. A standard variation of 2° is defined for the slope surface comprising talus, taking local surface variations into account, since the talus surface is relatively rough due to large variations in block size. A standard deviation of 1° for roughness is also applied for the areas defined as talus with vegetation in transect #5.

The friction angle suggests that every rock tossed on a slope segment steeper than the friction angle continues to move downward. In other words, all of the rocks continue to the bottom of the talus in transect #1 and #2, since the talus generally is very steep, while the deposited blocks are more evenly distributed along the other transects.

Table 6-2: Default parameters applied to the different slope segments during RocFall calculations.

Material	Coefficient of normal restitution		Coefficient of tangential restitution		Friction angle		Roughness	
	Mean	St.d.	Mean	St.d.	Mean	St.d.	Mean	St.d.
Bedrock outcrop	0.35	0.04	0.85	0.04	30	2	angle of segment	0
Clean hard bedrock	0.53	0.04	0.99	0.04	30	2	angle of segment	0
Soil with vegetation	0.3	0.04	0.8	0.04	30	2	angle of segment	0
Talus cover	0.32	0.04	0.82	0.04	30	2	angle of segment	2
Talus with vegetation	0.32	0.04	0.8	0.04	30	2	angle of segment	0*

* indicates that a standard deviation of 1 was used during the calculations of transect #5.

The RocFall simulation results correlate well with the developed talus and observations of blocks outside the talus along the eastern valley side. The calculated run out lengths can be found in Table 6-3 and are visualized in Figure 6-7. Figure 6-6 shows the calculation results for transect #2. The blocks tend to follow the topography closely, indicated by the bounce height envelope (C), and the energy generally decreases downward as the rocks loose energy from interactions with the ground (D). The blocks stop at the boarder of the talus where the slope decreases rapidly and where similar sized blocks are observed (B). The results are believed to represent large rock falls in a realistic way.

The modeled run out beneath *Daurmålsfjellet*, transect #5, generally stops in the middle between the source area and the settlement. Some rocks are modeled with a long run out, but they still deposit 130 m from the settlement. The area shows little rock fall activity from remote investigations that are consistent with the appearance of dense forest cover. Transect #6 and #7 along the western valley side both show longer modeled run out than has been observed for the talus. Results from transect #6 generally reveal low values for kinetic energy and bouncing height, while results from transect #7 show high energy values down to the valley floor. The inclination in this area is near the friction angle, and minor changes in roughness/friction angle cause the blocks to deposit higher up in the valley side.

Table 6-3: Horizontal location of end-points determined from RocFall simulations.

Horizontal location of end-points [m]					
	Minimum	**Maximum**	**Median**	**Mean**	**St.d.**
Transect 1	479.5	555	544.9	544.2	8.9
Transect 2	401.7	459.4	432.1	432.9	8.2
Transect 3	398.5	567.8	509.9	507.6	20.2
Transect 4	228.9	356.6	284.2	291.9	21.3
Transect 5	156.7	514.5	332	312.8	45.7
Transect 6	48.3	337.4	247.2	226.9	43.8
Transect 7	391.6	483.8	459.4	457.9	9.4

Figure 6-6 (on the next page): RocFall simulation results for transect #2. A) Slope profile for transect #2 with the applied soil type marked in vertical sections. Two point seeders are marked as an x on the slope by the arrows, and the rock fall paths are visible in the upper part of the section. Downward to the rock fall paths match the slope. B) Rock fall run out represented by horizontal location of rock endpoints. C) Bounce height envelope for the rock fall blocks representing the height above the slope. The values are generally low indicating small jumps and rolling. D) Total kinetic energy along the slope with a distinct peak as the rocks free fall over the crest in the upper part of the slope.

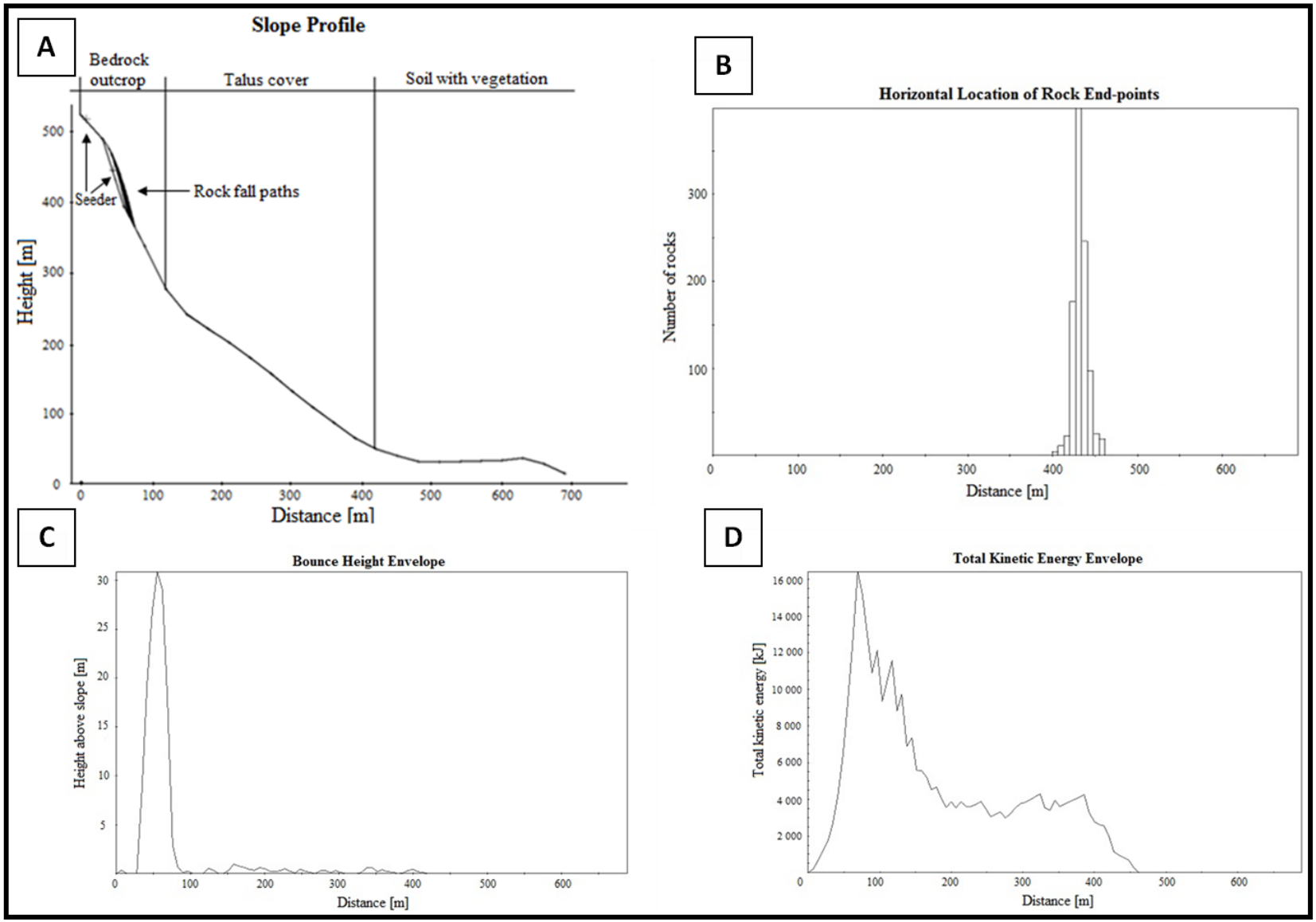
A
Slope Profile
Bedrock outcrop
Talus cover
Soil with vegetation
Seeder
Rock fall paths
Height [m]
Distance [m]
B
Horizontal Location of Rock End-points
Number of rocks
Distance [m]
C
Bounce Height Envelope
Height above slope [m]
Distance [m]
D
Total Kinetic Energy Envelope
Total kinetic energy [kJ]
Distance [m]

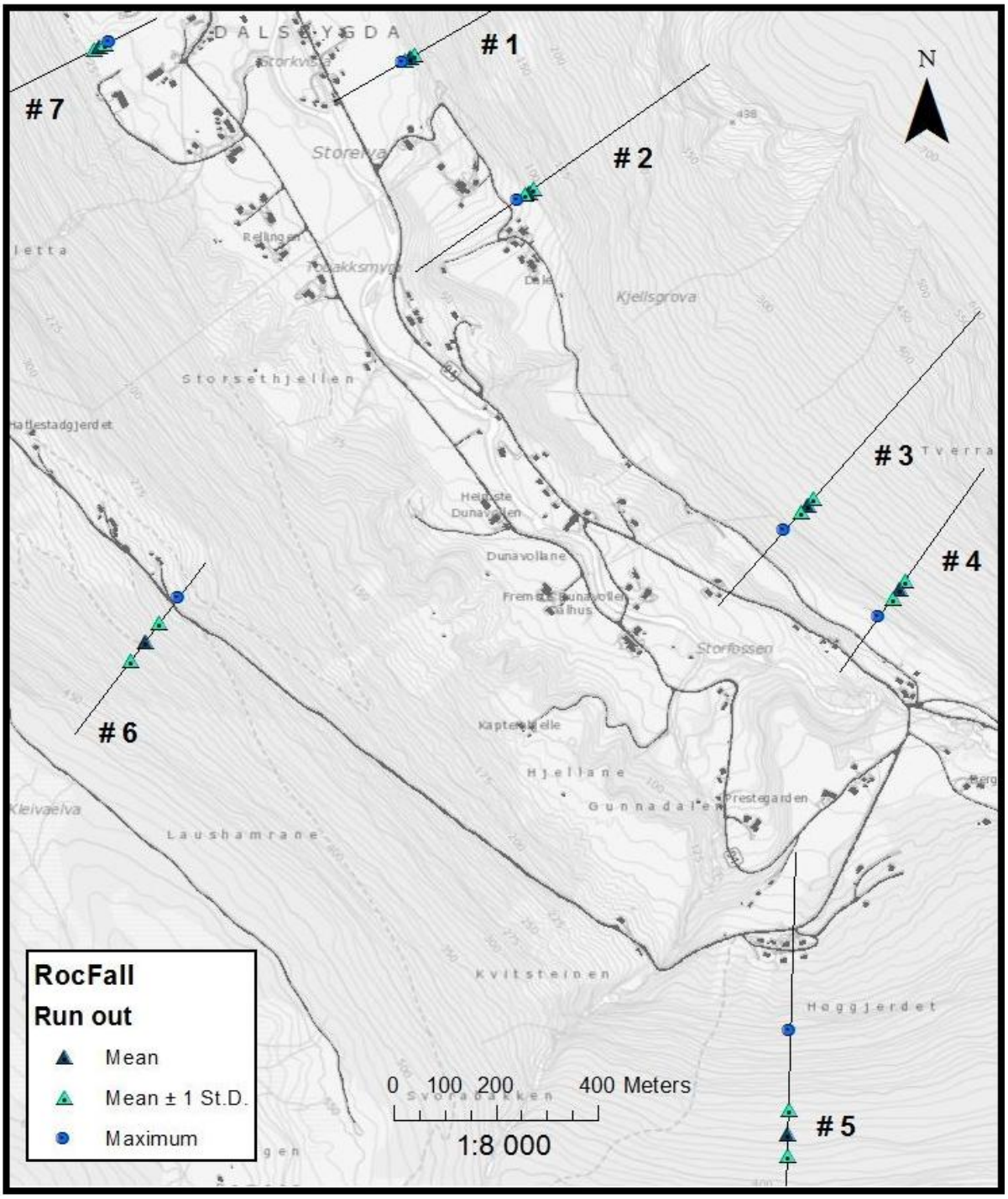

Figure 6-7: RocFall model results showing the mean and maximum run out for modeled rock falls. Notice how the different topographic conditions cause different spreading in transect #1 and #2 versus #5 and #6. Note that some of the modeled transects start outside the picture frame.

6.2.3 Rockyfor3D

Rockyfor3D is a three dimensional simulation program for rock falls which calculates trajectories of individually falling single rocks. The model is a 'probabilistic process-based rock fall trajectory model' which means it incorporates physically based deterministic algorithms with stochastic approaches and can be used for both single slope and regional scale investigations (Dorren, 2012). The trajectories are calculated by a series of parabolic free fall and rebounds from the ground (Dorren, 2012). Generally speaking, the model consists of three modules (Figure 6-8) where the first one is the calculation of the trajectories based on a digital elevation model (DEM). During each step of the model, the rocks fall direction can be toward one of the cells with a lower elevation value; hence, it moves down slope. In the second module, the energy loss from a possible collision with a tree is calculated and a new energy content and position are calculated. The third step processes the velocity of the rock after a rebound on the ground, an action which causes energy to dissipate due to the surface roughness (Stoffel et al., 2006). Sliding is not modeled and rolling corresponds to successive small-scale free falls and rebounds. Since the model also takes impacts against trees into account (Dorren, 2012), it is widely used in research on the protective properties of forest against rock falls.

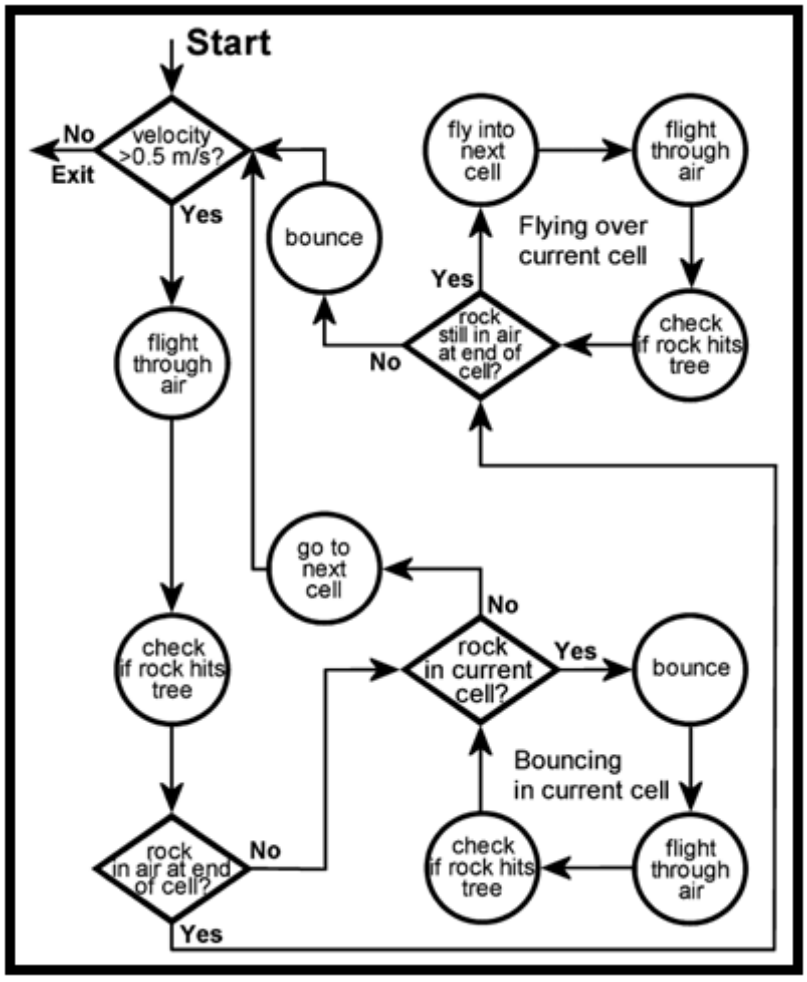

Figure 6-8: Flow chart of the Rockyfor3D simulation of rock falls (Dorren et al., 2004).

The input required is thoroughly explained in the user manual (Dorren, 2012) and can be developed using the software of QGIS and SAGAGIS. During this project, the program ArcMap was utilized, a part of the ESRI ArcGIS system. The input consists of three main components in terms of 10 raster data sets (ascii files) including a digital elevation model (DEM), information about the source area (block shape, density and block size in 3 dimensions which define the volume) and information about the surface conditions (soil type and surface roughness). In addition information about forest conditions may be added.

Considerable effort was expended in the determination of input parameters as both geographical extent and numerical values had to be defined. Rockyfor3D demands extensive input regarding the area from the user, and it is, therefore, important to know how the different input affects the model. Sensitivity studies were performed regarding resolution, volume, shape and density of rock fall blocks, forest cover, roughness values and the number of simulations that were performed for each source cell. The sensitivity studies revealed large effects of small changes in different parameters that emphasize the importance of being critical to modeled results. A short review of the sensitivity studies can be found in the discussion.

The following describes the input parameters used in the final calculation. The calculation is performed with a resolution of 5x5 m where the digital elevation model is re-sampled from a 1x1 m laser scan using the cubic convolution methodology. This spatial resolution is within the recommended values between 2x2 and 10x10 m (Dorren and Heuvelink, 2004). Ground parameters are determined for the entire area: the mountain side, the talus and the valley floor. Examples of the geographic distribution of source areas, roughness values and soil type can be found in Figure 6-10. Source areas are defined as all areas steeper than 45° which consists of bedrock (Figure 6-10A). The source areas are given the density 2700 kg m^{-3}, a volume of 3.9 m^3 distributed in a rectangular block with the respective height, width and length of 1.3, 1.5 and 2.0 m. Forest is not taken into account as it showed little mitigating effect against such large rock falls.

Soil type is the parameter which represents the elasticity of the underground with the area being divided into polygons representing water, bedrock, scree and soil cover (Figure 6-10C). Surface roughness, representing obstacles lying in the slope, are represented by three ascii-files which respectively hold the height of the obstacles in 70, 20 and 10 % of the areas

extent (Figure 6-10B). These values were obtained in the field looking in the downward direction, see Figure 6-9. The observations are evaluated together with the proposals for values for different surface types, and homogenous areas are drawn based on these observations, available maps and aerial photos.

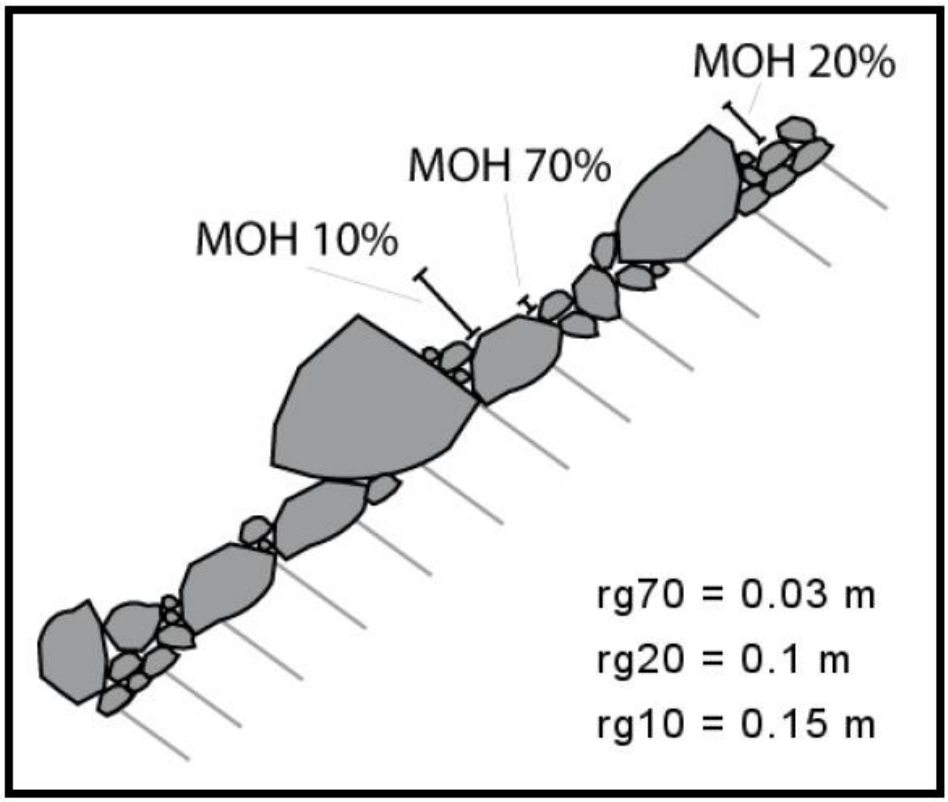

Figure 6-9: Sketch of the mean obstacle heights (MOH) representative for 70%, 20% and 10% of the surface along the slope, representing the RG-values for an area (Dorren, 2012).

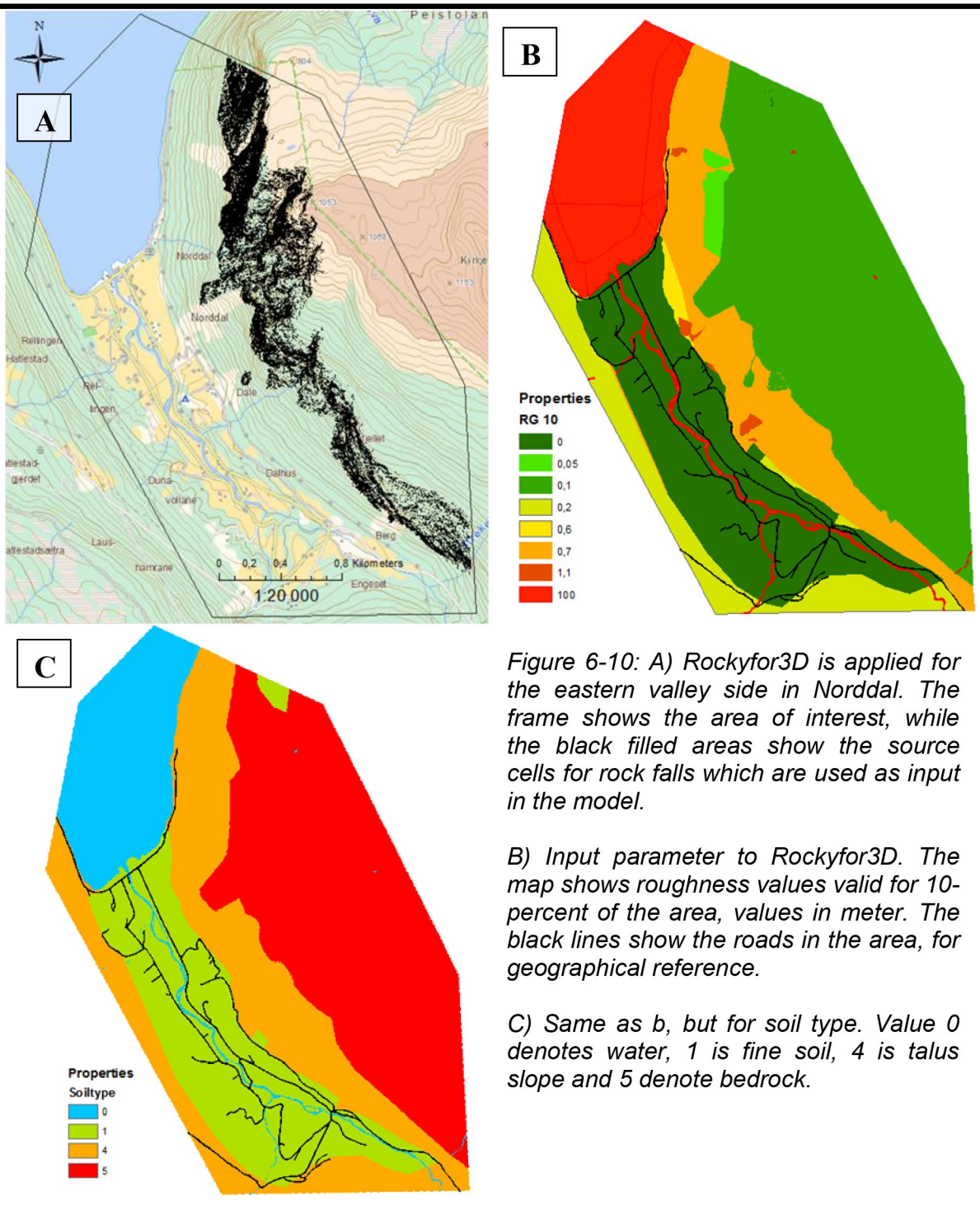

Figure 6-10: A) Rockyfor3D is applied for the eastern valley side in Norddal. The frame shows the area of interest, while the black filled areas show the source cells for rock falls which are used as input in the model.

B) Input parameter to Rockyfor3D. The map shows roughness values valid for 10-percent of the area, values in meter. The black lines show the roads in the area, for geographical reference.

C) Same as b, but for soil type. Value 0 denotes water, 1 is fine soil, 4 is talus slope and 5 denote bedrock.

Results

Rockyfor3D offers a variety of different results in form of raster files. Figure 6-11 shows the mean of the maximum kinetic energy values of all simulated blocks in a given cell. This includes both rotational and translational kinetic energy (Dorren, 2012) and shows that the modeled kinetic energy several places near settlements are more than 30 and 300 kJ, which is used within landslide hazard mapping in Switzerland (Jaboyedoff et al., 2005). The most important result for hazard mapping is the one showing the number of blocks with deposits in each cell. This is shown in Figure 6-12A together with the absolute maximum velocity measured in each cell (B), mean of the maximum passing height of all blocks passed through a cell (C), and the reach probability; P(R) in each cell (D). The latter map shows whether it is probable (high values) or improbable (low values) that a rock arrives into a given cell. This is calculated using the equation

$$P(R) = \frac{Nr\ passages\ x\ 100}{Nr\ simualtions\ from\ each\ source\ cell\ x\ Nr\ sourc\ cells} \qquad \textit{Equation 5}$$

If the calculated energy lines from Rockyfor3D are compared with commonly used ones, it may be observed that the run out calculated from Rockyfor3D generally lay within earlier suggested values. The Rockyfor3D calculations generally reveal α-values higher than 33° with some long run outs having α-values between 29 and 33°.

The results generally show that the settlement near the talus slope lay within the reach of rock falls according to the model and the input used, but most of the blocks will deposit within the talus.

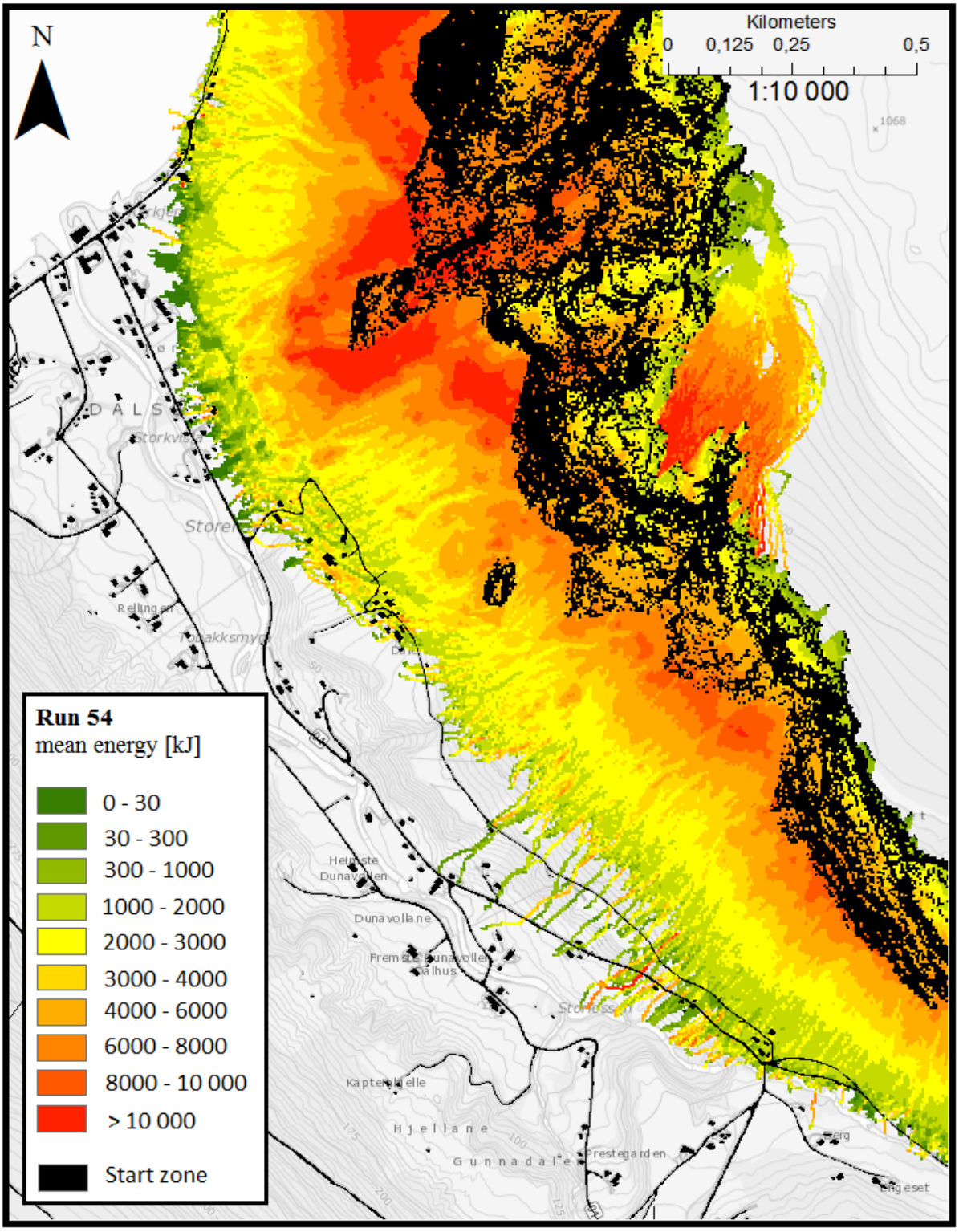

Figure 6-11: Results from Rockyfor3D run 54 showing the mean of the maximum kinetic energy (translational + rotational) of all simulated blocks in a given cell. The spatial resolution is 5x5 m.

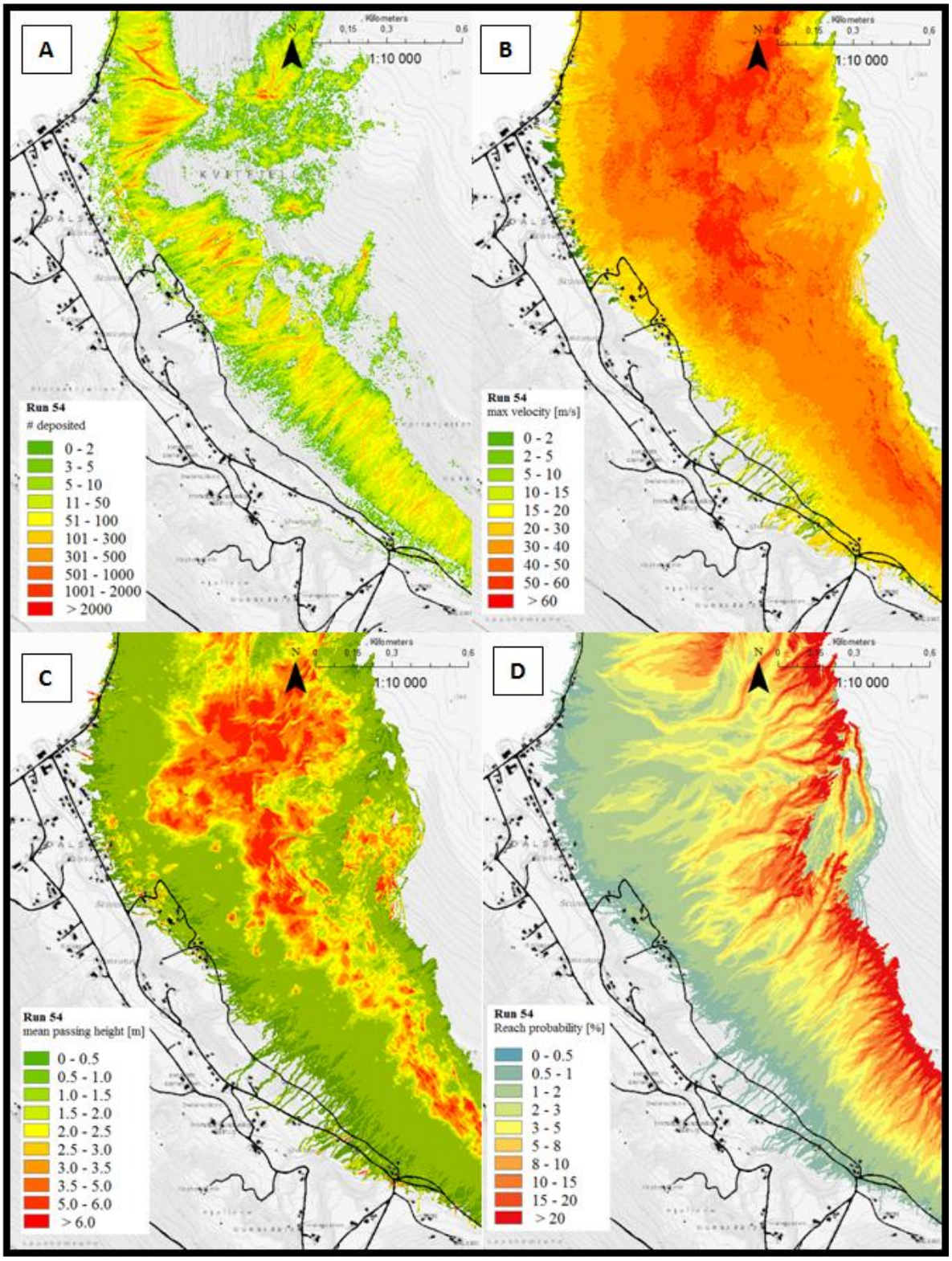

Figure 6-12: Results from Rockyfor3D. A) Number of blocks deposited in each cell. B) Maximum measured velocity in each cell. C) Mean passing height of the blocks in each cell. D) Reach probability for any given cell.

6.2.4 Comparison of rock fall models

Figure 6-13 shows modeled rock fall run out from the α,β-model, RocFall and Rockyfor3D model. The α,β-model and RocFall results show calculated run out length from the start point in the respective transects, while Rockyfor3D shows number of rock fall blocks deposited in each 5x5 m grid cell.

The most striking feature is the little consistency in the results. The α,β-model is the simplest model based on simple topographic parameters. Its calculated run out is generally the longest, but this could be related to the fact that the α,β-model are based on maximum run out from known events. In some case, the model predicts run out which seems unlikely from field observations (slope #5). RocFall is also calculated along transects but takes the movement, energy and friction into account. The model is very sensitive to friction angle in connection to the slope angle, and the run out, therefore, coincides with the slope and talus formation in steep areas. The results obtained generally seem more comparable with field observations. Rockyfor3D is the most complex model requiring detailed input regarding both source blocks and soil properties, as well as taking detailed topographical conditions into account. The model reveals depositional patterns, where most of the blocks deposit inside the talus, but some areas experience higher rates of rocks deposited outside the talus than others. This is thought to represent how the micro topography influences the rock fall path and, thus, provides valuable information. Rockyfor3D is thought to represent the possible large, single rock falls very well. This is due to the detailed input required, which represent the local conditions. Rockyfor3D has computed tens of thousands of rock fall trajectories which together with the large block size used make an impression of frequent rock falls outside the talus and near the settlement. Field investigations revealed that this does not appear to be the case; therefore, results must be evaluated carefully.

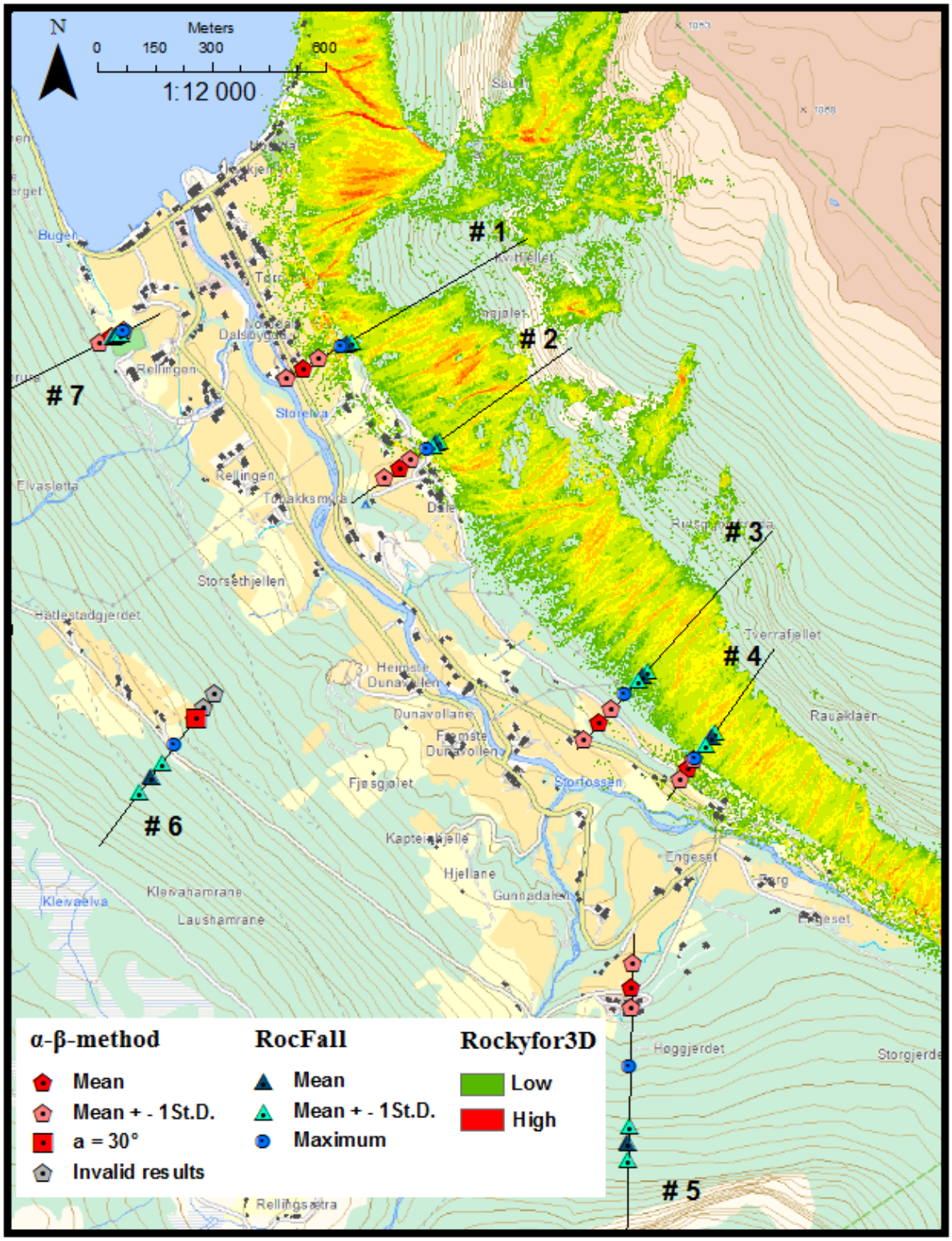

Figure 6-13: Calculated rock fall run out from the α,β-model, RocFall and Rockyfor3D model. The α,β-method and RocFall show calculated run out length from the start point of the respective transects, while Rockyfor3D shows number of rock fall blocks deposited in each 5x5 m grid cell.

7 Debris flows and debris slides

7.1 Quaternary mapping

The detailed work of the Norwegian Geological Survey (NGU) found in Stokke (1983) regarding exploitable materials in the *Norddal* valley gives detailed insight in the Quaternary geology in *Norddal*. Especially the western valley side, which is densely vegetated, is well mapped regarding ravines and depositional fans that give important information regarding determination of debris flow and debris slide hazards in the area. The map in Figure 7-1 shows the geomorphologic features related to mass movements in the area. It is based on the aforementioned work by NGU, a study of aerial photos and personal field observations.

The valley of *Norddal* is covered by large amounts of material from glaciers and melt-water rivers deposited during and after the last glaciations. The moraine material is unevenly distributed between the eastern and western side of the valley, which indicates a westerly direction of the last regional ice movement with most of the moraine material located in the western valley side (Stokke, 1983). The eastern side is almost completely covered by rock fall deposits, and the central part consists of fluvial and glacio-fluvial material. Four big glacio-fluvial terraces can be found along the sides: (1) *Daleterrassen, (2) Dalsreinane, (3) Herdalsterrassen* and *(4) Nordhjellane*, see Figure 7-1. The terraces are thought to be remnants of a large terrace crossing the valley from *Daleterrassen* to *Løshamrane*, possibly formed during a temporary stop in the glacial retreat or an advance of the ice front (Stokke, 1983). Several terrace pits are also visible. *Daleterrassen, Nordhjellane* and *Herdalsterrassen* have all been investigated regarding resources and are estimated to contain 2.7, 1.4 and 1.3 million m^3 of exploitable material, respectively (Stokke, 1983). The terraces include clay that could cause problems during construction work (Dale, 2012). A sketch of a cross section of the valley can be found in the geology portion of the area description, see Figure 4-6.

The thick continuous moraine material along the western valley side is exposed to constant erosion. This erosion and depositional processes from water, debris flows and slides are visible, partially covering and eroding the glacio-fluvial terraces lying along the valley floor

(Stokke, 1983). Also, the eastern valley side shows signs of present and previous redistribution of material from debris flows.

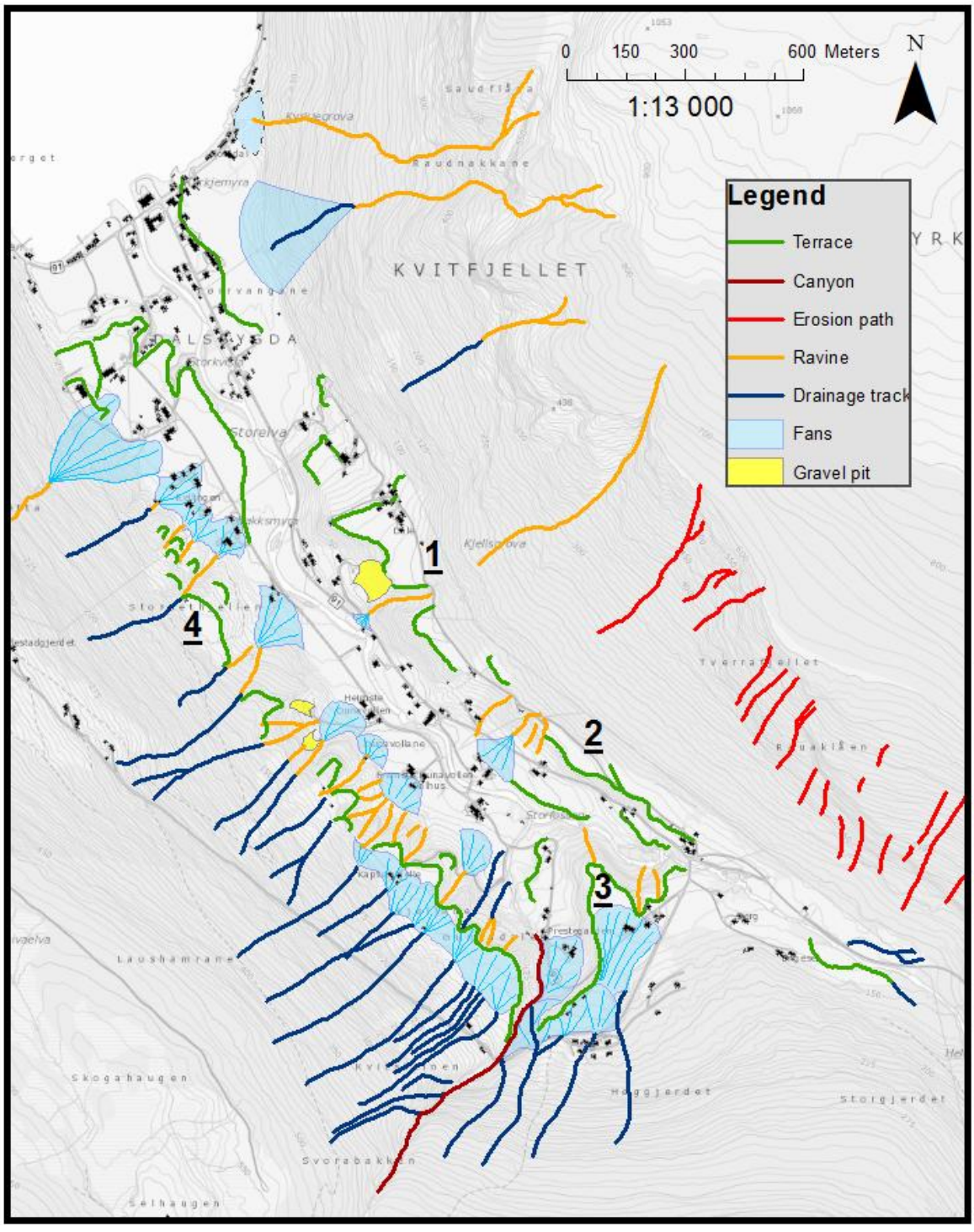

Figure 7-1: Geomorphologic map over Norddal, mainly based on Stokke (1983). Drainage tracks represent features in soil determined from Stokke (1983), while erosion paths are vegetation free tracks mainly on bedrock determined from field work and aerial photos. The numbers determine the names of the main glacio-fluvial terrace remnants, see text for explanation.

7.2 Field work

The western valley is completely covered by moraine material, which in some places is covered by debris flow deposits and, also, rock fall deposits in some minor areas. The valley side holds two major streams: *Dyrdøla*, located in the southern corner, and *Hatlestadelva*, which is located more north and has its origin in the catchment below the mountain *Middagshesten*. In addition, a swamp area below *Middagshesten* provides the entire area with water. Aerial photos show clear drainage from the swamp and down toward the valley side. The high rate of water flow is clearly evident when one walks on the old road, which is now only suitable as a walking path. Water drains almost continuously along the path, and several places show clear evidence of erosion, especially where the road blocks small ravines that act as drainage paths for the water. A number of residents also expressed concern about this situation regarding the old road damming up water, especially during heavy rainfall. Also, very distinct signs of erosion are seen along the road to *Rellingsetra* located at the flat above the valley side just outside the mapped area.

The vegetation cover changes from dense fields of planted spruce, which prevent all sunlight from reaching the ground and, therefore, leaves it completely vegetation free, to forests of young deciduous forest of different kinds. This forest is very dense and, most likely, stabilizes the ground as it takes up water and its roots bind the soil. Branches, dead trees and leaves could also attribute to blocking and damming of culverts and drainage paths, which is especially critical along the old and new road.

Figure 7-2 (A-C) shows an open pit in the glacial-fluvial terrace of *Nordhjellane*. It consists of layered deposits, mostly of sand size, but layers of clay up to 20 cm wide are also present. A distinct layer of unsorted material is present in the upper part between sorted materials. These are probably debris slide deposits which indicate that the moraine cover in the valley side was unstable already during the melting period. This conclusion coincides with Stokke (1983). It could also be till depositions from a temporal advance of the glacier during the retreat. Figure 7-2B also reveals a small slide in a grazing area. Figure 7-2D shows a distinct ravine beneath *Daurmålsfjellet* together with two scars from previous activity (Event # 13 and # 2 in Appendix D).

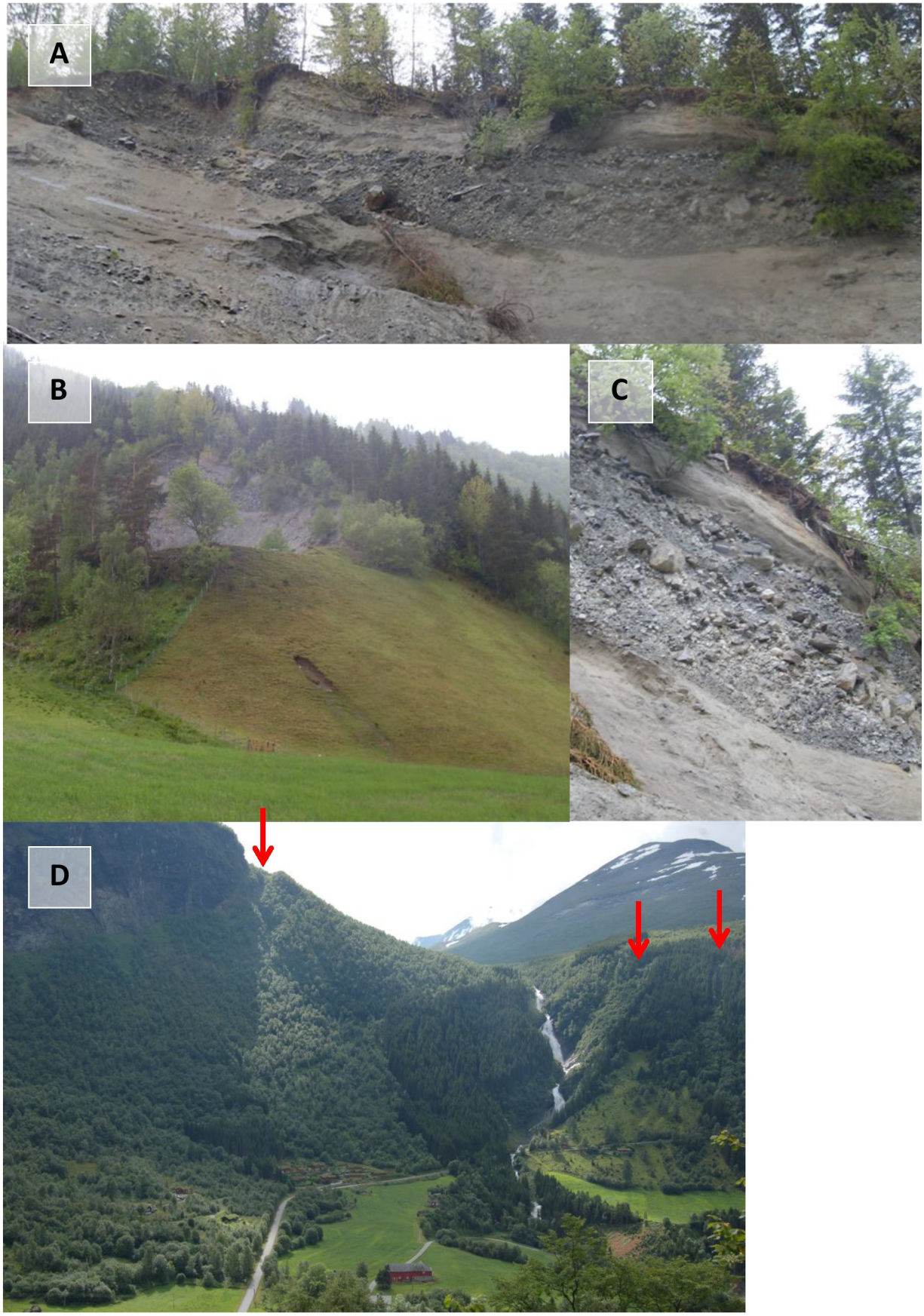
A
B
C
D

Figure 7-2 (previous page): A) Glacio-fluvial deposits in the Nordhjellane terrace. Sorted deposits of sand and clay with evident bedding, interrupted by unsorted material, which is thought to be debris slide deposits. Picture from a gravel pit. B) Small slide in an area which today is used for grazing, a common sight in the area. C) Close up photo of the unsorted layer. No sorting and size range from sand to boulders give an indication of the source; till deposits from the above lying valley side, or moraine deposited from a temporary advance during glacial retreat. D) Overview photo of the south-western part of the valley. Daurmålsfjellet is located in the left and an evident ravine is visible right beneath the top (arrow). Also, scars from two debris slides are visible right in the picture. The first dammed the river (#13 in Appendix D), while the second is thought to be the one from 1975 (#2). The latter started by a small forest road in the upper part of the valley side during heavy rain (Photos: N.A. Walberg).

The eastern valley side also shows evidence of ongoing processes related to debris flows redistributing material on the talus slope. Large amounts of available material are present in the valley side above the settlement, both in ravines (Figure 7-3A, C) and on the planar talus slope. In addition to *Kyrkjegrova*, another large fan is visible by the church indicating that debris flows in this area reach all the way to the valley floor (B). This fan shows clear evidence of how the debris flow path has changed over the years, as several geomorphologic features such as levees from different events are present. The outer part of the fan is cleared and used as agricultural land today. Also, snow- and slush avalanches are thought to redistribute material on the talus slope. Figure 7-3D shows newly deposited levees on the planar slope, which is thought to originate from a slush avalanche when the slope was snow covered, as little signs of erosion are present. Figure 7-4A shows the depositional fan by *Kyrkjegrova*, where mass is removed as a mitigation measure (Anda and Flataukan, 2002). Figure 7-4B shows massive deposits from repeating debris flow and snow avalanche events in a similar ravine 500 m north of *Kyrkjegrova*, outside the mapped area.

Figure 7-3 (next page): A) Large amounts of loose material are present in the ravines in the eastern valley side. These ravines hold seasonal streams during heavy rainfall and snow melt, and probably also debris flows and snow avalanches (Photo: N.A. Walberg). B) Large fan deposits by the church. The fan is built up by several events over a long period after the last glaciations, and the upper parts show signs of recent activity (Photo: Luzia Fischer, NGU). C) Another ravine holding a small stream in the eastern valley side (Photo: M. Lund) D) Fresh deposits of levees which are thought to originate from a small slush avalanche on the talus slope (Photos: N.A. Walberg).


A
1 meter
B
C
D

Figure 7-4: A) The lower part of Kyrkjegrova where deposits have been removed to lead new slides away from the settlement. B) Massive deposits from recurring events of debris flows, rock falls and snow avalanches 350 m north of the outermost settlement (Photos: M. Lund).

7.3 Debris flow susceptibility mapping

In the development of a national debris flow susceptibility map for Norway, *Norddal* is used as one of five test sites used for model calibration. The aim of the survey is to use present available information to determine and model possible debris flow paths and run out lengths on a national scale, so that a susceptibility map covering all areas potentially affected by an event can be determined (Fischer et al., 2012). Preliminary results show that the major challenge is determination of starting zones, while the run out modeled corresponds well with observed events. The challenge in determination of start zones is related to the topographic parameters and hydrological settings necessary for debris flow initiation, as these parameters depend on the geological settings which vary throughout Norway (Fischer et al., 2012). The presented result for *Norddal* in Figure 7-5 is preliminary, as the final calibration of the model and the determination of a final susceptibility map is not performed. The results can, therefore, not be used to determine hazard zones in agreement with the building law of Norway. The preliminary results from Fischer et al. (2012) correlates well with the existing observations from Quaternary geology in *Norddal*, and are used in this project to support the view of *Norddal* as an area which experiences debris flow development that might act as a threat against settlement and infrastructure.

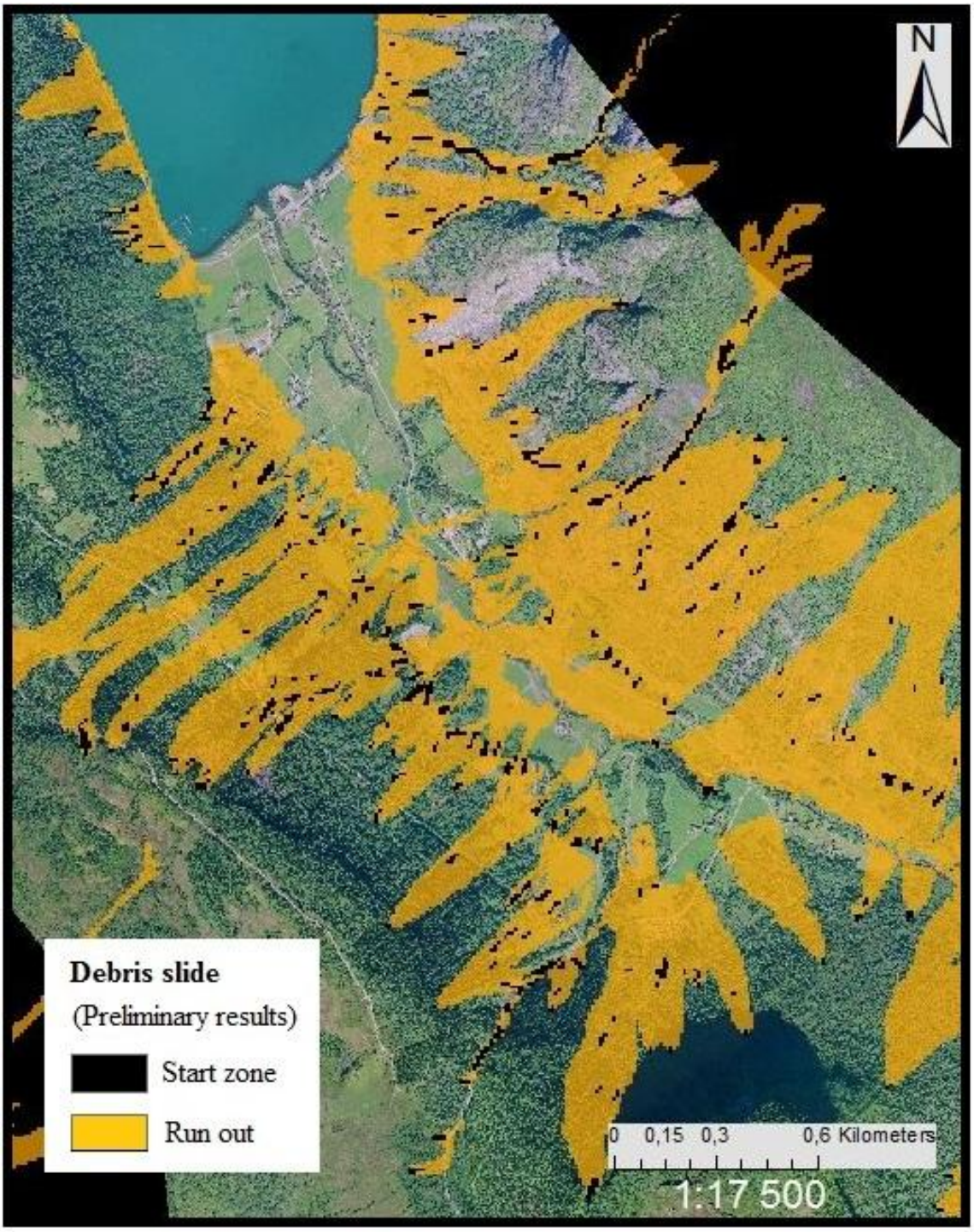

Figure 7-5: Preliminary results from national debris flow susceptibility maps for Norddal. New criteria for start zones will be made, and these results modeled run outs may, therefore, be incorrect. Especially along the eastern valley side are there uncertainties regarding the validity of these preliminary calculations. The results are based on a 25 m resolution digital elevation model (Fischer et al., 2012).

8 Snow avalanches and slush avalanches

8.1 Field work

Large parts of the valley sides surrounding *Norddal* are steep enough for snow avalanches to occur, but large areas are also covered by forest which is thought to prevent snow avalanche release (Breien et al., 2013). The steep areas in the western valley side consist of dense forest of deciduous trees or planted fields of large spruce trees. As long as the vegetation conditions remain as today, meaning no large harvesting operations or other incidents that harm or reduce the forest cover, the forest cover is assumed to prevent avalanche occurrences in this valley side. The same applies to the southern portion beneath *Daurmålsfjellet*, where the areas steeper than 30° are either covered by forest or so steep (>60°) that snow will slide down little by little as it deposits.

The eastern valley side consists of large areas on the talus steep enough for snow avalanches to occur. A picture taken from the opposite side of the valley, where some possible release areas are sketched, can be found in Figure 8-1. The talus is only partly covered by vegetation, and snow avalanches in this area can, therefore, not be excluded. Figure 8-2D shows an example of a number of trees which are bent and broken from a small avalanche within the talus. The side holds several ravines, e.g. *Kyrkjegrova,* which do experience snow- and slush avalanches as well as other mass movement processes. Figure 8-2A, B and C show, respectively, the upper track, a close-up of the transition zone from bedrock to the upper part of the talus, and the channeled path down slope on the talus. Deposits from a small snow- or slush avalanche were observed in the lower part of the ravine during the first field trip. Above the steep valley side, which is not visible from the valley floor, the terrain gently rises up toward *Kyrkjefjellet*, see Figure 8-1. The last area toward the top is vegetation free and between 30-45° which can act as a release area for snow avalanches. The area below consists of low and sparse vegetation that might be covered by snow during winter. A snow avalanche release from *Kyrkjefjellet* might reach the valley floor, which may have occurred in the early 1980's, see Chapter 8.2.3 regarding recreation of an avalanche near *Berg*.

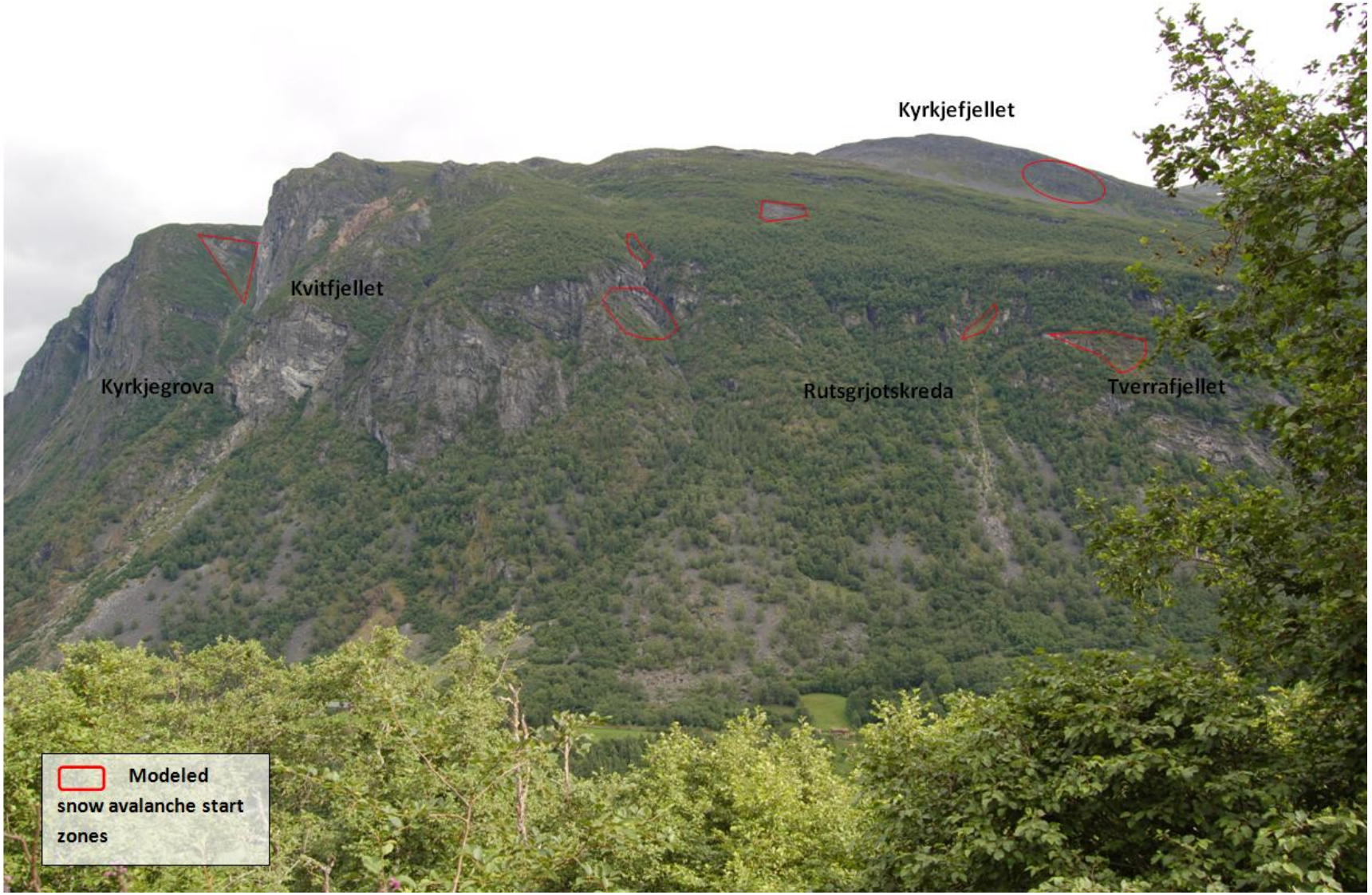

Figure 8-1: Overview of the eastern valley side showing the ravine Kyrkjegrova, the mountain face Kvitfjellet and Kyrkjefjellet (1153 m.a.s.l.). The red lines show approximate extent of some of the start zone modeled in RAMMS (Photo: N.A. Walberg).

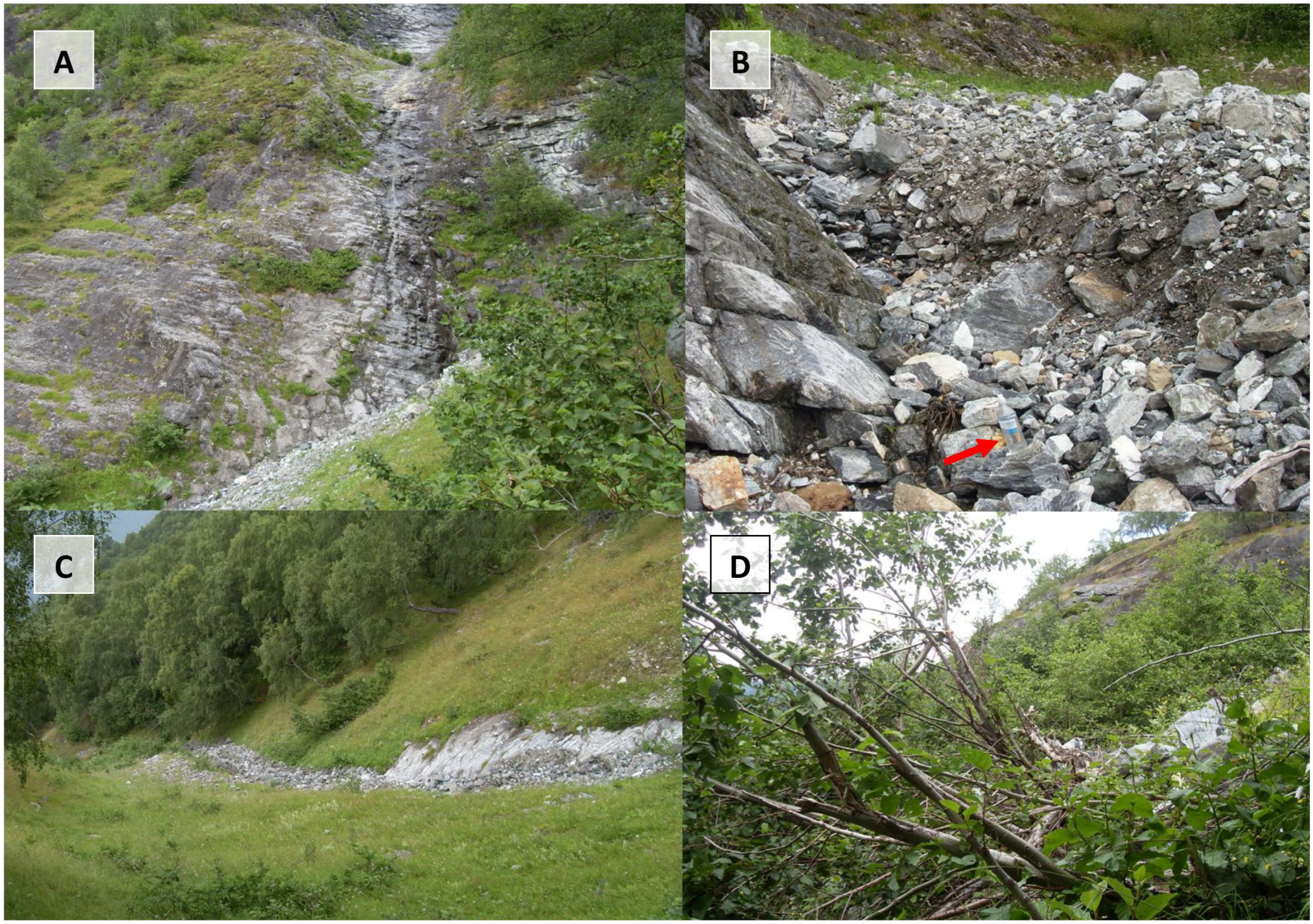
A
B
C
D

Figure 8-2 (previous page): A) Kyrkjegrova taken from the top of the talus and upwards. This ravine is known to experience both snow avalanches and debris flows. B) Close up photo of the transition from bedrock to loose material at the top of the talus slope. Arrow points to water bottle for scale. C) Large amounts of material are deposited in "terraces" down slope in the ravine. A small soil slide is partly visible in the right edge, adding more material. D) Broken trees caused by a small snow avalanche at the talus (Photo: N.A. Walberg)

8.2 Snow avalanche modeling

8.2.1 α,β-model for snow avalanches

The α,β-model is a simple empirical model which uses the 10º-point in the terrain to estimate the run out length for a snow avalanche (Lied and Bakkehøi, 1980; Bakkehøi et al., 1983). The relationship between the run out length represented by α and the 10º-point β is found to be

$$\alpha = 096\beta - 1.4° \qquad \text{Equation 6}$$

The standard deviation is 2.3º and the correlation value R = 0.92 (Bakkehøi et al., 1983).

This relationship is determined by looking at 206 avalanche events with known run out lengths in Norway. The relationship allows one to determine the angle between the starting point and the maximum run out of an avalanche using the angle β between the 10º-point and the starting zone of the avalanche (Figure 8-3).

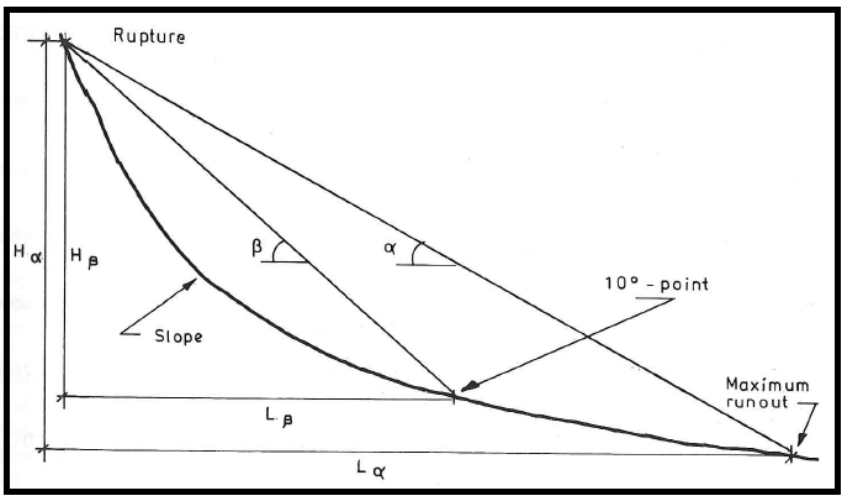

Figure 8-3: Schematic view of parameters included in the α,β.model (Lied and Bakkehøi, 1980).

The α,β-model is applied along 6 transects in the eastern valley side where snow avalanches are thought to occur. The start point is set at the upper end of the transect, and the 10°-point is determined from a slope map of the area as the point where the mean slope of the terrain

drops under 10°. This created a problem along transects #2, #3 and #4 where remains of a glacio-fluvial terrace are present. Here the terrain flattens out for up to 100 m on the top of the terrace before it steeply dips down to the river located centrally in the valley. The α,β-method is not developed for such types of terrain; therefore, resolution of the problem was attempted by making two calculations. One using the 10°-point located on the top of the terrace where the mean slope first drops under 10° and the second one beneath the terrace where the terrain again flattens out. The last parameter needed is the horizontal distance between the source and the respective β-point, and then the α-value and respective run out length was calculated using Equation 6. The result can be found in Table 8-1 and is visualized in Figure 8-4, where the run out length is determined from Equation 6 and represented by green squares. The extra calculations using the β-values from the 10°-points located beneath the terrace are marked as red triangles. The variation in run out is shown as one standard deviation in each direction and is marked by the respective symbols in slightly lighter colors.

Table 8-1: Input values and results for the α,β-method for snow avalanches.

α,β-model snow aval.	Slope 1	Slope 2	Slope 2-2	Slope 3	Slope 3-2	Slope 4	Slope 4-2	Slope 5	Slope 6
Height top [m.a.s.l.]	405	726	726	809	809	594	594	1088	496
Height 10°point [m.a.s.l.]	42	105	48	128	58	113	84	133	146
Dist. 10°-point - top [m]	460	917	1065	901	1106	627	706	1584	416
β-top [°]	38,3	34,1	32,5	37,1	34,2	37,5	35,8	31,1	40,1
α-top [°]	35,3	31,3	29,8	34,2	31,4	34,6	33,0	28,4	37,1
α-top + 1 std [°]	37,6	33,6	32,1	36,5	33,7	36,9	35,3	30,7	39,4
α-top - 1 std [°]	33,0	29,0	27,5	31,9	29,1	32,3	30,7	26,1	34,8
Dist. α-top [m]	512	1020	1185	1002	1230	697	785	1763	463
Dist. α top + 1 std [m]	471	933	1082	920	1126	641	720	1606	427
Dist. α top - 1 std [m]	558	1118	1303	1094	1349	761	859	1946	504

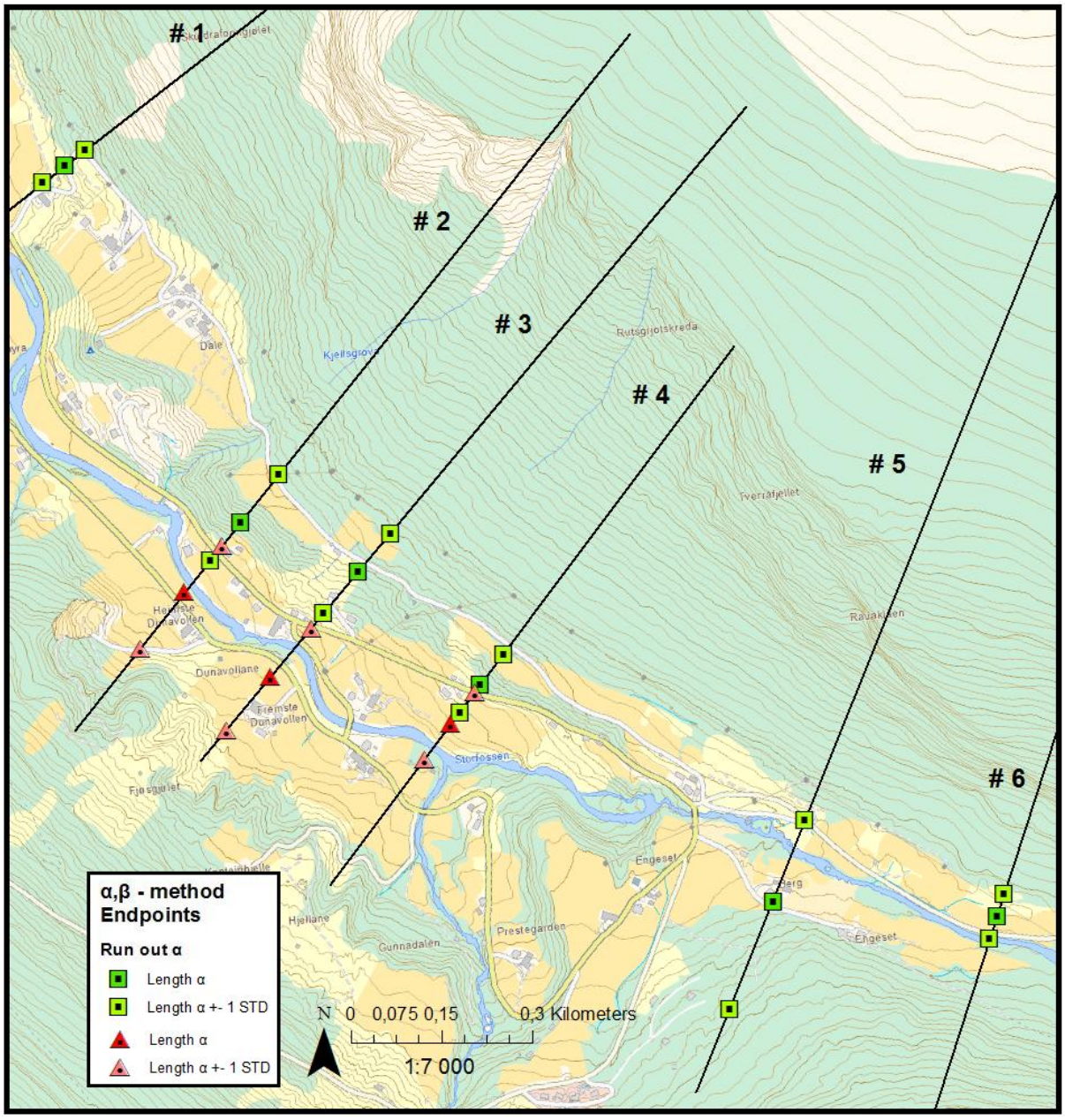

Figure 8-4: Results from the calculated run out from the α,β-model. Green squares represent results obtained from the conventional 10°-point at the lower part of the talus, while the red triangles in transect #2, #3 and #4 represent the extra set of calculations performed due to the presence of a glacio-fluvial terrace along these transects, thus using a 10°-point beneath the terrace.

8.2.2 AVAL-1D

AVAL-1D is a snow avalanche simulation program based on numerical calculations and can be used to compute both dense flow and powder snow avalanches. The program was developed by the Swiss Federal Institute of Snow Avalanche Research (SLF) from many

years of research. Since 1999 has it been available for practitioner and is today a commercial product widely used for hazard mapping in Europe.

The program calculates run out distances, velocities and pressures exerted by the avalanche along the avalanche path. The calculations are based on differential equations which describe conservation of mass, movement and energy using the finite difference method (Christen et al., 2002). Jamieson et al. (2008) did a sensitivity analysis of the model and found that small changes in input parameters could lead to large differences in calculated run out length. This is especially important to consider when the friction angle μ is close to the critical slope of the run out area (μ=~ $\tan^{-1}$ *slope).*

The required input and methodology are thoroughly described in the user manual and *quick-start-document* (Christen et al., 2002; SLF, 2005). The slope is characterized by X- and Z-coordinates describing length and height, and the intervals used satisfy the requirements in the best possible way without losing too much information about the terrain. The interval between the points should ideally be 80-220 m to smooth the terrain according to the calculation steps found in SLF (2005), which is meant to represent the snow filling small depressions in the terrain during an avalanche. The input intervals used are basically 100 m, but exceptions occur to assure that the terrain is represented in the best possible way. Each section also has a specified avalanche width, which is estimated from the terrain and probable avalanche size, together with a set of friction parameters. These are identical as for RAMMS, and can be found in Table 8-3 in Chapter 8.2.3.

The results determined from the calculations can be found in Table 8-2 and are visualized in Figure 8-5. Figure 8-6 displays an example of the output from the AVAL-1D calculation for slope 1. The uppermost graph shows the topography consisting of several sections with varying length and slope, where the uppermost (outlined in blue) represents the start zone with the mean fracture depth determined (1.5 m). Following is a plot of the maximum flow height (blue graph), maximum velocity (red graph) and maximum pressure (green graph) along the slope. The last and lowermost graph shows the run out length to the end of a pre-defined high (30 kPa) and low (0.3 kPa) pressure zone. The values represent the hazard zone limits in Switzerland (Jaboyedoff et al., 2005). These run out lengths are plotted for all the calculated slopes in the map found in Figure 8-5.

Table8-2: Results from AVAL-1D calculations.

Track	Duration	Max velocity	Max flow height	Volume	Mass	Distance to end of:	
						High pr. zone	Low pr. zone
	[s]	[ms^{-1}]	[m]	[m^3]	[t]	[m]	[m]
Slope 1	66	33,16	1,6	20538	6161	648	729
Slope 2	97	35,11	2,08	37998	11399	1040	1140
Slope 3	254	28,04	1,34	9639	2892	930	1150
Slope 4	126	28,68	1,03	9722	2917	730	830
Slope 5	151	29,03	2,57	89586	26876	1620	1670
Slope 6	61	27,32	0,86	9752	2926	460	520

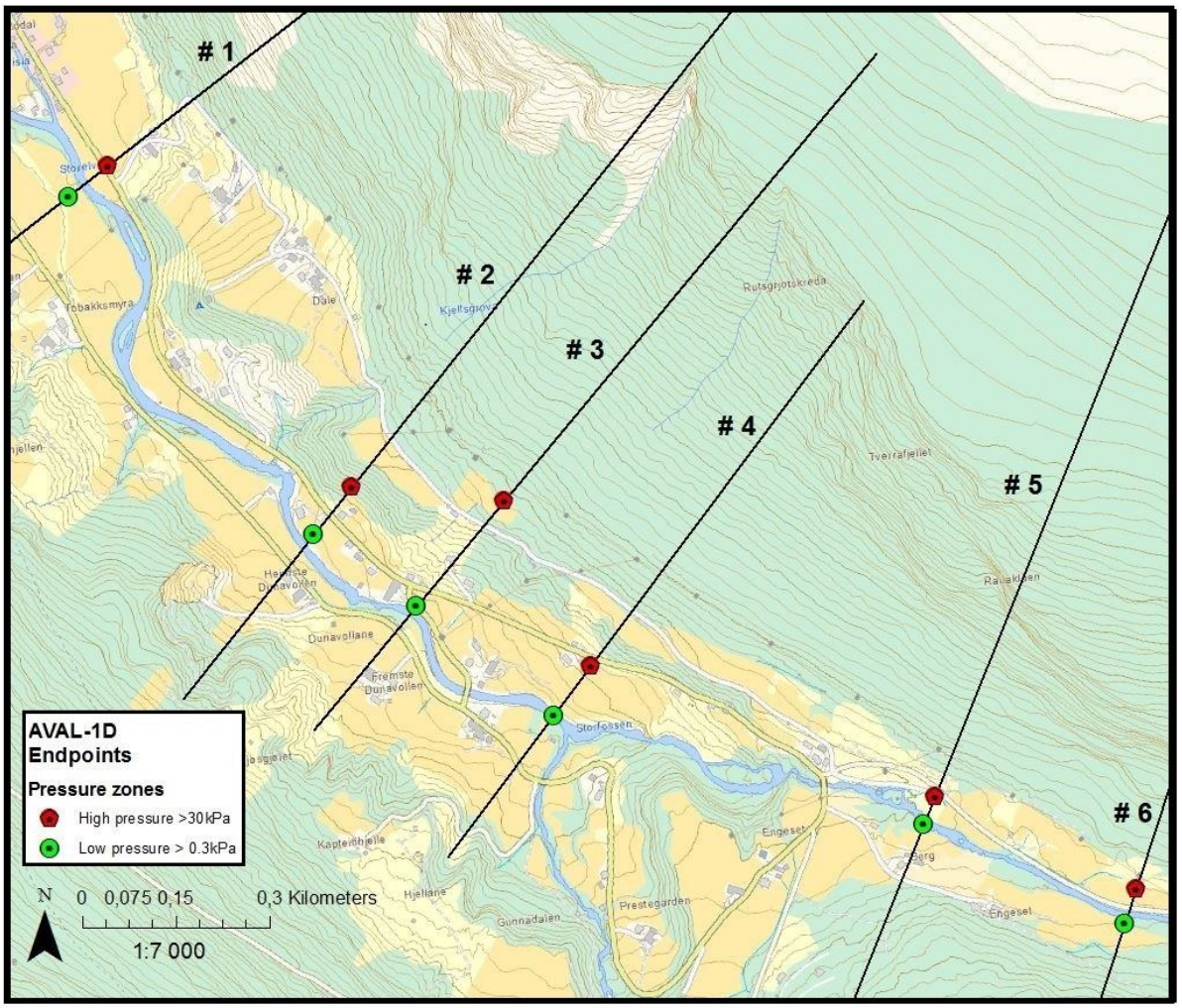

Figure 8-5: Distribution of endpoints for high (30 kPa) and low (0.3 kPa) pressure zones determined from AVAL-1D. Note that some of the modeled paths reach outside the shown area.

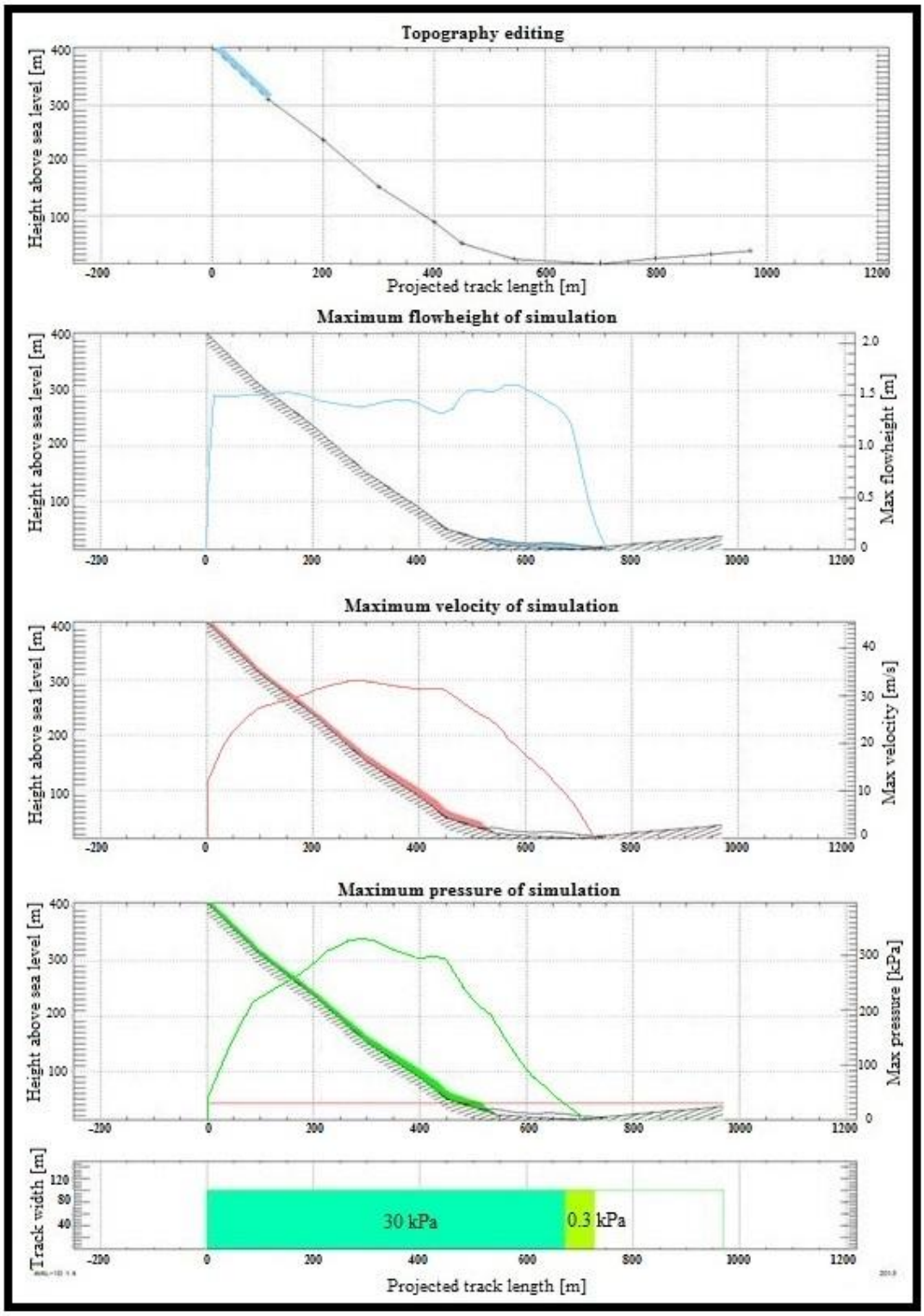

Figure 8-6: Graphical results from transect #1 determined from AVAL-1D. The uppermost graph shows the slope segments defining the slope, as well as the release area marked in blue. The graphs below show the maximum flow height, velocity, and pressure distributed down the track, while the lowermost one show endpoints of high and low pressure zones.

8.2.3 RAMMS

RAMMS (RApid Mass MovementS) is a two-dimensional numerical simulation program which was designed as a functional tool for snow avalanche researchers by the "avalanche, debris flow and rock fall" research unit at *Institute for Snow and Avalanche Research* (SLF) which is part of the *Swiss Federal Institute for Forest, Snow and Landscape Research* (WSL) (Christen et al., 2008; Christen et al., 2010; SLF, 2011). The model development, which is a constantly ongoing process, is based on widespread experiments with snow movements in a large chute and full scale experiments in the Vallée de la Sionne test site located in Switzerland.

RAMMS is developed as a tool to solve avalanche related problems such as avalanche hazard mapping. Since it is developed in Switzerland, the mathematical model used follows the Swiss calculation guidelines. This means that the Voellmy-Salm model (Salm, 1993) is applied in RAMMS, but due to limitations regarding the calculation of velocities during the avalanche, an additional flow model is implemented. This is based on growth and loss of kinetic energy during an avalanche and is denoted as a *random kinetic energy* (RKE) model. The model couples kinetic energy with the parameters included in the Voellmy-Salm model, which makes them dynamic, and the compounded model gives a better result for the velocity, entrainment and deposition (Christen et al., 2010). Inputs needed for RAMMS to carry out numerical simulations are a digital elevation model, friction parameters, release zone areas and height of the fracture which determine the initial snow volume (Christen et al., 2010).

Table 8-3: Input friction values used in RAMMS calculations. Notice that the altitude thresholds are reduced with 500 m compared to the default values.

RAMMS friction parameters			
Altitude [m.a.s.l.]			
	> 1000	500 - 1000	< 500
Open slope			
μ	0.155	0.170	0.190
ξ	3000	2500	2000
Channelled			
μ	0.210	0.220	0.240
ξ	2000	1750	1500
Gully			
μ	0.270	0.285	0.300
ξ	1500	1350	1200
Flat			
μ	0.140	0.150	0.170
ξ	4000	3500	3000

The modeling of snow avalanches performed by RAMMS in this study consists of two parts. One is to try to replicate a known avalanche, and the other is to model the run out of possible avalanche tracks determined from field observations and aerial photos. When modeling the

run out of possible new avalanches, a return period of 300 year is chosen. This is to ensure that the simulations use parameters which do not underestimate the run out, but do simulate large, seldom events which can be associated with the highest consequences, and it is the value nearest to Norwegian requirements. The friction values used can be found in Table 8-3, where μ refers to dry Coulomb friction and ξ the squared drag velocity coefficient. The altitude limits are reduced by 500 m compared to the default values from Switzerland. This is meant to reflect the different temperatures with elevation between Switzerland and Norway, and thus snow properties (Gauer, 2013). The calculations do not take vegetation cover or the influence of buildings into account, so eventually momentum loss or protective effects from vegetation or infrastructure in the area are not determined. Source areas are determined from field work, aerial photo studies, terrain analysis and vegetation conditions.

Reconstruction of historical snow avalanche near *Berg*

A snow avalanche is reported to have come down the eastern mountain side, crossing the river and causing a window to break in a house near Berg. This occurred early in the 1980's, but the exact year and date have not been successfully determined. The reason to recalculate this event is to determine the validity of the simulation program. Although very little is known about the avalanche, a successful recalculation with realistic input values predicts that the outcome from the model in similar conditions, where information does not exist about previous snow avalanches, might be dependable. This in comparison with no successful recreation, which suggests that the model will not manage to simulate a known event, and the results of other simulations, therefore, must be considered with much more care and uncertainty. RAMMS is a well-proven simulation program developed over time using field observations and experiments, but it is considered wise to re-validate in a new area.

The snow avalanche in the 1980s was reported as "coming over the ridge" which was confirmed since modeled release areas beneath the ridge didn't cause run outs beyond the river. Topographic conditions led to the southern hillside of *Kyrkjefjellet* which could be the source area. Here the inclination lays around 40°, and both the map and aerial photo show little or low vegetation. Simulations soon displayed that a large snow avalanche from this area may reach over the river and to the houses near Berg. Different sizes and locations of

the source area along the hillside were simulated, most of them showing that an avalanche reaching the houses near Berg were possible, as one part of the avalanche seemed to follow a small depression in the terrain down toward the houses. Figure 8-7 shows the result from a simulation of an approximate 350 m wide avalanche with an average snow depth of 1.5 m in the source area. This is a large avalanche (63 000 m^3), but the topography in the source area and meteorological conditions at the Norwegian west coast make such an event realistic.

The results in Figure 8-7 show maximum values for velocity, pressure and flow height for the computed avalanche. As can be observed from the results, the modeled maximum velocity, pressure and flow height in front of the houses are relatively low. The snow avalanche modeled is a dense snow avalanche and does not take pressure waves in front of an avalanche into account. The actual avalanche might have been a powder avalanche where the associated pressure wave might have caused the damage. Large avalanches, especially dry avalanches, can gain high velocities, and snow-air mixtures with higher density than the surrounding air could behave like heavy gasses and are pushed in front of the avalanche. Pressure waves usually occur in front of dry avalanches which flow off a cliff but could also occur as a result of terrain formations. Pressure waves could cause damage relatively far from the snow avalanche itself, while the effect on the sides of the avalanche decline rapidly (Hestnes, 1980).

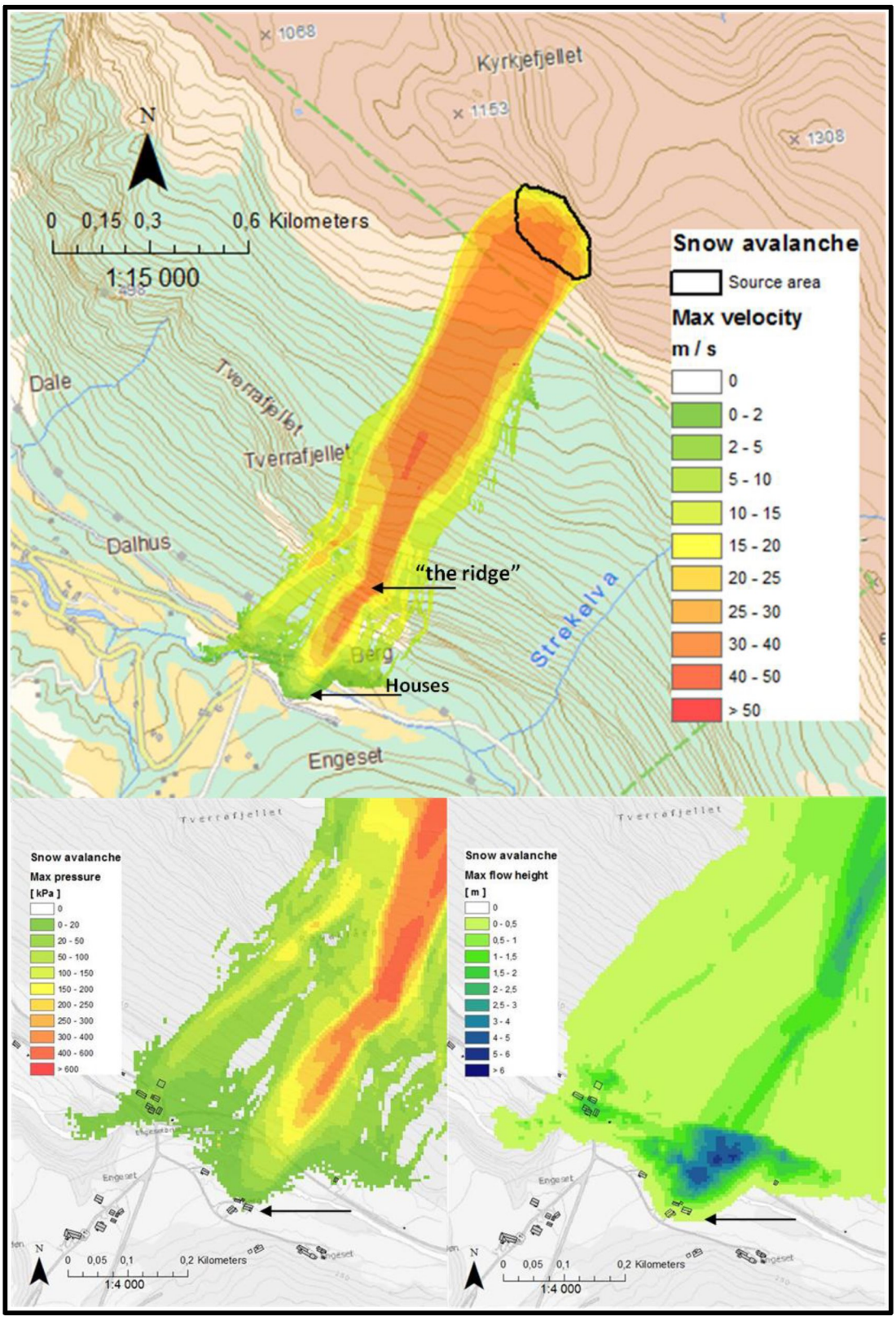

Figure 8-7: Recreation of a known avalanche which reached the houses near Berg early in the 1980's using RAMMS snow avalanche simulation program.

Run out modeling for *Norddal*

The modeled results show that there is a possibility that large snow avalanches from the previous mentioned start zones reach infrastructure and houses. It is important to remember that it is worst-case scenarios which have been modeled and, therefore, not the yearly events of which one has direct experience. The average snow height used is 1.5 m and the modeled volumes varies from 5 300 - 33 000 m^3. An example may be observed in the modeled result from the *Kyrkjegrova* in Figure 8-8, which almost yearly experiences snow avalanches, but usually do not cause any threat, because they stay within the gully. The modeled results assumed a total of 1.5 m of snow release in the entire possible start zone, while normally just 1/10 or less of this area probably releases, something which is estimated from vegetation cover in the release area. Most of the start zones consist of vegetation free areas within forested areas. Based on empirical evidence, it is often assumed that an avalanche needs to have 50-100 m of fall before the effect of forest can be neglected. NGI has completed a report regarding how forest cover affects snow avalanche hazard in Norway, partly based on results conducted in the Alps (Breien et al., 2013). Birches, which are the predominate type of tree along the upper eastern valley side, need to have a density of 250 stems per decare with a mean diameter at breast height (DBH) of 10 cm to meet the posted requirements for snow avalanche protection forest in the Alps, measured as percentage of crown cover. NGI points out that such values are not widespread in Norway, and that birches near the tree line in Norway often show a low and wide appearance. NGI concludes that studies based on conditions in the Alps cannot be directly applied to Norway (Breien et al., 2013). Vegetation and forest cover below the release areas is therefore not taken into account in the following snow avalanche simulations. This is because the forest cover in the eastern valley side of *Norddal* is discontinuous and partly sparse. In addition, the effect from deciduous forest cover on snow stability is still regarded as uncertain (Breien et al., 2013), and snow avalanche release in this sparse forest can therefore not be excluded.

Since all possible source areas most likely do not release at the same time, as modeled in Figure 8-8, the three starting zones which interfere are modeled separately (Figure 8-9).

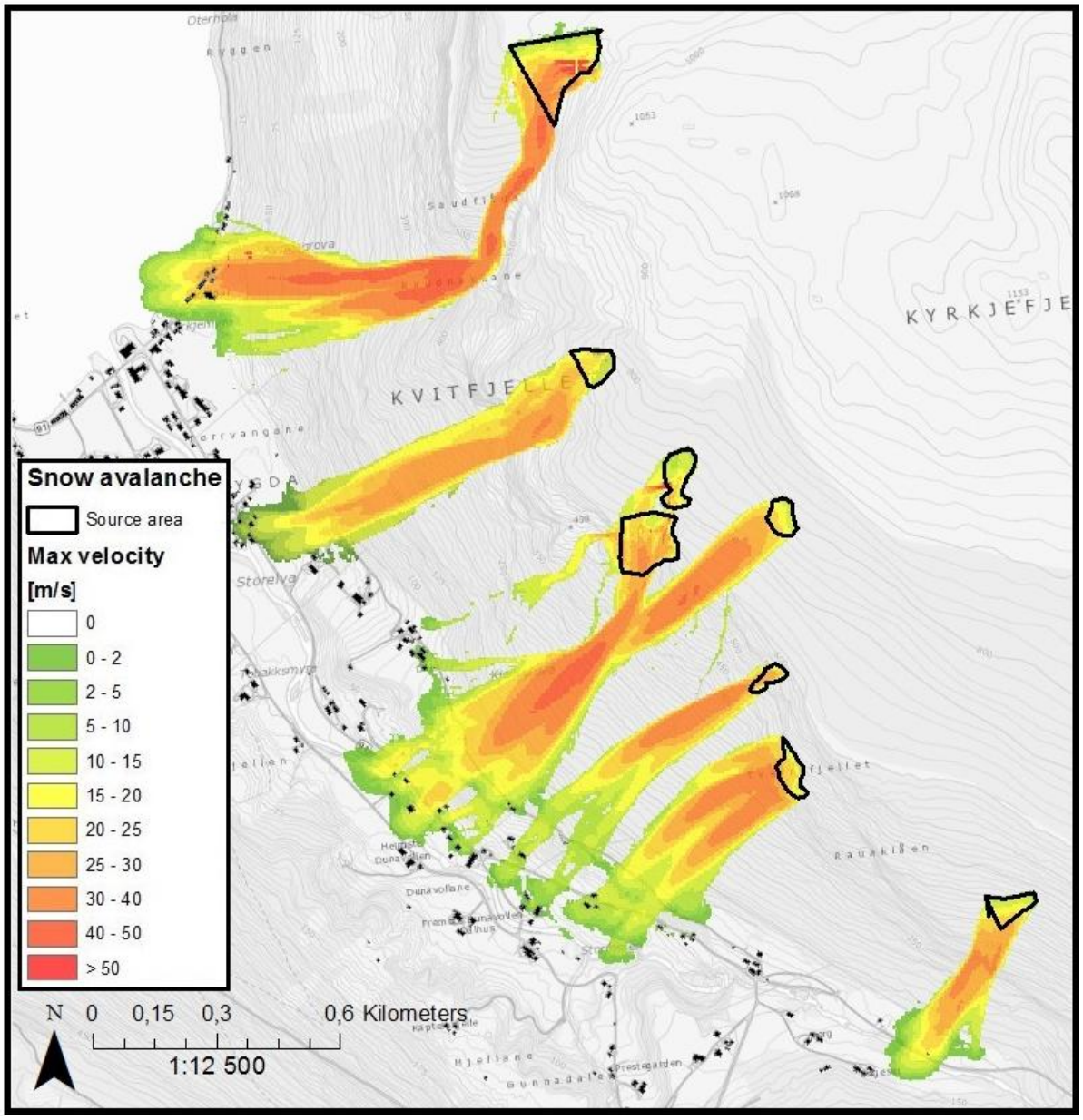

Figure 8-8: Results of RAMMS modeling the possible run out from source areas determined from field observations and aerial photo. The modeled snow avalanche volumes varies from 5 300 - 33 000 m^3. Roads and buildings are highlighted for easier geographical reference.

8.2.4 Comparison of snow avalanche models

Figure 8-10 shows the run out lengths determined from both RAMMS, AVAL-1D and the α,β-model. Notice that the RAMMS and AVAL-1D results show maximum pressure [kPa], while the α,β-model show the predicted run out length [m].

The α,β-model and AVAL-1D calculations are performed along transects which are determined prior to the calculations. They are determined in areas where avalanches are thought to possibly occur and represent the steepest part of the slope perpendicular to the elevation contour lines. As the hillsides are not completely planar, the steepest path is hard to determine and seldom follows a straight line. The transects will, therefore, be a simplification of the real avalanche path. The result from this effect are clearly visible along transect #2, #3 and #4 where the RAMMS simulation show that the avalanche will follow a curved path towards the valley bottom. This is due to micro-topographic conditions which will guide the snow such as depressions, ridges and ravines. This effect cause the results from the α,β-model and AVAL-1D calculations to show slightly too long run outs, as an avalanche probably would have followed a more curved path. The fact that RAMMS takes local topography into account is its greatest advantage compared with the other two models, since it determines the avalanche path. Another important aspect is that the α,β-model is not developed for complicated terrain variations, such as uphill slopes in the run

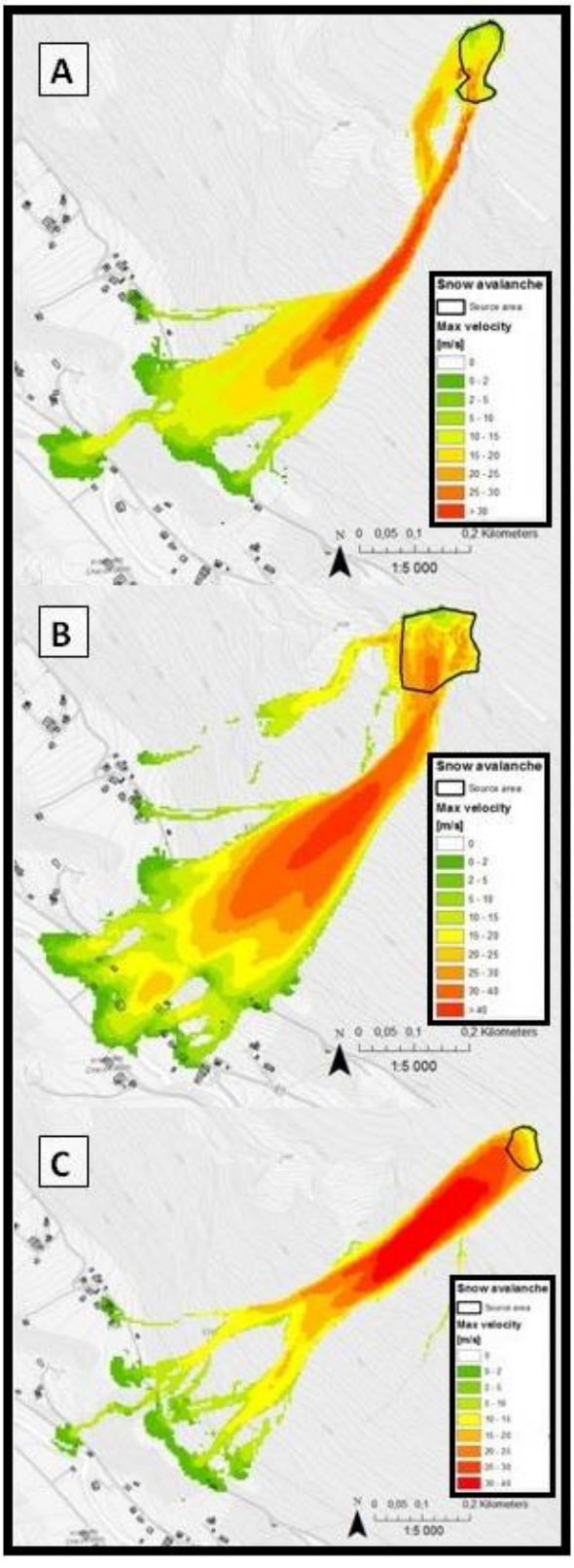

Figure 8-9: Start zone B, C and D modeled separately in RAMMS.

out zone. This implies that the results from transect #5 in Figure 8-10 must be cautiously evaluated.

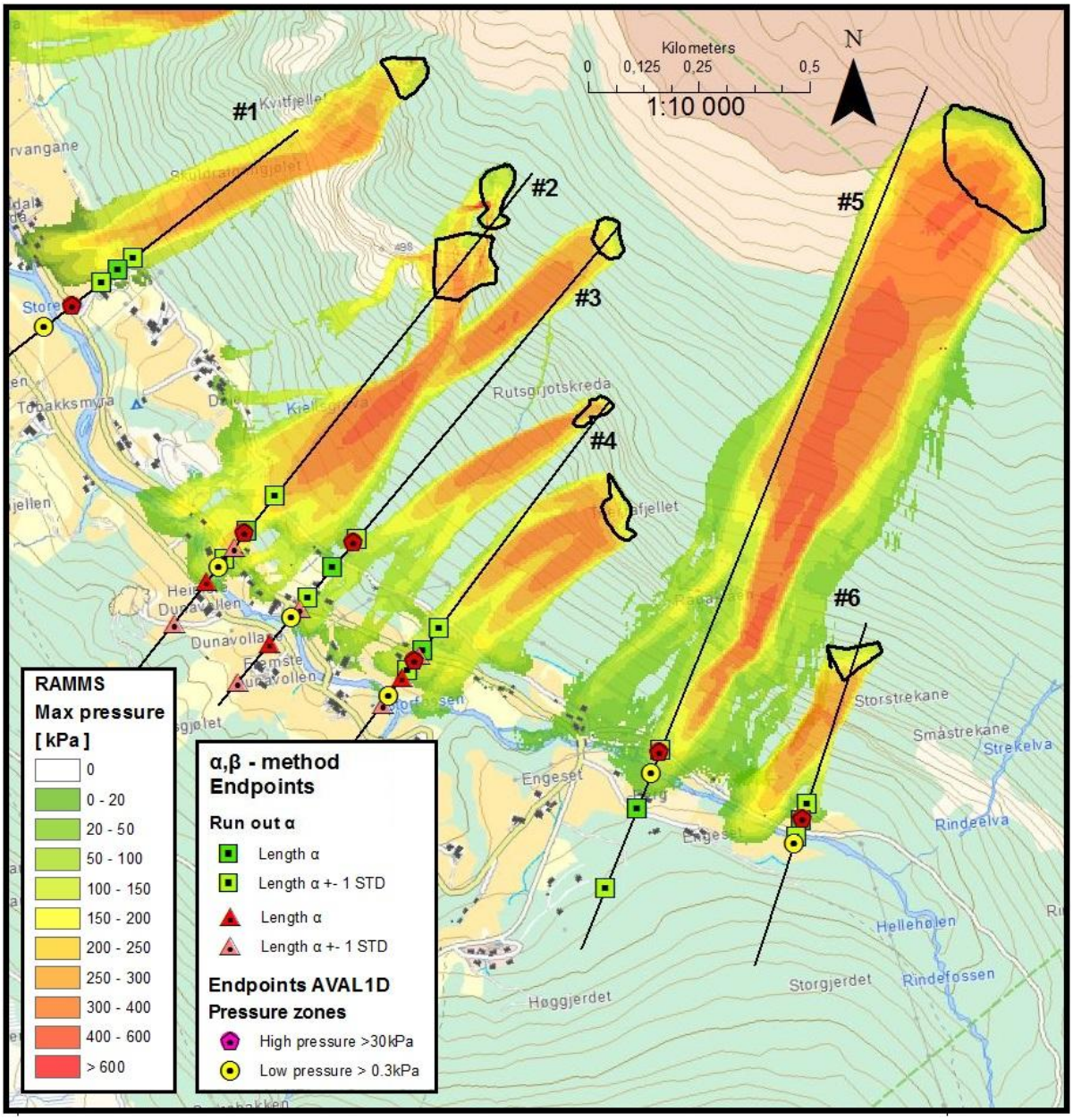

Figure 8-10: Calculated snow avalanche run out lengths from RAMMS, AVAL-1D and the α,β-model. Notice that the RAMMS and AVAL-1D results show maximum pressure in [kPa], while the α,β-model show the predicted run out [m]. RAMMS reveal that the snow avalanches seldom follow a straight path, which was the assumption in the two other models.

9 Hazard maps

Hazard maps regarding landslides and snow avalanches have been prepared according to current regulations (TEK10, 2012) and guidelines from NVE (2012b). The hazard zones are determined from available information regarding existing susceptibility maps, geological and topographical maps, historical records and interviews, field investigations, meteorological conditions and model experiments.

Hazard zones are determined for the extent of potential considerable damage caused by landslides

- with nominal annual probability 1/100
- with nominal annual probability 1/1000
- with nominal annual probability 1/5000.

The mapped area is divided into four parts during the following hazard zone assessment due to topographic conditions and similarities in the areas. The different parts can be found in Figure 9-1, and is in the following denoted part A-D. The hazard from the different mass movement processes are explained separately for each part and can be viewed in conjunction with the different hazard maps.

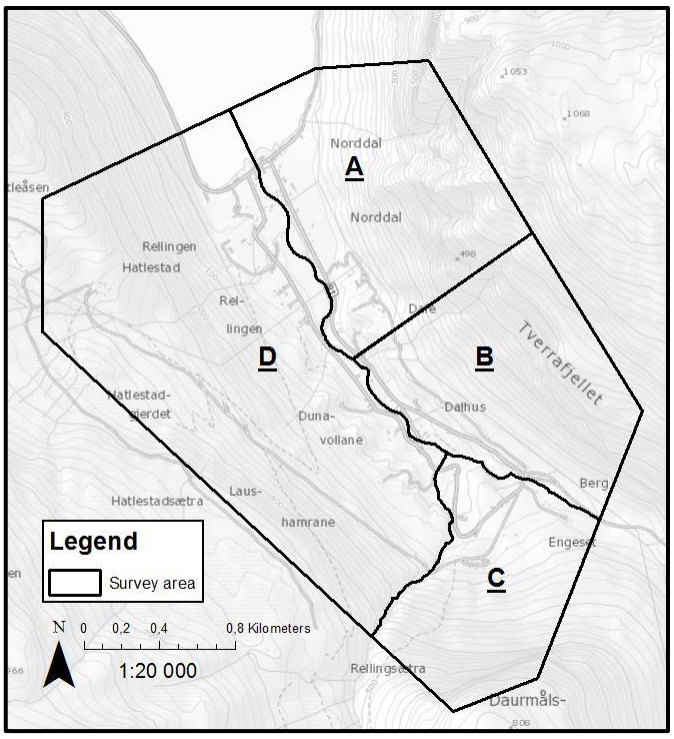

Figure 9-1: Area division during the following hazard zone assessment.

Separate hazard maps are produced for rock falls and rock avalanches (Figure 9-2), snow avalanches and slush avalanches (Figure 9-3) and for debris slides and debris flows (Figure 9-4). The final hazard zone is determined from the process having the longest run out at each location, according to prevailing practice, and it is this map which should be used during land use

planning (Figure 9-5). The hazard maps are valid for the current situation. Change in vegetation cover or implementation of mitigation measures could change their validity.

9.1 General overview

Norddal has experienced large mass movements related to loose soil, snow and bedrock. In the steep eastern valley side (A, B), rock falls occur every year, and long run outs of single blocks outside the talus are reported and deposits are observed. Yet, it is the potential for large snow avalanches along large parts of the mountain side that determines the hazard zones. The western valley side (D) is covered by a thick cover of till and is prone to debris flows and partly rock falls. The hazard from debris flows and debris slides determine the total hazard zones in this area and for the slope beneath *Daurmålsfjellet*, south in the valley (C).

9.2 Part A: eastern valley side – north of *Kjellsgrova*

The mapped area stretches from the northernmost settlement north of *Kyrkjegrova*, southwards along the mountain side to *Kjellsgrova*, see Figure 9-1. The mapped area includes all the settlement in the north eastern part of *Norddal*, including *Dale.* This area is dominated by rock falls with a rock avalanche occurring in 1996, leaving deposited blocks almost all the way out to the nearest house. Snow avalanches may occur in the ravines and are together with rock falls considered the determinative hazards in the area.

9.2.1 Rock falls and rock avalanches

A massive talus along the mountain side is developed from repeated rock fall and rock avalanche activity. The mountain holds several outcrops consisting of vertical rock faces with distinct fracturing, e.g. *Kvitfjellet*. Many overhanging blocks, fresh scars and presence of water are observed, indicating the possibility for future activity. Several fresh rock fall deposits and scars on the vegetation are observed within the talus. The extent of the talus determines the 1/100 hazard zone.

A rock avalanche of 10 000 m^3 occurred in 1996 from *Kvitfjellet*. Large boulders were deposited at the end the talus and smaller ones deposited outside the talus in the cultivated land. The nearest blocks were deposited 30-50 m from the nearest houses located centrally in the valley. The cultivated land was cleared of stones from a similar event prior to the 1996 landslide, indicating similar events have happened before. A rock fall reached the power line in the lower part of the talus in November 2011. Single rock fall blocks are still present in the field and near the houses at *Dale*, indicating the possible run out of similar blocks. The reported run out from the *Kvitfjellet* rock avalanche and present rock fall deposits outside the talus represents the 1/1000 hazard zone in this area. Results from rock fall run out models correspond well to observed rock fall deposits in this area, but show that rock falls may reach longer than the 1996 event. Results from the rock falls models contributes to the extent of the 1/5000 hazard zone.

9.2.2 Snow avalanches and slush avalanches

The mountain side holds four distinct ravines, *Kyrkjegrova,* a nameless one by the large fan behind the church, *Skuldrafonngjølet* and *Kjellsgrova.* All these display geomorphology in terms of 30-45° steep vegetation free areas in the upper part which is compatible with snow avalanche release. The ravines also collect snow during north-westerly winds, which often is present during snow fall. Except for *Kyrkjegrova* located north in the area, there is no certain historical evidence of snow avalanche release in these ravines. The planar talus side is generally more than 30° steep, and the forest cover is discontinuous, which makes the talus slope itself a possible snow avalanche release area. Field observations revealed one fresh snow avalanche event and one slush avalanche event on the talus. Observations of old levees and channels, especially on the large fan, indicate that rock fall material on the talus was redistributed by slush avalanches and/or debris flows. The surface roughness is generally high, which will tie the snow to the substrate. This could be covered by snow forming a new sliding layer; therefore, a snow avalanche release from the planar talus slope can not be excluded. Small snow avalanches within the talus and in the ravines are determining the 1/100 hazard zone.

Results from snow avalanche run out modeling in this area show possible run out lengths from large snow avalanches that will reach significantly outside the talus slope. The different

models are consistent with these predictions. Despite little information regarding large historical events in the area, parts of the area are considered prone to snow avalanches. The terrain features in terms of distinct ravines which could collect large amounts of snow, and modeled run out are particularly emphasized in the 1/1000 and 1/5000 hazard zone determination for snow avalanches.

9.2.3 Debris slides and debris flows

The same ravines referred to as a possible snow avalanche paths in the previous section could hold debris flows as well. Seasonal water flow during heavy rain and during the snow melt period are present, and the ravines holds large amounts of material which could be entrained. Observations of old levees and channels, especially on the large fan by *Kyrkjemyra*, indicate that rock fall material on the talus are redistributed by debris flows and/or slush avalanches. The large fan by *Kyrkjemyra* gently extends out into the field, but only water rich parts consisting of fine-grained material are observed deposited here. Cuts in the depositions of *Kyrkjegrova* and *Oterhola*, the latter located slightly north of the mapped area, show repeating events of debris slides and snow avalanches. The material on the upper portion of the planar talus consists of sand and gravel that can possibly release as debris slides and debris flows during high water saturation or as a result of rock fall impacts. Such events are not thought to reach outside the talus due to the high surface roughness in the lower part of the talus, and are regarded as decisive for the 1/100 hazard zone. Debris slide and debris flow initiation in the middle and lower section of the talus is not considered likely due to the large block size and high permeability.

Areas outside the talus are not regarded as particularly vulnerable to debris flows and slides. The hazards are mostly focused around the existing fans and beneath the ravines, something which is considered in the determination of the 1/1000 and 1/5000 hazard zone. The preliminary results from debris flow susceptibility mapping by NGU are not considered reliable in this area. The preliminary model holds large uncertainties regarding definition of starting zones and low spatial resolution, and the model is not created for local detailed investigations. Local geomorphology is, therefore, emphasized in the hazard zone determination.

The glacio-fluvial terrace present centrally in the valley, *Daleterrassen*, steeply dips toward the river with a height difference of up to 50-60 vertical meters. Clay has been revealed during construction work in this slope; therefore, care should be taken if further work is considered. Scars from small slides are visible, but it is unknown if any of them are natural or if they are connected to grazing or human activity. The steep side of the terrace are therefore included in the 1/1000 hazard zone.

9.3 Part B: eastern valley side – south of *Kjellsgrova*

The mapped area stretches from *Kjellsgrova* in the north and southward to the end of the village toward *Herdalen*, see Figure 9-1. Rock fall occurs regularly in the area, but usually deposits within the talus although ancient boulder deposits are located in the fields. Two large snow avalanches were reported in the area, and the possibility of large snow avalanches becomes the dominating factor in the hazard zone determination.

9.3.1 Rock falls and rock avalanches

The mountain side differs from the previously mentioned one in that large vertical rock outcrops, such as *Kvitfjellet*, are not present in this area. The mountain side appears smoother, but still holds several steep parts in place (>70°), especially around *Tverrafjellet* and *Rauklåen.* The altitude of this steep section drops consistently towards the south causing the talus developed beneath to decrease in extent as well. The fracturing is not so distinct in this area. Deposits after what is probably an old rock avalanche are present around *Kjellsgrova* as several blocks approximately 10 m and more in diameter are observed. The average block size seems to decrease toward the south, but boulders in the lower part of the talus are present all the way. The lower part of the talus is densely vegetated with deciduous forest and mosses covering the blocks; no fresh rock fall blocks was detected in the lower areas. The upper and middle parts show signs of fresh rock fall deposits. Large boulders present in the cultivated land outside the talus toe are thought to originate from rock falls.

Local inhabitants spoke about yearly rock falls within the talus and rock falls and snow avalanches reaching all the way to the upper small farm road. Sparse settlement in the area is

implicated as a result of relatively high frequency of landslides and snow avalanches. Fresh rock fall deposits and information about high rock fall activity within the talus are determining the 1/100 hazard zone.

The run out models taking roughness into account show a shorter run out than the topographic α,β-method in the northern part where the talus has its largest extent. Observation of several rock fall boulders in the field on *Dalsreinene*, some which are regarded as moved and some which are not, indicate that a rock fall run out modeled from the α,β-model is plausible in this area. Rock fall blocks deposited in the fields and local information determine the 1/1000 hazard zone, while run out from the α,β-model contributes to the extent of the 1/5000 hazard zone in this area.

9.3.2 Snow avalanches and slush avalanches

The gentle form of the sparsely vegetated mountain side and talus formation, with major parts having an inclination between 30-45°, makes the area prone to snow avalanches. The vegetation is not considered dense or high enough to prevent snow avalanche release in between or above the vegetation cover. The steeper vegetation free areas along *Tverrafjellet* show evident erosion tracks which are thought to be derived from minor snow avalanches and/or rock falls. These areas are considered to steep (>60°) for large snow amounts to build up, but less steep areas are located in between.

The ravines of *Kjellsgrova* and *Rutsgrjotskreda* could hold channeled snow avalanches and slush avalanches, and a large snow avalanche in the 18th century is reported in this area, destroying former settlement. Remnants of a small slush avalanche were evident during field work. Sparse settlement in the area today is implicated as a result of the high frequency of snow avalanches and rock falls. A snow avalanche was reported reaching over the river near Berg in the 1980's. This probably released in the concave slope beneath *Kyrkjefjellet* (1000-1120 m.a.s.l.). The release area is located above the tree line and model results reveal that snow avalanches from this area could reach the valley floor.

Topography and sparse vegetation do not exclude the possibility of snow avalanche release along the mountain side. The modeled run out from such events, as well as information about snow avalanches reaching the upper road, are determinative for the 1/100 hazard zone.

Several ravines and depressions can collect snow, and in addition, snow avalanches may release and travel almost a thousand vertical meters from *Kyrkjefjellet*, located out of sight from the valley floor. The modeled and reported run out from such events is used to define the extent of the 1/1000 and 1/5000 hazard zones.

9.3.3 Debris slides and debris flows

The mentioned ravines of *Kjellsgrova* and *Rutsgrjotskreda* may act as debris flow paths during periods were they occur as small creeks, especially during the snow melt period. Large amounts of material are present in the depressions which could be entrained during high discharge, causing debris flows. The water path near *Kjellsgrov*a is evident all the way to the valley floor, but a slide will probably deposit its material and loose energy before this point. The visible remnants from channels in the lower part are densely vegetated and reveal no signs of present activity. The other ravine spreads out on the talus, suggesting that the possible debris flow will quickly loose energy. The fine-grained material in the upper part of the planar talus is of pebble size; therefore, water will probably drain before water pressure can build up.

Debris slides and debris flows are not thought to occur regularly in this area and no signs of debris flow activity were detected during field work, except for the deposits that were most likely a small slush avalanche. The hazard can not be excluded but run outs outside the talus slope are not regarded as likely, and the 1/100 hazard zone therefore tightly follows the extent of the talus, with some safety margin added for the higher return periods. Extra caution should be made along the ravines and depressions as they may act as channels for debris flows. The ravine of *Kjellsgrova* is therefore included in the 1/1000 hazard zone all the way to the valley floor. This is also the case for the steep side of *Daleterrassen*.

9.4 Part C: *Daurmålsfjellet*

The area is located in the southern portion of the valley, bounded by *Daurmålsfjellet* and the rivers *Dyrdøla* and *Herdøla*, see Figure 9-1. The large vertical cliff could act as a source area for rock falls, despite the infrequently observed activity. Snow avalanches would probably not occur during present conditions, but some houses at Berg could be affected by snow avalanches crossing the valley floor from the eastern mountain side. Steep slopes covered by

till, evident drainage tracks and depositional fans make debris flows and debris slides the controlling hazard type in this area.

9.4.1 Rock falls and rock avalanches

Daurmålsfjellet holds a vertical cliff of more than 200 vertical meters. The rock fall activity seems much lower than along the eastern valley side, which is confirmed by people in the area. The talus formation is vegetated by forest and grass all the way up to the cliff itself. No distinct rock fall paths in the forest are evident, which often is the case if rock falls occur in forested areas. The reason for the apparently low activity might be because the mountain consists of quartzite and/or the aspect of the cliff, which may be favorable related to the structural geology in the area.

Although the activity seems low, a large vertical cliff like this poses the threat of rock falls and rock avalanches. The topography beneath is quite gentle which causes varying run out lengths determined from the models. The run out predicted from RocFall seems more realistic than the one from the α,β-model, and is used to determine the extent of the 1/100 hazard zone. From the longest run out modeled by RocFall and the little signs of present activity, it is interpreted that rock falls will not reach the existing settlements within a return period of 1000 years. Since the α,β-model reveals that such long run outs theoretically are possible and behavior of large failures is difficult to predict, the settlement is included in the extent of the 1/5000 hazard zone.

9.4.2 Snow avalanches and slush avalanches

No reported events or signs of snow avalanches are present in the area. The cliff itself is too steep for snow to accumulate, and only small areas beneath are steep enough for snow avalanche release. These areas are densely vegetated, and a release is not regarded likely during the present conditions. Toward *Dyrdalen*, there are some steeper areas, but the dense planted spruce forest is regarded as enough to prevent snow avalanche release. Large changes in vegetation cover in this area, such as logging, will affect the conditions regarding snow avalanches and should not be performed without further analysis.

The settlement in the south eastern part of the area can be affected by large snow avalanches coming down the eastern valley side.

9.4.3 Debris slides and debris flows

The Quaternary map (Figure 7-1) shows that the slope is covered by a thick layer of continuous till. Quaternary mapping performed by NGU (Stokke, 1983) revealed evident drainage tracks along the western flank between *Daurmålsfjellet* and *Dyrdøla*, where the lower part today holds settlements. The drainage tracks end up in fluvial deposited fans on the glacio-fluvial terrace. The remnants are not easy to detect if one is not aware of them, but aerial photos show clear erosion tracks within the previously mentioned spruce forest, indicating also present activity. The fans are deposited in flat terrain with no sign of coarse material, but this material could have been displaced during clearing of agricultural land. No concerns regarding debris flows in this area were expressed, but the steep slope covered by till and presence of drainage tracks in the forest express a potential for debris flow occurrence. The 1/100 hazard zone includes the upper part of the valley side (≥ 20°), while the 1/1000 hazard zone includes the mapped drainage tracks and fans. The flat topography of the outermost fans is thought to rapidly decrease the energy of a possible debris flow, leaving the settlement on these fans outside the hazard zone determined for a 1000 years return period. Three other newly built houses (after 2003) at contour line 150 more eastward are also outside the mentioned hazard zone due to different topographic conditions and lack of evident drainage tracks, but these areas are included in the 1/5000 hazard zone. Some houses eastward in the mapped area, towards *Herdalen*, are included in the 1/1000 hazard zone due to locally steep terrain located above the houses.

9.5 Part D: western valley side

This area includes the whole western valley side from the river *Dyrdøla* to the end of the village by the fjord, see Figure 9-1. Snow avalanches are not regarded as a threat due to dense vegetation cover, while rock fall hazard is present especially in the northern part. The controlling factor for the hazard zone determination in this area is the run out of possible debris flows.

9.5.1 Rock falls and rock avalanches

Rock falls occur almost along the entire valley side. By *Laushamrane*, south in the area, a small talus is present above the road. A steep section parallel to the valley side is acting as the source for these rock falls. The talus is partly covered by forest and is decisive for the 1/100 hazard zone. Observations, topographic conditions and models show that the rocks usually stop above the road (1/1000 hazard zone), while the maximum run out from α,β-model is used to determine the extent of the 1/5000 hazard zone.

Another steep section goes from *Hatlestadgjerdet* all the way towards the fjord. Also, here is a dense vegetation cover present, but scree deposits and open rock fall paths in the forest are visible from aerial photos, especially in the north. The dense forest probably has a preventive effect on small rocks, but larger blocks are reported reaching almost to the valley floor. The 1/100 hazard zone is determined from visible rock fall deposits within the forest, and extends all the way down to the valley floor. Modeling results reveal the possibility of rock fall run out reaching the valley floor, and it must be expected that rock falls can reach the fields right beneath the forest covered slope within a return period of 1000 year and higher.

9.5.2 Snow avalanches and slush avalanches

Large parts of the valley side are between 30-60° steep, but the entire valley side is covered by dense forest. Since snow avalanches seldom release in such dense forests, no detailed mapping has been performed regarding snow avalanches along this valley side. The exception can be slush avalanches occurring by the river *Hatlestadelva* or from the marshlands beneath *Middagshesten*, but the run out from such events are considered to be covered by the debris flow mapping. The settlement at *Hatlestadgjerdet* and *Hatlestad* located up in the hillside is not threatened from any possible snow avalanche release from higher elevation outside the mapped area, but the river *Dyrdøla*, south-west in the area could possible be dammed by snow avalanches from the south-eastern side of *Middagshesten.*

Large changes in vegetation cover in this valley side, such as logging, could create open fields where the terrain is steep enough for snow avalanche release and should not be performed without further impact analysis.

9.5.3 Debris slides and debris flows

The Quaternary mapping performed by NGU (Stokke, 1983) gives detailed information about the geomorphology in the western valley side. The valley side is covered by ravines and distinct drainage tracks which cut into the thick continuously till cover, especially the southern portion. The glacio-fluvial terrace in the valley floor, *Nordhjellane*, is strongly affected by erosion and debris flows, and in several places debris flow deposits are detectable (Stokke, 1983). Field observations this summer revealed dense vegetation, large amounts of water draining down along the entire valley side and a large amount of available material. Some individuals expressed worries regarding all the water present in this valley side and the landslide database does reveal several large debris slides and debris flows reaching all the way to the valley floor. Concern was especially expressed regarding the presence of an old road crossing the valley side. Erosion due to blocked culverts can increase the chance of debris slide initiation.

Generally, the entire valley side is exposed for debris slides and debris flows. The hazard zone is determined with background in the detailed Quaternary mapping and field observations. The 1/100 hazard zone follows the transition from the valley side to the valley floor, while the 1/ 1000 and 1/5000 hazard zones are based on the depositional fans beneath the ravines.

The estimated run out from the preliminary susceptibility map regarding debris slides and debris flows are consistent with the mentioned Quaternary mapping and field observations. The exception is some modeled debris flow paths above *Hatlestadgjerdet*, which are not regarded as threatening for the settlement, as it has to travel up to 600 m in forest and across a field in terrain gentler than 25°. Another exception is made for a house/cabin near the road across *Dyrdøla*, where a small area is left out of the 1/100 nominal probability hazard zone. This is due to local topography and field observations.

9.6 Maps

The following section contains the hazard maps for *Norddal*:

- Rock falls and rock avalanches (1:16 000) – Figure 9-2
- Snow avalanches and slush avalanches (1:16 000) – Figure 9-3
- Debris flows and debris slides (1:16 000) – Figure 9-4
- Total hazard map (1:12 000) – Figure 9-5

The maps will also be available from www.nve.no.

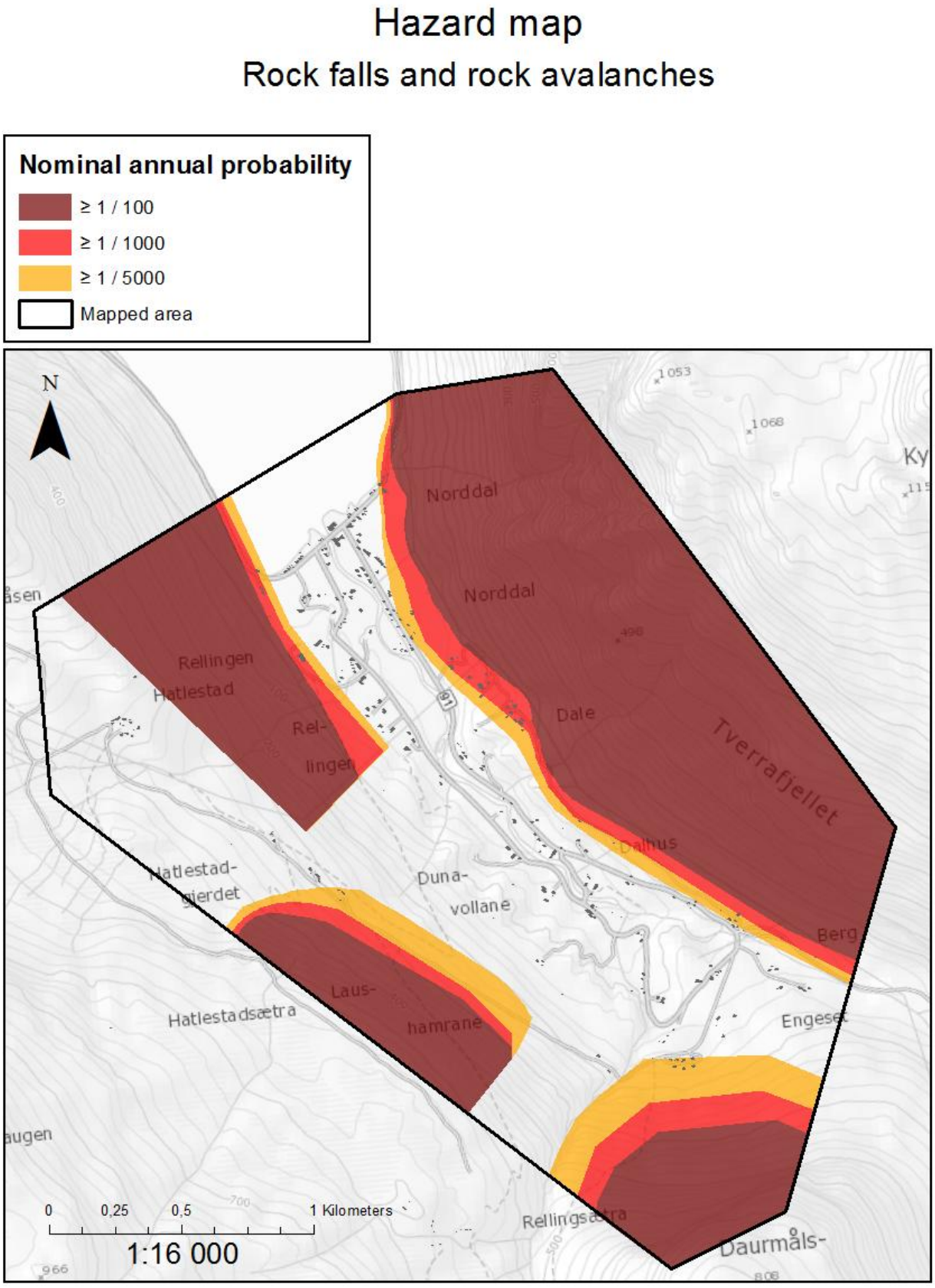

Figure 9-2: Hazard map for rock falls and rock avalanches

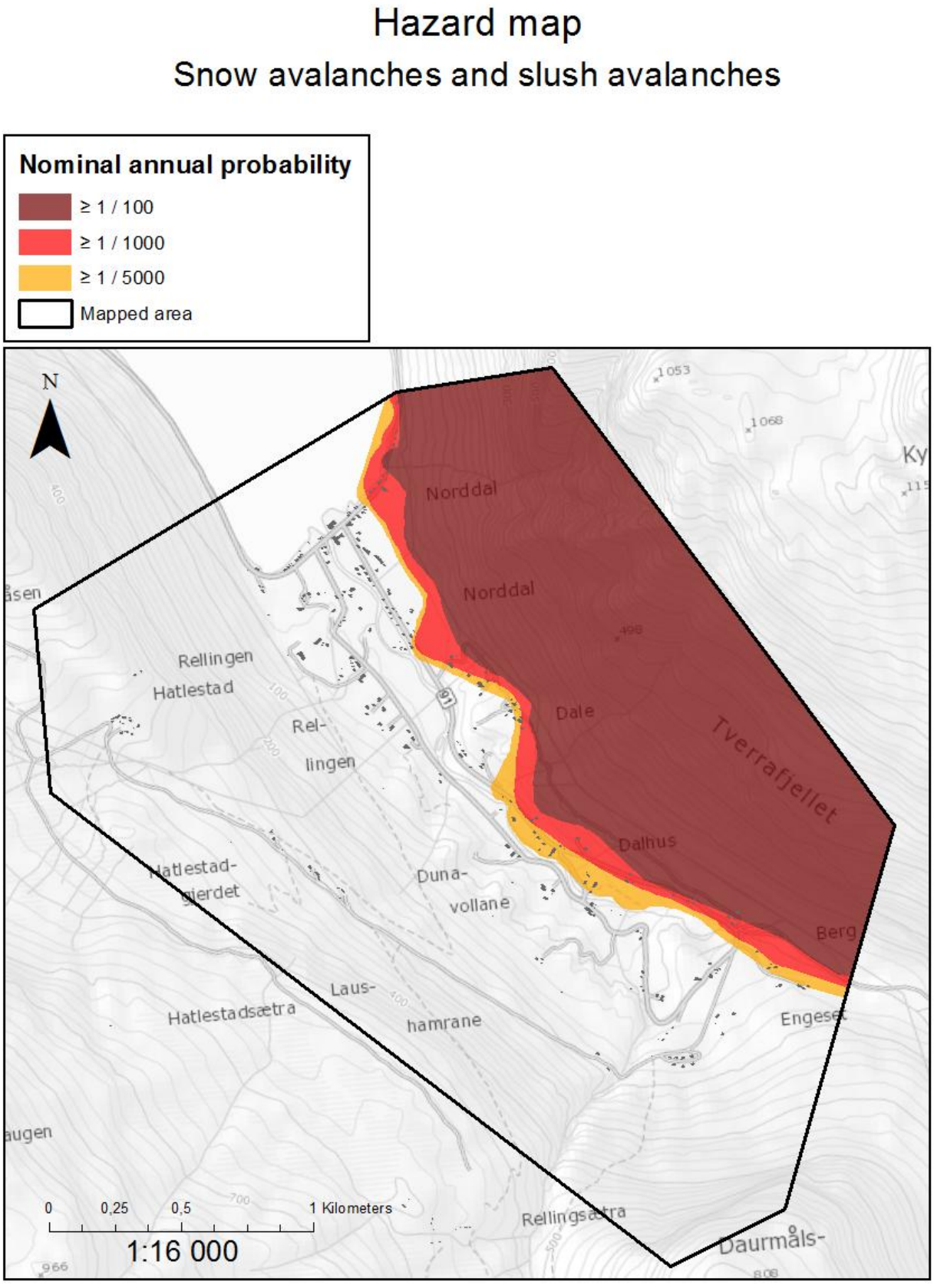

Figure 9-3: Hazard map for snow avalanches and slush avalanches.

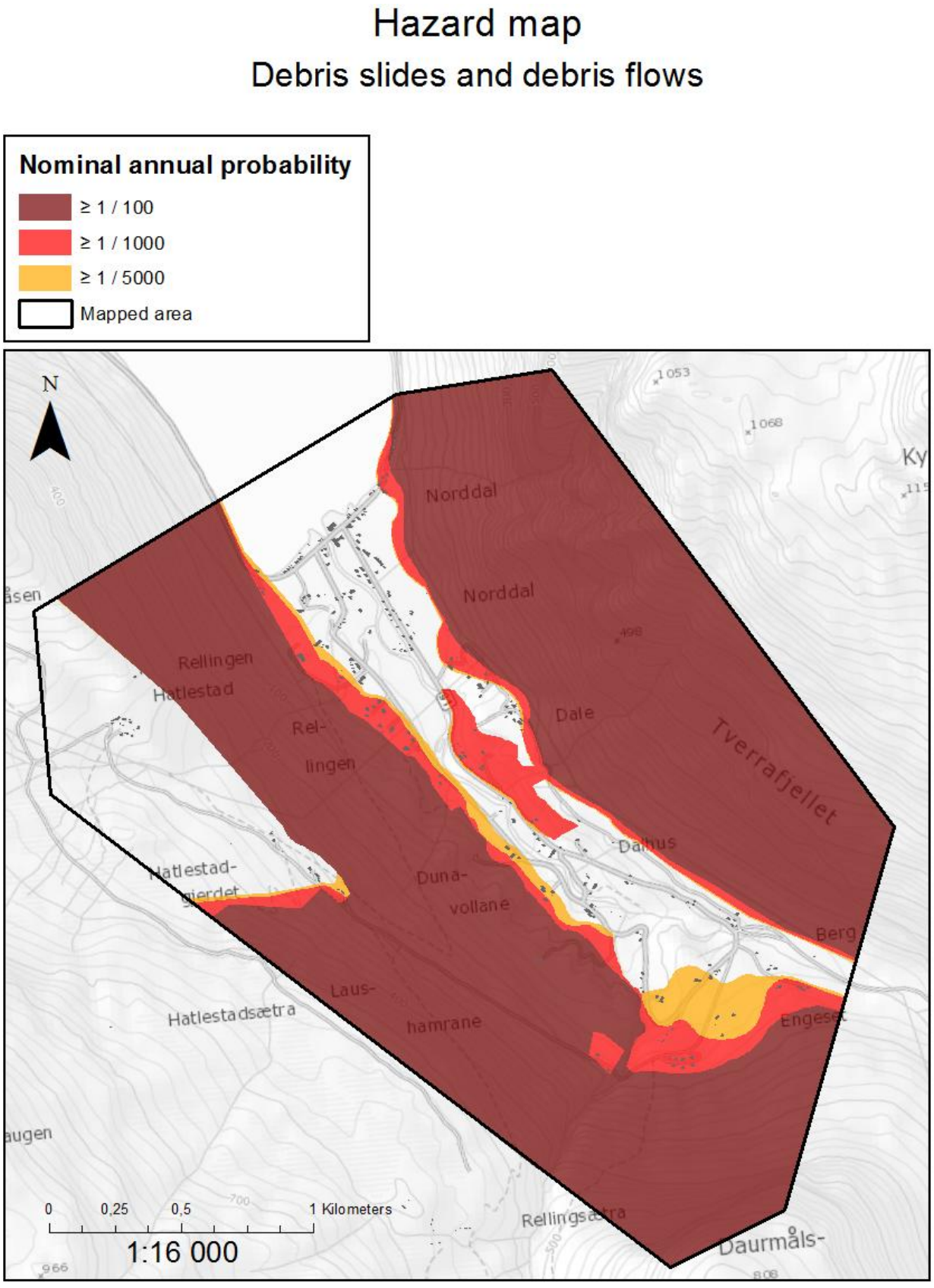

Figure 9-4: Hazard map for debris slides and debris flows.

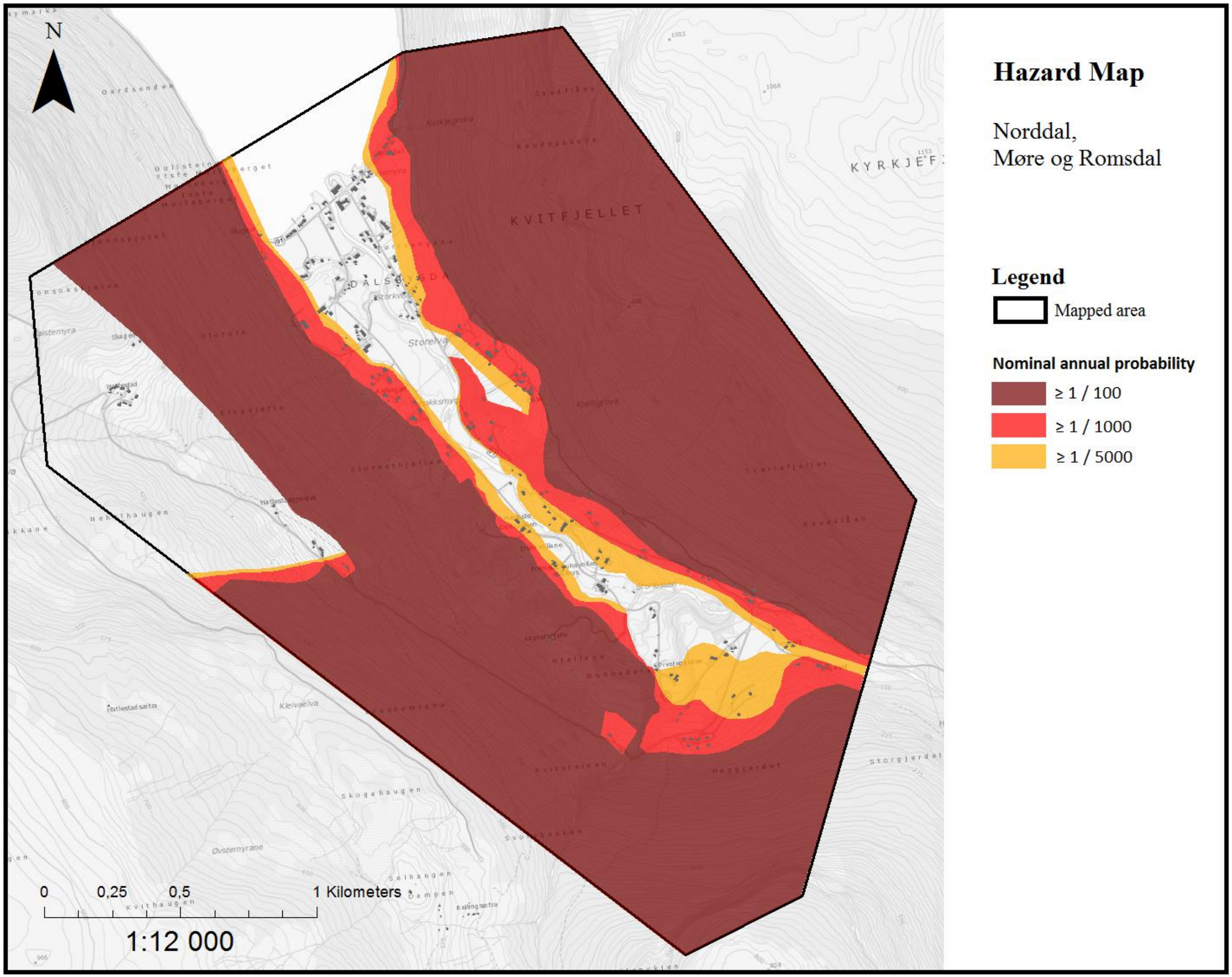

Figure 9-5: Total hazard map for Norddal, Møre og Romsdal.

9.7 Other hazards

9.7.1 Rock slides

The present detailed landslide hazard mapping does not take large failures with volumes > 10 000m^3 in bedrock into account, such as rock slides. The reason is that the dynamics of such events, and thus run out, is hard to predict. The same applies for the triggering factors for such events which are not fully determined. In *Norddal, Kvitfjellet* is the most evident rock slide threat, and the risk is determined as moderate in a regional survey mentioned in Chapter 5.4 (FylkesROS, 2011).

9.7.2 Tsunami from a rock slide into the fjord

After speaking with more than 20 inhabitants in *Norddal*, it has emerged that the possible threat of a tsunami following a rock slide at *Åkneset*, *Sunnylvsfjorden*, is their most prominent concern. This unstable mountain side shows present movement up to 20 cm per year and is under continuous monitoring with an evacuation plan existing in case of failure. A slide would likely cause a tsunami with an estimated runup height in *Norddal* of 2-3 m that would arrive in Norddal 7 minutes after the initiation. The runup could increase to 7-10 m if the entire unstable area (35 mill m^3) slides at once (Blikra et al., 2006). Several other unstable mountain slopes exist in the area such as *Hegguraksla* in *Tafjorden*. During the last 8-9000 years, the frequencies of large rock slides in *Tafjorden*, *Geirangerfjorden* and the inner part of *Sunnylvsfjorden* are estimated to be 5 events per 1000 year (Longva et al., 2009). New rock slides with tsunami initiation must, based on history and topography in the area, be expected, but projects related to prediction, monitoring and early warning are ongoing, working to decrease the risk for the coast communities in the area (Åknes/Tafjord Beredskap IKS, 2012).

9.7.3 River damming and flooding

Three flash flood events caused by damming of the rivers above *Norddal* are known to have occurred (Chapter 5.2), indicating that river damming is an existing threat. Flash floods and normal flooding are not take into account in this report, but can pose a threat for exposed areas near the rivers. The threat from flooding also applies to *Hatlestadelva* and seasonal creeks in the area.

10 Discussion

10.1 Climate

10.1.1 Interpolation of climatic data

The frequency analysis regarding return periods for extreme precipitation events revealed large uncertainties despite the availability of local meteorological observations. SeNorge.no offers interpolated meteorological data for 1x1 km grid cells for all of Norway, but uncertainty in the models must be taken into account. This is due to the precipitation pattern in Norway, with large differences between west and east, large topographic variations, as well as few observation stations widely spread throughout the country. Similarly, frequency analysis using interpolated values will always contain uncertainties, but accurate results can be obtained in areas with low topographic variability located near observational stations (Alfnes, 2007).

Time series of meteorological data in Norway seldom exceeds 100 years of data. Normal time spans are around 20 – 60 years. Such an amount of data is not enough to interpolate important precipitation values for a 1000 year period which would be desirable within landslide hazard mapping. A common rule of thumb is that valid interpolations can be made for time spans three times the length of the observational series (Taurisano, 2013b). Interpolations beyond this should be interpreted with caution. An ongoing project at NVE is addressing this issue as a contribution to improve landslide hazard assessment.

10.1.2 Future climate scenarios and landslides

There is a relatively broad consensus that the climate in Norway is changing toward a warmer and wetter climate. The GeoExtreme Project (www.geoextreme.no) discussed changes in climate and the influence on landslide and snow avalanche hazard in Norway. The climate in western Norway in the near future (50-100 years) is expected to include a higher frequency of intense precipitation events, generally more precipitation and warmer temperatures which have implications for the landslide and snow avalanche activity. Increased frequency of high precipitation rates will increase the frequency of debris slides and debris flows. Higher temperatures will reduce the risk of snow avalanches at 500-1000

m.a.s.l. but increase the hazard of wet snow and slush avalanches. Changes in precipitation patterns could also increase the hazard for landslides and snow avalanches in areas where they have not previously occurred (NOU, 2010). Landslides and snow avalanches are not only dependant on climate and weather but on the local conditions, also. Detailed forecast and predictions for the future are not possible, but Kronholm and Stalsberg (2009) developed a regional distribution for debris slide and snow avalanche hazards in Norway. For the region including *Norddal*, the results show a small increase in snow avalanche frequency and no change in debris slide frequency. The results do not take other parameters than meteorological into account such as local topography, geology, increased tree line or artificial influence on the local conditions. Increased probability of landslides due to climatic change does not necessarily lead to increased damage and/or loss of life. Through common sense, respect for building laws and landslide hazard mapping in vulnerable areas, it is possible to manage the outcome of tomorrow's climate (Jaedicke, 2009).

10.2 Sensitivity analysis regarding Rockyfor3D

Sensitivity analysis was performed for the input parameters used in Rockyfor3D. The model required large amounts of input data based on information obtained during field observations with regard to geographical extent and numerical values of properties reflected in the source and run out area. The results are determined in Figure 10-1 which shows the effects of the changed parameters relative to the run out length of modeled rock falls. The order is displayed in the legend, where the upper parameter in the legend represents the upper layer in the figure. The spatial resolution during calculations is 5x5 m, if nothing else is stated.

A) Change in block density

The change of density is associated with the fact that the mountain side consists of several rock types: gneiss, dunite and quartzite. The extent of the different rock types, shown in Figure 4-4, is not regarded as accurate enough to use in the model, as it does not appear consistent with observations. The solution was to check the density of gneiss (2700 kg m^{-3}) versus the density of quartzite (3200 kg m^{-3}). The results showed that the denser blocks may have a significant longer modeled run out in some areas.

B) Change in block shape

The change in block shapes shows that the ellipsoidal and spherical blocks reach further out into the flat field than the rectangular blocks, in some areas as much as 80 m. This is probably because they are given the opportunity to roll along the surface (modeled as small jumps according to the user manual (Dorren, 2012)), and it is, therefore, important to take this behavior into account if such source blocks are present. A significant difference between the spherical and ellipsoidal blocks is not detectable.

C) Change in block size

The block sizes are increased and decreased with 50% of the initial length, width and height of the blocks, leading to a significant change in volume. The run out increases with rock size (and weight), but the amount varies locally according to the underlying terrain. This implies that it is important to determine a reasonable block size to use during field investigations to assure that the most realistic run out is calculated.

D) Change in roughness values in the talus

The collection of roughness values requires the most attention in the field, and the user manual emphasizes that the model is sensitive against these values. The roughness values are, therefore, also the input parameter which has taken the most time to establish accurately during this project. While working with the model, it is confirmed that these values are very important regarding deposition of the modeled blocks. Smooth areas don't experience deposition in the talus slope at all, but it begins immediately outside the area if the roughness values increase. This can be seen in Figure 10-1D where the first deposition closely follows the polygon of talus extent marked by arrows. The same feature causes that depositional free areas seem to occur in locations where the roughness goes from higher to lower value indicated by an arrow in Figure 10-1A.

Depositional pattern reveals that a higher roughness causes a shorter run out and that small rocks are more sensitive to small roughness changes than the larger ones. The longest modeled run out length does not seem to necessarily change as much as the general pattern, although low roughness values cause more blocks to travel further. There appears to be no doubt that the roughness values must be prepared cautiously in order to obtain realistic run out predictions.

E)Change in calculation resolution

Increasing the resolution should, theoretically, give more accurate and realistic run out prediction. Three different spatial resolutions within the recommended values are used: 2 m, 5 m and 10 m spatial resolution. The highest resolution, 2x2 m, generally shows a more site specific depositional pattern than the lower resolutions, probably because it includes small terrain formations as depressions and small ridges. The model with the highest resolution models significantly more rock falls than the coarsest one, theoretically 25 times more as one 10x10 m source cell contains 25 source cells of 2x2 m resolution. This coincides well with the actual number of simulations which is 782 900, 3 123 600 and 19 563 100 for the 10x10 m, 5x5 m and 2x2 m resolution. Worth to mention is that the higher resolution generally increases processing time significantly and the finest resolution (2x2 m) uses 3.5 hrs. The maximum run out length for the different resolutions changes throughout the area, but it appears that in some areas the middle resolution, 5x5 m, leads to a shorter run out length than the coarser and finer resolutions. The reason for this is not clear. In other areas, it has as long or longer run out than the others. It is, therefore, difficult to draw a conclusion from the existing results, but the number of simulations in the different calculations probably play an important role in the developed pattern.

F) Change in number of simulations

Rockyfor3D allows the investigator to set the number of simulations that can be generated from each source cell. 1, 10, 100 and 500 simulations are performed from each source cell. From the results, it is observed that one simulation is not enough to reflect the actual rock fall run out in some areas, as most of the block stops within the talus slope. The run with 500 simulations shows a more distinct pattern than the run with 10 simulations, but the run out length for these are longer than for the run with 100 simulations in some areas. This is the same pattern which is revealed for the different resolutions, but only appears on some parts of the area. An explanation for the pattern is not determined.

Figure 10-1 (next page): Results from sensitivity studies of Rockyfor3D.The figure shows how change in input parameters affect the modeled rock fall run out. A) Change in density of rock fall blocks. B) Change in shape of rock fall blocks. C) Change in size of rock fall blocks. D) Change in surface roughness. E) Change in calculation resolution. F) Change in number of simulated rock falls from each source cell.

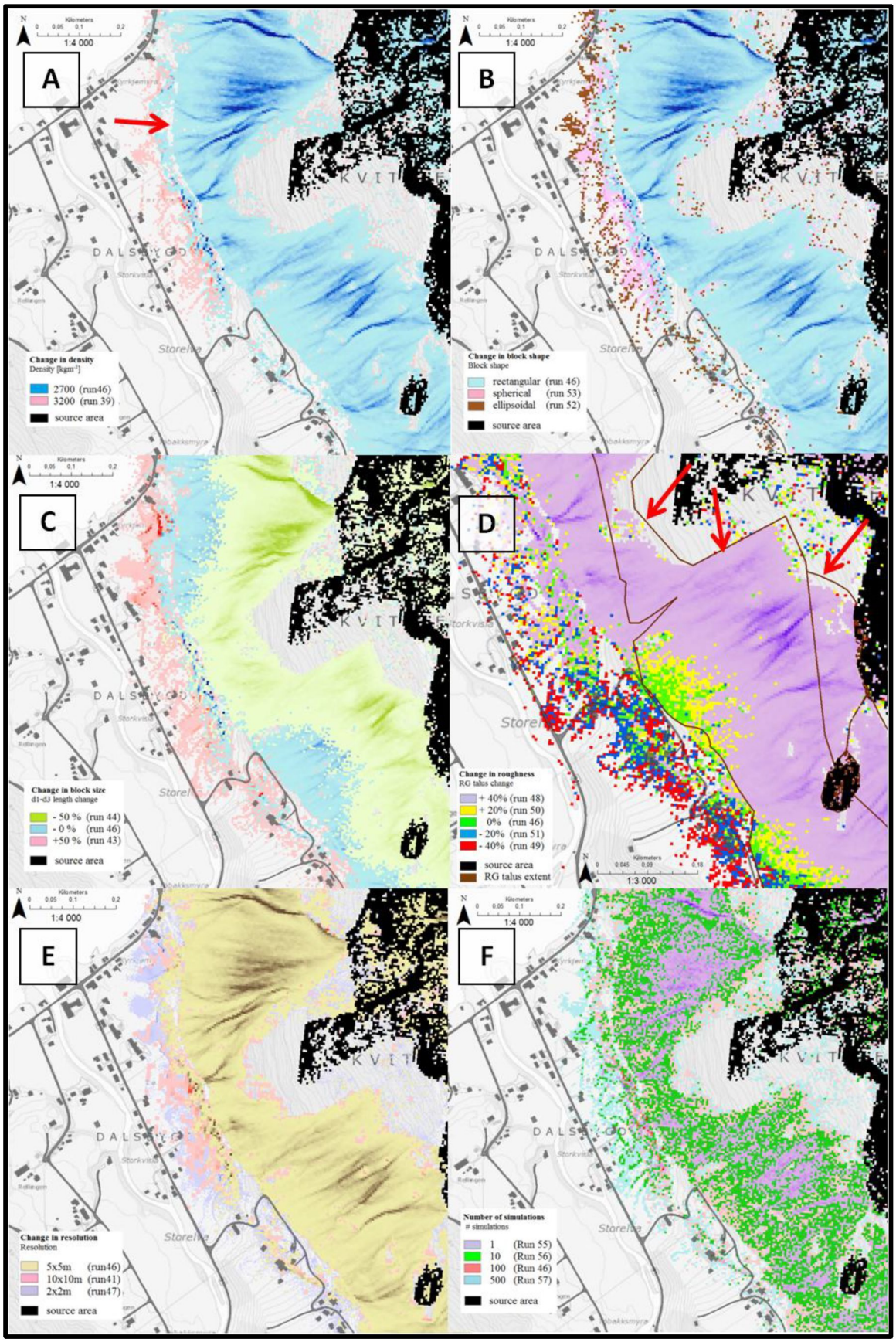
A
Change in density
Density [kgm-3]
2700 (run46)
3200 (run 39)
source area
B
Change in block shape
Block shape
rectangular (run 46)
spherical (run 53)
ellipsoidal (run 52)
source area
C
Change in block size
d1-d3 length change
- 50 % (run 44)
- 0 % (run 46)
+50 % (run 43)
source area
D
Change in roughness
RG talus change
+ 40% (run 48)
+ 20% (run 50)
0% (run 46)
- 20% (run 51)
- 40% (run 49)
source area
RG talus extent
E
Change in resolution
Resolution
5x5m (run46)
10x10m (run41)
2x2m (run47)
source area
F
Number of simulations
simulations
1 (Run 55)
10 (Run 56)
100 (Run 46)
500 (Run 57)
source area
1:4 000
1:3 000

F) Effect of forest

Rockyfor3D gives the opportunity to take forest cover into account. This can be done either by using the coordinates of all the single trees and their diameter at breast height (DBH) or by a set of rasters giving the density of stems per hectare, mean and standard deviation of DBH, and the percentage of coniferous trees. This information is used to create a file of randomly spread trees according to the values and extent given. This was performed in a test on the western valley side, which is densely covered by forest. The values used can be found in Table 10-1, but the results did not show any clear effect from the dense forest. This was probably due to the large block size chosen [3 m³], and is consistent with other surveys. From these tests, it was decided not to take forest cover into account. Implementation of forest cover can be a valuable tool in local rock fall hazard assessments in areas with dense forest and small rock fall blocks. An abundance of research on forest as a protection measure against rock falls has been performed, e.g. by Stoffel et al. (2006); Dorren and Berger (2010).

Table 10-1: Input values for the forested areas in Rockyfor3D calculations. Two calculations are performed with varying number of trees and mean DBH. Data was obtained from field observations and the extent of the forest cover from aerial photos.

	Forest type	# trees	Mean DBH	StD DBH	Coniferous
		[ha^{-1}]	[cm]	[cm]	[%]
Run 1	Coniferous forest	900	40	10	95
	Deciduous forest	2500	18	5	5
Run 2	Coniferous forest	2500	30	10	95
	Deciduous forest	4444	15	5	5

Final remarks on the sensitivity studies

The sensitivity studies did not reveal any surprising results, such as the fact that a large, heavy block normally travels further than a smaller, lighter one. It is interesting to note the amount of difference in run out length changes/uncertainties in the input parameters may cause. It is important to remember that the terrain, represented by a digital elevation model, acts as the basis for the model. Several detected changes in run out are not consistent across the valley side, which implies an underlying effect from terrain variations and the importance of terrain for rock fall run out. The results obtained here are from a limited set of experiments in one area, but they, nonetheless, still show how an important result, calculated run out, might differ noticeably by just small changes in one or more input parameters. This

should be taken into account when model results are evaluated during landslide hazard mapping.

10.3 Use of models in landslide hazard mapping

One of the main objectives in landslide hazard studies is to predict the dynamic behavior and properties of rock falls, snow avalanches or debris flows as they move down a mountain side. Accurate and realistic prediction of trajectories, run out distances and velocities is essential to develop a hazard map of high utility value (Dorren, 2003; Christen et al., 2012). The use of numerical models is an old and constantly developing assessment to help establish and predict this information. Numerical simulation is very difficult as the dynamic processes are controlled by different types of movement mechanisms in interaction with the surroundings (Christen et al., 2012). A large variety of both empirical and process-based models exist. While empirical models provide fast and approximate run out information, a process-based model can provide a more precise result and offer additional information, but the model also requires more effort and software to perform the mapping (Dorren, 2003).

The advantage of simple empirical models, like the α,β-model, is the minor effort and input required. Empirical models are often expressed as a geometric relationship based on topographic features which are simple to recognize in the field. Valid results require similar conditions in the area of interest that are consistent with the original events on which the model is based. This is not the case for all modeled transects in *Norddal*, see transect #2, #3 and #5 in Figure 8-4. A glacio-fluvial terrace creates implications for the first two transects, while direct interpretation of the latter provides an indication of possible snow avalanche run out high up in the opposite valley side. Another disadvantage is that it does not take size of the avalanche into account; for example, a 10 m wide avalanche receives the same calculated run out as a 100 meter wide one. A significant advantage of more complex models, such as RAMMS, is that the model reveals how the terrain will influence the direction of movement of a landslide or snow avalanche, which is extremely useful information, and also takes size of release area and volume into account.

As the physics within a model and model input will always be a simplification of the real system, the model output will never predict reality, and can, therefore, only provide an indication of the behavior and run out of an actual landslide. During the last decade, several

programs have been developed into versions of 2D and 3D, allowing an informative and elaborate graphical user interface. As long as the physical model is not further developed, the misconception of a better and more realistic model outcome could result.

Process-based models, such as Rockyfor3D, allow the user to determine detailed input parameters. If the model itself does not simulate realistically, the output will not reflect reality regardless of how accurately the input is perceived. The opposite also applies; a well-proven model can provide unrealistic results if the input used is incomplete and inaccurate. Another realization which users of models like Rockyfor3D need to be aware is that the model computes the number of simulations requested. Often, large numbers of simulations are computed to reveal potential depositional patterns that can give an impression of high rock fall activity if you only take the modeled results into account. A model does not make reference to the return period of an event. The actual rock fall activity of a location can only be revealed from field observations, historical events and communication with local inhabitants. The use of run out models is, therefore, only one of several tools in a landslide hazard assessment. The results must be evaluated cautiously and in connection with additional information.

10.4 Other methods within landslide hazard mapping

Several other methods can be applied to provide useful information for a landslide hazard assessment. In the following, four methods are briefly described. These methods were not applied in the present assessment due to limited time, resources and/or suitability.

10.4.1 Excavation pits

Subsurface investigations can be made by digging pits in the soil. This could be done on fans beneath distinct ravines and gullies where debris floods are thought to regularly occur or beneath soil covered valley sides. Pits can reveal previous landslide activity by the presence of deposits, and the time of deposition can, in some cases, be dated using radiocarbon dating methods. Stratificated deposits can contain evidence regarding the type of process involved, and deposits from repetitive events can provide information to determine the frequency. An

example of this can be found in Sletten (2004). Information collected from such pits is local information and, therefore, gives limited information about the surrounding areas. Interpretation and evaluation of landslide deposits require experience and knowledge regarding soil and depositional processes. Internal environmental, health and safety (EHS) routines in NVE also demand structural measures when excavations exceed 1.5 m, which requires more time and equipment (Taurisano, 2013b). Due to the challenges associated with interpretation of deposits and limited spatial extent of the data collected, this method is most suitable in local investigations.

10.4.2 Geophysical surveys

Geophysics comprises several sub-surface investigative methods. The most common are seismic and ground penetrating radar (GPR), but a great variety of methods exist using different material properties to distinguish various substrates from each other. Geophysics is widely used within quick-clay mapping, but it can also be used for other landslide types. Lecomte et al. (2012) used, among other methods, seismic, GPR and electrical resistivity tomography (ERT) to investigate a complete debris flow system in *Jotunheimen*, Norway. Similar to the aforementioned excavation pits, interpretation of geophysical results requires detailed knowledge about the methodology and experience from similar conditions. Separating material of comparable properties, such as different landslide deposits and the surrounding soil, can be very challenging. An advantage is that a large area can be surveyed relatively fast.

10.4.3 Helicopter survey

Helicopter survey is in certain circumstances the only way to obtain information regarding possible source areas for rock falls and rock slides in inaccessible mountain faces. The method allows one to determine information from various angles, and several locations can be investigated in relatively short time. The disadvantages are high cost and occasionally low availability; the use of a helicopter must often be decided and reserved a long time in advance.

10.4.4 GigaPan photography

GigaPan photography allows one to create digital images with billions of pixels that provide a very high resolution image. A GigaPan, which is an abbreviation for gigapixel panoramas, is a set of hundreds to thousands of photos that are combined to create a single highly detailed photograph resulting in excellent depth and clarity. The photos are taken by using a robotic camera mounts, which may be used with nearly all types of digital cameras (GigaPan, 2013). This technology allows one to create detailed images of mountain sides and cliffs from distance and can be utilized to study fractures and joint systems in inaccessible mountain faces. The method is relatively new and can, in some cases, provide the same information as the more expensive helicopter surveys.

10.5 The effect of forest on landslide hazard zonation

In the conducted landslide hazard mapping of *Norddal*, the presence of forest cover is taken into consideration in the evaluation of the type of mass movement processes that can occur in the different areas. This is especially apparent in the western valley side where snow avalanches are excluded due to dense forest cover. A forest influences wind, precipitation, solar radiation and temperatures in the surrounding micro-climate, all parameters that are important regarding landslide initiation. Forest cover will, in most cases, reduce the landslide hazard (Breien et al., 2013).

NGI is involved in a project to determine how forest cover influences the hazards from snow avalanches, rock falls and debris slides in Norway. The first report regarding forest as a mitigation measure has recently been completed. It illustrates how forests influence landslide hazards and proposes criteria that can be implemented for protection forests in Norway (Breien et al., 2013).

With regard to snow avalanches, the focus of the report is on preventing a release and suggests criteria regarding coniferous forests as protection forests. It concludes that most of the planted fields of spruce in Norway satisfy these criteria within a reasonable margin and could, therefore, potentially be given the status as a protection forest. Regarding deciduous forest, no distinct criteria are determined, since birches especially near the tree line in

Norway are short and broad compared to their lowland relatives. Since the anchoring effect and effect on snow layers from deciduous forest in Norway still are regarded as uncertain, further research is needed. It is expected that protection forest criteria for deciduous forest in Norway will be prepared in the future (Breien et al., 2013).

Protection forests with regard to rock falls focus more on the forests' role as a physical barrier, an effect which is not questioned (Perret et al., 2004). When considering the protective measure of a forest against rock falls, both properties of the forest and the rock fall must be taken into account. NGI (Breien et al., 2013) suggests minimum values regarding rock fall block sizes and forest properties; see Table 10-2, where the block size represents the blocks which can be stopped by the respective forest properties.

Table 10-2: Minimum values for protective forests in relation to rock falls (Breien et al., 2013).

Block size	DBH*	Density
[m^3]	[cm]	[trees/ha]
< 0.05	12 - 20	> 600
0.05 - 0.2	20 - 35	> 400
> 0.2	> 35	> 200
1	40	> 350
< 2	50	> 300
> 2	special evaluation	
> 5	no effect	

* mean tree diameter at breast height

A landslide hazard assessment must take vegetation and forest cover into account. It is a general view that snow avalanches don't release in dense coniferous forests, but in areas of deciduous forest, sparse and/or low vegetation, special attention is required. Forest cover also reduces energy and run out of especially small rock falls, but it cannot be expected to stop all the rocks even if it satisfies the requirements for protective forests. It only reduces the annual probability of rock falls reaching the underlying terrain. Vegetation, also, improves slope stability through changes in hydrological and mechanical properties of the root – soil matrix, and, thus, reduces the risk of debris slides and flows (Stokes et al., 2008). Still, debris slides and debris floods occur in densely forested slopes, as in *Kvam* in *Gudbrandsdalen* during heavy rain in June 2011 (Figure 2-3) and, therefore, forest cover cannot exclude the hazard from potential debris slides and debris flows in a till-covered slope.

10.6 Guidelines / regulations

In the regulations encompassing safety against natural hazards (TEK10), which acts as the basis for landslide hazard assessments in Norway, hazard zones should be classified as areas with probability of "damages or substantial inconvenience" in response to the different safety classes. This can be interpreted differently from agency to agency or person to person. Buildings in Norway often have a weak structure since they are mainly made of wood, and, thus, don't have the strength to withstand slow moving slush avalanches or debris flows. This should be taken into account in hazard zoning, but provokes the scenario of two neighboring houses, one of wood and one of concrete which, theoretically, could be located on each side of a hazard zone. Vague definitions of regulations can create different outcomes depending on interpretation of the rules. The same applies to nominal properties which must be taken into account. There is no certain way to determine exactly what a 1/1000 or 1/5000 landslide event will be like. This requires that conditional judgment is applied and, therefore, make it personal dependant. In areas where no distinct landslide or snow avalanche paths can be defined, such as along open, steep valley sides, hazard zones should be determined for 30 m wide sections perpendicular to the slope. In case of direct interpretation of this rule along a 3 kilometer long mountain side prone to snow avalanches, statistically one snow avalanche from the mountain side should reach the end of the hazard zone every 10^{th} year. This interpretation is seldom used in Norway today.

Typical practice within the Norwegian scientific environment is to use the dominant process to determine the extent of the hazard zone, although more processes may occur in the area (NVE, 2012b). Dependable frequency analysis is hard to determine. A hazard zone of 1000 years return period is determined from substantial reported events in the area, field observations of landslide deposits or from analytical evaluation of how far a large infrequent slide will reach in the area. As more areas in Norway are mapped under the auspices of NVE, it is important to determine an agreed upon interpretation of the governmental regulations, so one can ensure that all mapped areas possess the associated safety class based on the correct foundation.

10.7 Hazard zone determination in *Norddal*

10.7.1 Limitations

As mentioned previously, this hazard assessment addresses rock falls and rock avalanches, debris slides and debris flows, and snow avalanches and slush avalanches. Floods, flash floods from river damming, rock slides and their secondary effects, such as tsunamis, are not taken into account. The assessment also takes into account the predicted changes of climate conditions in the near future (50-100 years). The changes are thought to be increased rates of precipitation, such as rain, which can increase the frequency of debris slides, and increased hazard from wet snow avalanches as the temperature increases. Change in vegetation cover, together with excavation in slopes covered by loose soil, is the single parameter which could substantially change the present presumptions used in the assessment. Multiple residents expressed opposition to the present fields of planted coniferous trees which cause little diversity in vegetation cover. Complete logging of these fields, which exists in the till-covered western and south-western slope (Figure 7-2) would drastically change the small-scale hydrological conditions in the area. This circumstance would again increase erosion and probability of debris slide and debris flow occurrence, and open new areas for snow avalanche release. In some areas, it would also decrease the mitigating effect against rock falls. If logging is considered, NGI provides guidelines regarding how to minimize the undesirable effects of logging (Breien et al., 2013).

A landslide hazard assessment is a compromise of efficiency, range and level of details; the need for expert judgment increases when the level of details decreases. This project is at the feasible level for an area of this size. More detailed surveys aimed at single objects like a house, for instance, can entail a higher level of details and, thus, require less expert judgment. This would necessitate increased time and detailed field work at the site location, but would not necessarily reveal major changes in the final hazard zones. In the case of Rockyfor3D rock fall modeling, a more detailed study could include measurements of thickness and location of each single tree in the area or more detailed surface roughness input data.

10.7.2 Challenges

Linking the probability and possible run out length is the major challenge in most landslide hazard zone assessments. *Norddal* shows a high potential for all types of mass movements, but detailed records for only a few large events are known. The exception is the 1996 *Kvitfjellet* rock avalanche and snow avalanche which caused damage near *Berg*, but it is unknown if the damage was caused by the avalanche or a pressure wave. One more large snow avalanche event was recorded, along with several large debris slides. No signs of these events were present near the settlement today, and interviews did not reveal any clarifying information. Removal of possible deposits from debris slides and rock falls in relation to agriculture must also be regarded, since the areas close to the slopes are mostly cultivated land.

10.7.3 Methodology

A statistical approach in terms of landslide history and geomorphology is used to define the hazard zones, when there is a lack of information and evidence from historical events that is considered important. The topography in *Norddal* generally shows a high potential for landslides and snow avalanches. Large events are reported within all mass movement types, and the geomorphology offers details about events which have occurred after the last glaciations (~10 000 BP). The extent of the talus reveals evidence about the reach of rock falls and rock avalanches, and fresh blocks reveal present activity. The same applies for debris slide and debris flows which have eroded and deposited on the glacio-fluvial terraces. Vegetation cover can expose vast information about the frequency of landslide events, as different trees have different growth rates. Adult spruce forests ready for logging in Norway normally have a growth rate of 70-80 years (snl.no, 2013), and if such are present in a valley side, one can assume that no large debris slides or snow avalanches occurred at this location during the last ~70 years. Common to these frequency estimations are the approximate values that are often based on relative order and must be assessed with this regard.

The hazard zones are determined from the available information and expert judgment. The importance of geomorphologic features, such as the talus, is emphasized and is often decisive for the 1/100 hazard zone for rock falls. A limited numbers of larger rock fall deposits are present outside the talus and are, together with modeled run out, used to

determine the 1/1000 hazard zone. The probable removal of a significant number of rock fall deposits from the fields is taken into account. The same applies for steep till-covered slopes and debris flow deposited fans when determining a hazard map for debris slides and debris flows. For snow avalanches, vegetation cover, topography and revealed landslide history are important in the hazard zone determination. The snow avalanche run out models are also a valuable tool which have been emphasized in the 1/1000 hazard zone determination. The 1/5000 hazard zone is more diffuse in its appearance, and the applicable information available is often limited. These are, therefore, often mapped near the 1/1000 zone if no additional information from maximum run out modeled or geomorphologic evidence indicates otherwise.

Hence, it is concluded that this project has obtained the necessary documentation for an appropriate landslide hazard mapping assessment according to the present regulations. Together, the methods used provide an accurate overview of the landslide and snow avalanche activity in *Norddal*. The scientific community performing landslide hazard analysis in Norway generally has the same methods and information available, such as access to run out models, digital elevation models and climatic data for entire Norway. Yet, the detail level of the work performed varies considerably within the different surveys and companies. Therefore, a common guideline explaining the methodology should be developed. This guideline should include mandatory methods for different scales of mapping, such as topographic and climatic investigations or certain models, but should also include methods which can be performed if they are thought to contribute to the target assessment and/or could include local assessments. These could include subsurface investigations or detailed run out modeling using local input parameters (Rockyfor3D). Most importantly, the guidelines should include how to connect the obtained results with the different hazard zones. This could involve specific methods to calculate return periods of extreme precipitation events and/or delineate which modeled pressures exerted from snow avalanches can be tolerated within each hazard zone. The latter may be inspired from the Alps, where Austria has snow avalanche hazard zones that are determined from both recurrence intervals and exerted pressure (Sauermoser, 2006).

11 Conclusion

The project has revealed the importance of using several methods in landslide hazard assessments. The meteorological conditions revealed a relatively high frequency of precipitation events favorable for landslide initiation, while the landslide database showed that these events seldom caused any landslides. The same applied for modeling which revealed large potential for long run outs, while inhabitants related that they seldom or never heard about events threatening the settlement or occurring in those target locations. Several methods needed to be applied to obtain a complete record of the danger posed by landslides and snow avalanches in a given area. As all methods hold various shortcomings and uncertainties, expert judgment is still regarded the most important one.

Various interpretations of governmental regulations and levels of expertise among surveyors will create implications since several areas throughout Norway are expected to be mapped by different companies. A variety of suitable methods exist, but the development of common guidelines should provide more specific information about what and how mapping should be done. The guidelines should be based on information and methods that are available and/or realistic to collect and include how the methods should be interpreted regarding the different hazard zones. An evaluation of the governmental regulations should be considered to determine if it is possible to implement new criteria which could be more closely related to the methods. However, it is still important to include expert judgment in the landslide hazard methodology since models nor statistical tools can replace expert judgment in the complex system of different hazards, their damage potential and frequency.

The meaning of landslide hazard mapping is to ensure that people and settlements are exposed to as low risk as possible, and to avoid locating new settlements in high risk areas. Damage caused by landslides and snow avalanches outside the hazard zones can not be excluded, but they are regarded as low probability events. A large part of the inhabitants in *Norddal* today live in an area which do not meet the governmental regulations. It is currently up to the local authority along with NVE to decide if any mitigation measures should be implemented to reduce the risk and meet the defined regulations.

References

Alfnes, E. (2007) Ekstremnedbør beregnet fra serier med gridbasert arealnedbør. *Met.no report 1/2007.* Oslo: Meteorologisk institutt. 21pp.

Anda, E. and Flataukan, J. (1998). *Planlagt hyttefelt på GN/BNR 51/3 i Norddalen - skredfare*. Brev til Norddal kommune, sektor for teknisk, næring og miljø, 25.04.2002.

Anda, E. and Flataukan, J. (2002). *Frådelingssak ved Dale i Norddalen - Skredfare*. Brev til Norddal kommune, 30.05.2002.

Anda, E. and Flemsætherhaug, B. (1996). *Skredet i Norddalen den 4.11.96 - fare for nye skred?* Brev til Norddal kommune, teknisk etat, 14.11.1996.

Anda, E. and Holten, B. (1998). *Skredet ved Relling i Norddalen den 18. februar 1998*. Brev til Norddal kommune, teknisk etat, 26.02.1998.

Bakkehøi, S., Domaas, U. and Lied, K. (1983). Calculation of snow avalanche runout distance. *Annals of Glaciology, 4*, p.24-29.

Bjerrum, L. and Jørstad, F. (1968) Stability of rock slopes in Norway. *NGI Publication 79.* Oslo: Norwegian Geotechnical Institute. p.1-12.

Blikra, L. H., Anda, E., Høst, J. and Longva, O. (2006) Åknes/Tafjord-prosjektet: Sannsynlighet og risiko knyttet til fjellskred og flodbølger fra Åknes og Hegguraksla. *NGU Report 2006.039.* Trondheim: Norges geologiske undersøkelse. 20pp.

Brattlien, K. (2012). *Skredulykke Sorbmegaisa, Troms mandag 19.03.2012.* Retrieved 23.10, 2012, from http://www.ngi.no/upload/Snøskred/Ulykker/ulykker_2012_19mars_Sorbmegaisa.pdf

Breien, H., Høydal, Ø. A. and Sandersen, F. 2013. *Forslag til kritertier for vernskog mot skred - DEL 1*. Oslo: Norges geotekniske institutt, 48pp.

Christen, M., Bartelt, P. and Gruber, U. 2002. *AVAL-1D Numerical calculation of dense flow and powder snow avalanches. User manual.* Davos, Switzerland: Swiss Federal Institute for Snow and Avalanche Research, 136pp.

Christen, M., Bartelt, P., Kowalski, J. and Stoffel, L. (2008). *Calculation of dense snow avalanches in three-dimensional terrain with the numerical simulation program RAMMS*. Proceedings of the International Snow Science Workshop, Whistler, BC, Canada. p.709-716.

Christen, M., Bühler, Y., Bartelt, P., Leine, R., Glover, J., Schweizer, A., Graf, C., McArdell, B. W., Gerber, W. and Deubelbeiss, Y. (2012, 23-27th Apr.). *Integral hazard management using a unified software environment - numerical simulation tool "RAMMS" for gravitational natural hazards.* 12th Congress INTERPRAEVENT 2012, Grenoble, France. 10pp.

Christen, M., Kowalski, J. and Bartelt, P. (2010). RAMMS: Numerical simulation of dense snow avalanches in three-dimensional terrain. *Cold Regions Science and Technology, 63*, 1, p.1-14.

Dale, Å. (2012, Aug). [Personal communication - verbal, e-mail and mail correspondence].

Derron, M.-H. (2010). *Technical Report: Method for the susceptibility mapping of rock falls in Norway*. Geological Survey of Norway (NGU) and Institute of Geomatics and Risk Analysis, University of Lausanne, Switzerland. 22pp.

Dorren, L. (2003). Review of rockfall mechanics and modelling approaches. *Progress in Physical Geography, 27,* 1, p.69-87.

Dorren, L. 2012. *Rockyfor3D (v5.0) revealed - Transparent description of the complete 3D rockfall model*. ecorisQ paper (www.ecorisq.org). 31pp.

Dorren, L. and Berger, F. (2010). *New approaches for 3D rockfall modelling with or without the effect of forest in Rockyfor3D.* Geophysical Research Abstracts, EGU 2010. 12, 11pp.

Dorren, L. and Heuvelink, G. (2004). Effect of support size on the accuracy of a distributed rockfall model. *International Journal of Geographical Information Science, 18*, 6, p.595-609.

Dorren, L., Maier, B., Putters, U. S. and Seijmonsbergen, A. C. (2004). Combining field and modelling techniques to assess rockfall dynamics on a protection forest hillslope in the European Alps. *Geomorphology, 57*, 3, p.151-167.

eklima.no. (2013). *Eklima - free access to weather- and climate data from Norwegian Meteorological Institute from historical data to real time observations*. Retrieved 2013, last time 28.05, from www.eklima.no

Fischer, L., Rubensdotter, L., Sletten, K., Stalsberg, K., Melchiorre, C., Horton, P. and Jaboyedoff, M. (2012). Debris flow modeling for susceptibility mapping at regional to national scale in Norway. In Eberhardt et al. *Landslides and Engineered Slopes: Protecting Society through Improved Understanding*, p.723-729.

Furseth, A. (1987) *Norddal i 150 år 1837-1987.* Norddal kommune. 100pp.

Furseth, A. (2006) *Skredulykker i Norge.* Oslo: Tun Forlag. 207pp.

Furseth, A. (2009) *Dommedagsfjellet - Tafjordulykka 75 år etter*. Oslo: Samlaget. 175pp.

FylkesROS. (2011) Risiko- og sårbarheitsanalyse for fjellskred i Møre og Romsdal. Fylkesmannen i Møre og Romsdal, Møre og Romsdal fylkeskommune, and Norges geologiske undersøkelse. 105pp.

Førland, E. J. 1984. *Påregnelige ekstreme nedbørverdier*. Oslo: DNMI, 32pp.

Gauer, P. (2013, 11.04). [Personal communication - e-mail].

GigaPan. (2013). *GigaPan*. Retrieved 19.05, 2013, from www.gigapan.com

Gjelsvik, T. (1951) Oversikt over bergartene i Sunnmøre og tilgrensende deler av Nordfjord. *Norges geologiske undersøkelse 179.* Oslo: Aschehoug. 45pp.

Henderson, I., Saintot, A. and Derron, M. (2006) Structural mapping of potential rockslide sites in the Storfjorden area, western Norway: the influence of bedrock geology on hazard analysis., *NGU Report 2006.052.* Trondheim: Geological Survey of Norway. 83pp.

Hestnes, E. (1980) Skredfarevurdering. *Publikasjon 132.* Oslo: Norges geotekniske institutt. p.61-81.

Hestnes, E. (1985). A contribution to the prediction of slush avalanches. *Annals of Glaciology, 6*, p.1-4.

Hungr, O., Evans, S., Bovis, M. and Hutchinson, J. (2001). A review of the classification of landslides of the flow type. *Environmental & Engineering Geoscience, 7*, 3, p.221-238.

Jaboyedoff, M., Dudt, J.-P. and Labiouse, V. (2005). An attempt to refine rockfall hazard zoning based on the kinetic energy, frequency and fragmentation degree. *Natural Hazards and Earth System Science, 5*, 5, p.621-632.

Jaedicke, C. (2009). Økt skredfare kan avverges. *Klima, 1*, p.30-31.

Jaedicke, C., Solheim, A., Blikra, L., Stalsberg, K., Sorteberg, A., Aaheim, A., Kronholm, K., Vikhamar-Schuler, D., Isaksen, K. and Sletten, K. (2008). Spatial and temporal variations of Norwegian geohazards in a changing climate, the GeoExtreme Project. *Natural Hazards Earth System Science, 8*, p.893-904.

Jakob, M. and Hungr, O. (2005). *Debris-flow hazards and related phenomena*. Berlin: Springer. p.9-23.

Jamieson, B., Margreth, S. and Jones, A. (2008). *Application and limitations of dynamic models for snow avalanche hazard mapping*. Proceedings of the International Snow Science Workshop, Whistler, B.C. p.730-739.

Kronholm, K. and Stalsberg, K. (2009). Klima endringer gir endringer i skredhyppigheten. *Klima*, *3*, p.34-36.

Landrø, M. (2007) *Skredfare: snøskred, risiko og redning.* Oslo: Fri Flyt. 169pp.

Lecomte, I., Juliussen, H., Støren, E. W. N., Sauvin, G. C., Hamran, S.-E., Lavrientiev, I., Petrakov, D., Kutuzov, S. and Tissot, S. (2012, 3-5th September). *Geophysical Investigations of Unstable Mountain Slopes in Jotunheimen, Norway.* Near Surface Geoscience 2012 - 18th European Meeting of Environmental and Engineering Geophysics, Paris, France. 5pp.

Lied, K. (1992) Snø- og steinskred. Kartlegging og erfaringer. *Publikasjon 183.* Oslo: Norges geotekniske institutt. 19pp.

Lied, K. and Bakkehøi, S. (1980). Empirical calculations of snow-avalanche run-out distance based on topographic parameters. *Journal of Glaciology*, *26*, 94, p.165-177.

Longva, O., Blikra, L. H. and Dehls, J. F. (2009) Rock avalanches - distribution and frequencies in the inner part of Storfjorden, Møre og Romsdal County, Norway. *NGU Report 2009.002*: Geological Survey of Norway. 32pp.

NGU. (2012). *Geological database* Retrieved 15.11, from Geological Survey of Norway http://www.ngu.no/no/hm/Kart-og-data/nedlasting/

Norem, H. (2011) Veger og snøskred. *VD rapport 27.* Oslo: Vegdirektoratet. 94pp.

NOU. (2010) Tilpassing til eit klima i endring: samfunnet si sårbarheit og behov for tilpassing til konsekvensar av klimaendringane. In O. Flæte (Ed.), *Norges offentlige utredninger,10.* Oslo: Statens forvaltningstjeneste. p.44-56.

NVE. (2011a) Plan for skredfarekartlegging - delrapport jordskred og flomskred. In T. H. Bargel (Ed.), *NVE Rapport 16.* Oslo: Norges vassdrags- og energidirektorat. 62pp.

NVE. (2011b) Plan for skredfarekartlegging - delrapport kvikkleireskred. In T. Wiig (Ed.), *NVE Rapport 17.* Oslo: Norges vassdrags- og energidirektorat. 102pp.

NVE. (2011c) Plan for skredfarekartlegging - delrapport snøskred og sørpeskred. In A. Taurisano (Ed.), *NVE Rapport 18.* Oslo: Norges vassdrags- og energidirektorat. 44pp.

NVE. (2011d) Plan for skredfarekartlegging - delrapport steinsprang, steinskred og fjellskred. In G. Devoli (Ed.), *NVE Rapport 15*. Oslo: Norges vassdrags- og energidirektorat. 120pp.

NVE. (2011e) Plan for skredfarekartlegging - status og prioriteringer innen oversiktskartlegging og detaljert skredfarekartlegging i NVEs regi. In E. K. Øydvind (Ed.), *NVE Rapport 14*. Oslo: Norges vassdrags- og energidirektorat. 92pp.

NVE. (2012a). *Aktsemdkart for stein- og snøskred (NGI)*. Retrieved 08.02, 2013, from http://www.nve.no/no/Flom-og-skred/Farekartlegging/Aktsemdkart-for-sno--og-steinskred-NGI/

NVE. 2012b. *Faresonekartlegging for skred på oppdrag fra NVE- Kravspesifikasjon.* Norges vassdrags- og energidirektorat, 14pp.

NVE. (2013a) Faresonekart skred Odda kommune. In A. Taurisano (Ed.), *NVE Rapport 4*. Oslo: Norges vassdrags- og energidirektorat. 84pp.

NVE. (2013b) Faresonekart skred Årdal kommune. In A. Taurisano (Ed.), *NVE Rapport 5*. Oslo: Norges vassdrags- og energidirektorat. 118pp.

NVE Atlas. (2013). *NVE Atlas - Hydrological database*. Retrieved 2013, last time 20.05, from Norwegian Water Resources and Energy Directorate http://.atlas.nve.no

NVE Skredatlas. (2013). *NVE Skredatlas - Landslide database*. Retrieved 2013,last time 20.05, from Norwegian Water Resources and Energy Directorate http://skredatlas.nve.no

Oppikofer, T., Bunkholt, H. S. S., Fischer, L., Saintot, A., Hermanns, R. L., Carrea, D., Longchamp, C., Derron, M.-H., Michoud, C. and Jaboyedoff, M. (2012). Investigation and monitoring of rock slope instabilities in Norway by terrestrial laser scanning. *Landslides and Engineered Slopes: Protecting Society through Improved Understanding*, p.1235-1241.

Oppikofer, T., Fischer, L., Hermanns, R. L., Devoli, G., Bunkholt, H., Taurisano, A. and Eikenæs, O. (2011, 16-19th May). *Rockfall hazard mapping in Norway - how to prioritize areas?* Interdisiplinary Rockfall Workshop 2011, Innsbruck - Igls. 2pp.

Perret, S., Dolf, F. and Kienholz, H. (2004). Rockfalls into forests: Analysis and simulation of rockfall trajectories—considerations with respect to mountainous forests in Switzerland. *Landslides, 1*, 2, p.123-130.

Ramberg, I. B., Bryhni, I. and Nøttvedt, A. (2007). *Landet blir til: Norges geologi*. Trondheim: Norsk geologisk forening. p.178-181, 550-553.

Reite, A. J. (1966) Lokalglaciation på Sunnmøre. *NGU Årbok 247*. Oslo: Universitetsforlaget. p.262-287.

RocScience. 2002. *RocFall - Risk analysis of falling rocks on steep slopes. User's Guide.* RocScience. Retrieved 05.02.2013 from www.rocscience.com 63pp.

RocScience. 2003. *Advanced tutorial - Determining input parameters for a RocFall Analysis.* RocScience. Retrieved 05.02.2013 from www.rocscience.com 8pp.

Salm, B. (1993). Flow, flow transition and runout distances of flowing avalanches. *Annals of Glaciology, 18,* p.221-226.

Sandersen, F. (2012) *Snow avalanches.* Lecture in Geo 4180 - Geohazard and Mitigation. 25.10.2012. Institute for Geosciences, University of Oslo.

Sandersen, F., Bakkehøi, S., Hestnes, E. and Lied, K. (1997) The influence of meteorological factors on the initiation of debris flows, rockfalls, rockslides and rockmass stability. *NGI Publication 201*. Oslo: Norwegian Geotechnical Institute. p.97-114.

Sauermoser, S. (2006). *Avalanche hazard mapping—30 years experience in Austria*. Proceedings of the 2006 International Snow Science Workshop, Telluride, Colorado, USA. p.314-321.

seNorge.no. (2013). *Climate database from NVE, met.no and Kartverket.* Retrieved 2013, last time 25.05, from www.senorge.no

Sletten, K. (2004) Skredfarekartlegging i Vestfjorddalen. *Rapport 2006.023.* Trondheim: Norges geologiske undersøkelse. 41pp.

SLF. 2005. *AVAL-1D: Calculation steps for dense flow avalanches.* Institut für Schnee- und Lawinenforschung (SLF), Davos, Switzerland. Retrieved 09.02.2013 from www.slf.ch 2pp.

SLF. 2011. *RAMMS - A modeling system for snow avalanches in research and practice. User Manual v1.4 Avalanche.* Institut für Schnee- und Lawinenforschung, Davos, Switzerland. Retrieved 09.02.2013 from www.slf.ch 111pp.

snl.no. (2013, 27.02.2013). *Omløpstid - skogbruk.* Retrieved 25.05, 2013, from http://snl.no/oml%C3%B8pstid./skogbruk

SSB. (2012). *Statistisk sentralbyrå: Folkemengde*. Retrieved 10.12, 2012, from http://www.ssb.no/emner/02/02/folkendrhist/tabeller/tab/1524.html

St. Meld. (2008). *Samfunnssikkerhet - samvirke og samordning*. St. Meld. 22 (2007-2008). Oslo: Justis- og politidepartementet. p.24-26.

St. Meld. (2012) *Melding til Stortinget: Hvordan leve med farene - om flom og skred.* St. Meld. 15 (2011-2012). Oslo: Olje- og Energidepartementet.

St.prp. (2009). *For budsjettåret 2009: Del III - Forebygging av skredulykker*. St. Prp. 1 (2008-2009). Oslo: Olje- og Energidepartementet. p.104-111.

Stevens, W. D. (1998). *RocFall: a tool for probabilistic analysis, design of remedial measures and prediction of rockfalls.* Master of applied science, University of Toronto. Retrieved from www.rocscience.com 38pp.

Stoffel, M., Wehrli, A., Kuhne, R., Dorren, L. K. A., Perret, S. and Kienholz, H. (2006). Assessing the protective effect of mountain forests against rockfall using a 3D simulation model. *Forest Ecology and Management, 225,* 1-3, p.113-122.

Stokes, A., Norris, J. E., Van Beek, L., Bogaard, T., Cammeraat, E., Mickovski, S. B., Jenner, A., Di Iorio, A. and Fourcaud, T. (2008). *How vegetation reinforces soil on slopes Slope Stability and Erosion Control: Ecotechnological Solutions*: Springer. p.65-118.

Stokke, J. A. (1983) Kvartærgeologisk kartlegging med oppfølgende sand og grusundersøkelser i Norddal kommune, Møre og Romsdal. *NGU Rapport 1560/30.* Trondheim: Norges geologiske undersøkelse. 17pp. + app.

Stranda kommune. (2012). *Geiranger - Herdalen landskapsvernområde*. Retrieved 10.12, 2012, from https://www.stranda.kommune.no/artikkel.aspx?MId1=2&AId=151&back=1

Tafjord, A. B. (1977). *Vær og klima*. In S. Evensberget (Ed.), *Bygd og by i Norge - Møre og Romsdal*. Oslo: Gyldendal Norsk Forlag. p.104-114.

Taurisano, A. (2013a, 24.04). [Personal communication - e-mail].

Taurisano, A. (2013b, 15.05). [Personal communication - verbal].

TEK10. 2012. *Veiledning om tekniske krav til byggverk. Ch: 7. Sikkerhet mot naturpåkjenninger*. Direktoratet for byggkvalitet. Retrieved 07.11.2012 from www.dibk.no,

USGS. (2012). *Landslide Types and Processes*. Retrieved 22.11, 2012, from http://pubs.usgs.gov/fs/2004/3072/pdf/fs2004-3072.pdf

Varnes, D. J. (1958) Landslide types and processes. *Special Report 29.* Washington: Highway Research Board. p.20-47.

Varnes, D. J. (1978) Slope movement types and processes. *Special Report 176.* Washington: Transportation and Road Research Board. p.11-33.

Åknes/Tafjord Beredskap IKS. (2012). *Åknes - nasjonalt senter for fjellskredovervåkning*. Retrieved 15.12, 2012, from www.aknes.no

Appendices

Appendix A: Slope map

Appendix B: Place names

Appendix C: Observations

Appendix D: Historical landslides and snow avalanches

Appendix E: Maximum precipitation events

Appendix F: Glossary

Appendix A: Slope map

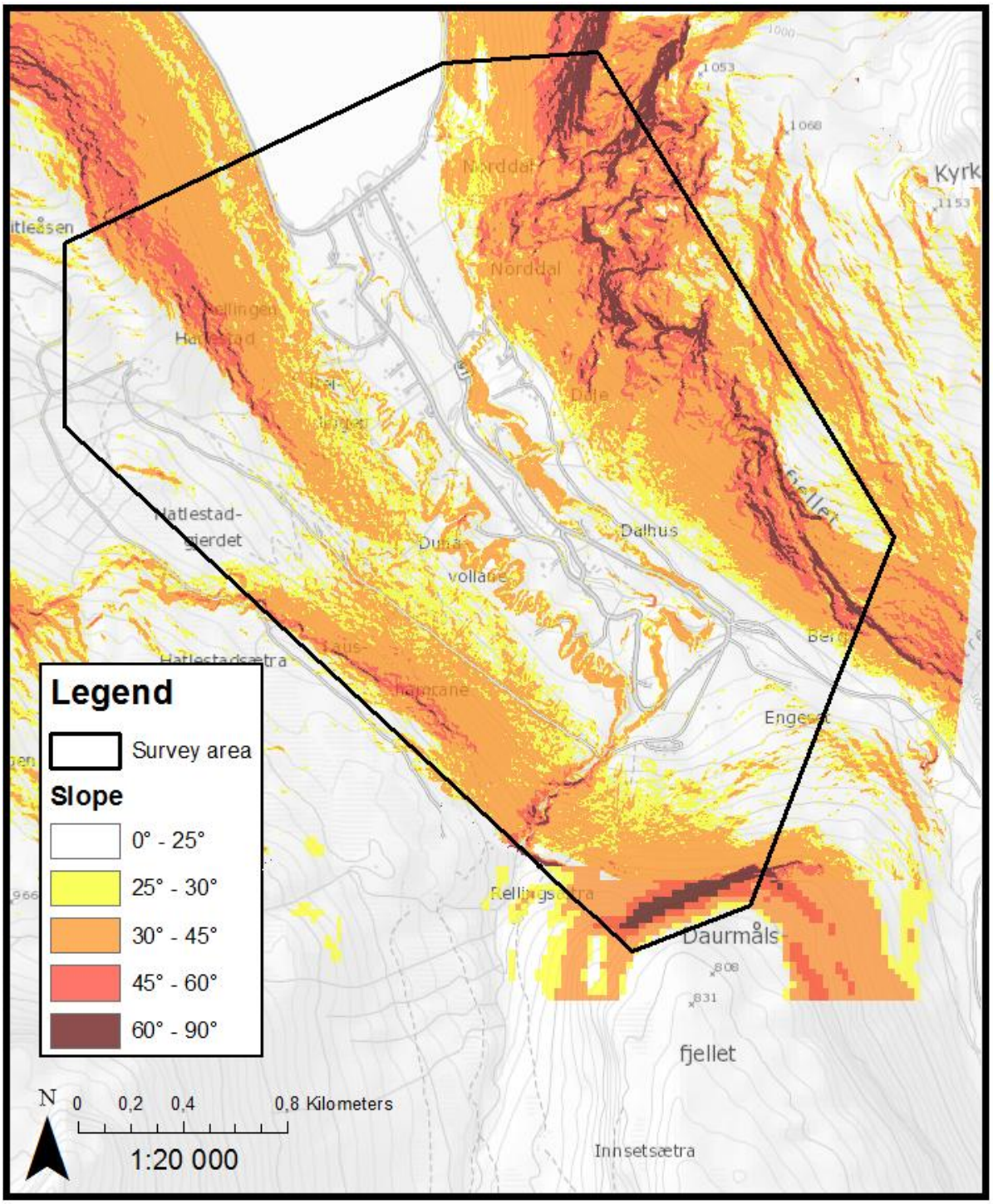

Appendix B: Place names

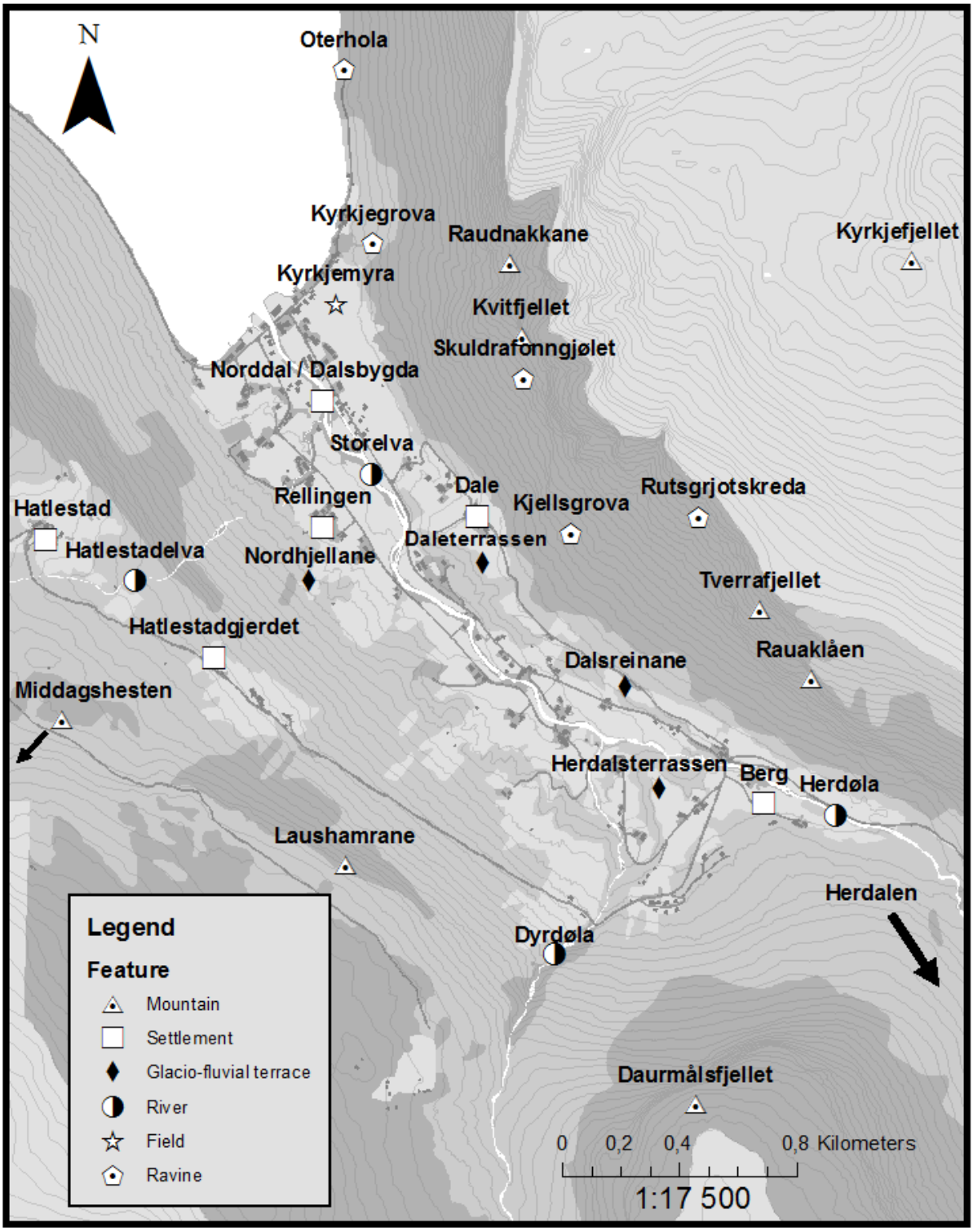

Appendix C: Observations

WP	Description
1	Beneath *Kyrkjegrova*. Masses are removed from the fan. House nearby.
2	Large pit showing stratificated deposits from several landslide events. Varying block size, from pebbles to boulders. Some clay/silt?
3	Fresh rock fall.
4	Fresh rock fall.
5	Fresh rock fall.
6	Deposited rocks decrease in size from the bottom (boulders) and upwards. “Sturzgradierung”.
7	A lot of available material in the ravine.
8	Very steep. Several loose blocks around and on the cliff. The ravine is certainly place for snow avalanches and debris flows.
9	Meadow in the upper part, visible scars after rock falls bouncing the ground. Every step taken in places where no vegetation is present causes material within 0.7 m in radius to start to slide downwards. Size < 20cm.
10	Drainage tracks.
11	Several overhanging blocks in the mountain side are visible from binocular investigations.
12	Completely vegetation free area. Small stones at the top and size increase to boulder size in the bottom. “*Sturzgradierung*”.
13	Well/spring. Dense vegetation, the ground is covered by mosses.
14	Well/spring.
15	Ravine / stream in dense vegetation. Several old and large trees present.
16	Dense vegetation cover, forest.
17	Talked to people. Rock fall should have deposited with in the church yard once.
18	Northern part of fan, several small channels have changed their paths.
19	Well /spring.
20	Several (2-3) ravines (1-2 m height) on the fan.
21	Water course / mass movement path. A lot of available material in the path. Mostly small rocks (pebbles, gravels), but also sand and blocks. Bad sorting.
22	Evident ravine, drainage track in the vegetation.

23	Talus. Roughness and vegetation information collected.
24	Talus. Roughness and vegetation information collected.
25	Talus. Roughness and vegetation information collected.
26	Talus. Mostly gneiss, rectangular shape, covered by lichens. Some grass and vegetation between the blocks.
27	Talus. Rock fall blocks, both gneisses and dunite.
28	Talus. Roughness and vegetation information collected.
29	Top of ravine, *Kyrkjegrova*. Transmission from loose material to bedrock. Small earth slide at the side of ravine.
30	Top of ravine. Water is present. Accumulation of material in natural dams.
31	Well / spring.
32	Well / spring. Lower part of large 1996 *Kvitfjellet* rock avalanche.
33	Remote investigations of *Kvitfjellet*. Several free hanging blocks. Distinct wedge; probably 30 m high. Lower part has fallen out.
34	*Kvitfjellet* 1996 rock avalanche deposits. Trees >50 cm crushed. Blocks > 3x2x1.5 m.
35	Smooth mountain side, broken trees from snow avalanche (?). Platy loose rocks, seems like sliding plane along a mafic (green) layer.
36	Large blocks covered by mosses in dense vegetation (>1,5x1x1 m). Many trees hold old scars/damages.
37	All blocks covered by mosses, no fresh deposits.
38	Fresh rock fall deposits on bedrock. From 1996 rock avalanche.
39	Smooth bedrock. Could act as snow avalanche release area, but no signs of erosion/sliding on mosses at surface. Also large block dammed small ones in 1996 path.
40	Broken trees from small snow avalanche.
41	Ridge beneath *Kvitfjellet*. It looks like another rock avalanche path south for fresh track, beneath the wedge.
42	Erosion tracks in soil consisting of ultramafic grains (green). Eroded 50 cm deep gully, 30 cm wide.
43	Overview: deposits from younger event and 1996 (red. most likely 2011). Also older deposits visible, meaning it has happened before.
44	Grazing area. Large blocks, partly covered by soil.
45	Well / spring.
46	Talus, blocks up to 2x1.3x0.8 m. Small section of bedrock above. Signs of fresh spalling in mountain face above.
47	Vegetation free polygon in scree. It looks very homogenous when it comes to gray scale and lichen covers. Some fresh rock fall deposits.

48	Talus - big fan? Generally covered by soil and grass, grazing area. Low roughness, but some large blocks (2x2x2 m). Remnants of old channels/lobes.
49	Large block (>4 m length) have "dammed up" tens of smaller ones (<0.5 m). Uncertain process type.
50	Old channel. 5-6 m deep. Old path of stream. Dense vegetation.
51	Small stream. 3-4 m high ridges / levees. Water flows underground from here.
52	Vegetation free area of blocks which appear homogenous regarding weathering/lichens. Rectangular blocks from 10x10x20 cm to 2x2x1 m.
53	Young birch forest, grass covered ground. Some creep.
54	Big open field with spread large, old birches. No fresh deposits and rocks totally covered by lichens.
55	Probably rock slide deposits. Large blocks >10x6x5 m. One like house. Rough terrain with large boulders.
56	Rock fall deposits gathered in field. Some probably removed and some which are likely not. Sizes from 90x170x250 cm to 150x300x680 cm.
57	Very dense alder forest, vegetated ground and soil present, but talus underneath with blocks up to > 1m in diameter.
58	Evident "*sturzgradierung"* from boulders below and small pebbles up towards the cliff.
59	Small pebbles (2x2x3 cm), planar surface under steep mountain. Seems like water have caused material to move on the surface.
60	2-3 fresh rock falls.
61	Spread birch forest; 25 cm in diameter, 5 m apart. Rocks covered by mosses.
62	Small ravine / melt water channel; < 50 cm. Also very abundant creep on some old birches, 30-40 cm in diameter, 10 m apart.
63	Old rock fall stopped against tree. Also several fresh ones, evident bumping marks in rocks uphill and remnants of crushed rocks.
64	Newly deposited levees of fine-grained material, levees < 50 cm. Probably slush avalanche.
65	Open vegetation free area, expect of some 30-60 cm wide birches. No sign of fresh rock falls.
66	Two fresh rock falls deposited 20 m apart.
67	Large boulder of house size.
68	Small ravine, melt water channel.
69	Two large boulders on each side of a forestry road. Small one: 7.6x1.6x3.2 m. One looks fresh, but probably washed out from glacio-fluvial deposits.
70	Boulder on concrete element. Rock fall?

71	Dense spruce forest, no vegetation on ground. Thick layer of needles cover the ground.
72	Rock fall boulder; 4.5x4.5x1.8 m.
73	Two rock fall boulder by road turn by the houses; 5x4x4 m.
74	Dense spruce forest. Soil covered by old boulders covered by needles. No living vegetation on the ground or fresh rock falls/marks on trees are evident.
75	Gravel pit. Layered deposits of clay/silt, sand and landslide deposits.
76	Top on gravel pit. Distinct forest covered ravine in the back side. Boulders here and there (approx. 1 m in diameter).
77	Well/spring in cavern.
78	Rock fall deposit in the field.
79	Rock fall boulder; 3.2x2.1x1.6 cm.

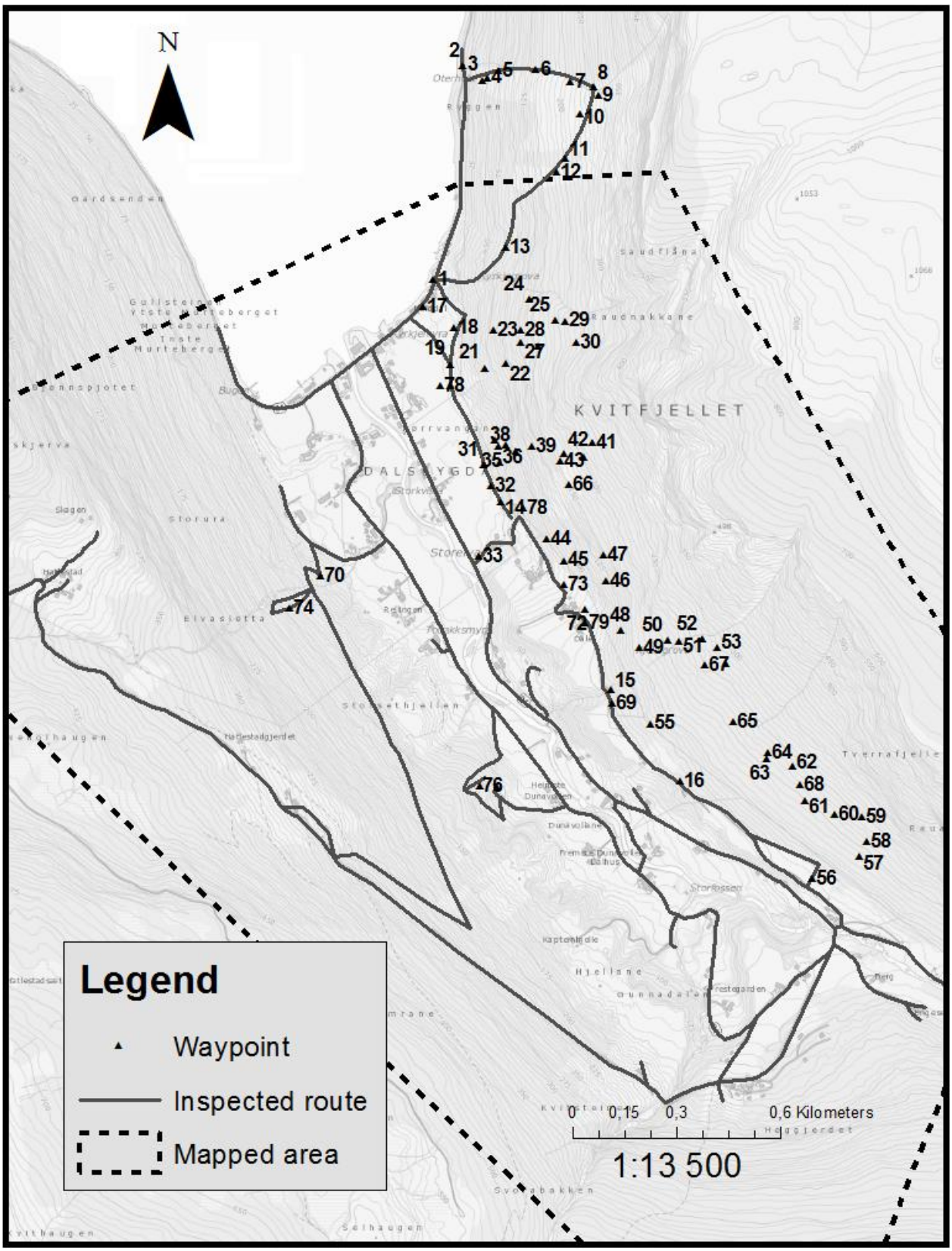
N
KVITFJELLET
DALSBYGDA
Legend
Waypoint
Inspected route
Mapped area
0
0,15
0,3
0,6 Kilometers
1:13 500

Appendix D: Historical landslides and snow avalanches

1	**Type: Snow avalanche**	**Date: 20.02.1850**
Location: *Dyrdøla*		
Description: "*Dalsbygda* in *Norddal*. One man was killed by a flash flood caused by ice damming as he was grinding grains in *Dyrdøla* river. This should have happened the same day as the *Storfonna* avalanche happened at *Rønneberg*, most likely during the mild weather which occurred in the district the 15th-20th February 1850."		
Source: NVE Skredatlas (2013)	Registered by: NGU, Astor Furseth	

2	**Type: Debris slide**	**Dato: 09.10.1975**
Location: Western valley side, *Norddal*.		
Description: "Two large earth slides happened in *Dalsbygda* 9th October 1975. This was expected as several small slides occurred the night before and the village experienced heavy rainfall. The large debris slides started by the small road high up in the valley side and went down into the valley, causing damages to agricultural land, a road and grazing land. The rivers did experience flooding during these days".		
Source: NVE Skredatlas (2013)	Registered by: NGU, Astor Furseth	

3	**Type: Rock avalanche**	**Date: 4th November 1996**
Location: *Kvitfjellet, Dale*.		
Description: "In November 1996, did a rock avalanche occur from *Kvitfjellet*. There is no settlement at this exact place, but it did deposit near some houses. The county geologist at the time, Einar Anda, did a review of the area after this event. Earlier similar events have occurred at the same location."		
Source: NVE Skredatlas (2013), Anda and Holten (1998)	Registered by: NGU, Astor Furseth	

4	Type: Debris slide	Date: 1743 and 1974
Location: *Relling* / *Dalhus*		
Description: *Dalhus, Nilsegarden*. During late autumn 1743 there were a lot of snow present in the mountains, but late in November did the weather turn mild with heavy rainfall. Landslides, snow avalanches and "remarkable large waterways occurred several places in the region. 17 farms and more than 20 smaller ones were damages, mostly in the inner parts of *Sunnmøre*. A rock- and debris slide came from *Dalhusberget* and hit the yard. At the time where the houses located at the *Relling* side, but they were removed to the north-eastern side of the river by the road to *Innset*. The time is unclear; also if there ware any fatalities. *Dalhusberget* is a known place for landslides, and the last debris slide happened in 1974."		
Source: NVE Skredatlas (2013)	Registered by: NGU, Astor Furseth	

5	Type: Snow avalanche	Date: 1690
Location: *Tverrafjellet, Norddal*.		
Description: "Snow avalanche (probably) around 1690. It came down *Tverrafjellet* at the head of the village. For a long time should a place called *Tuftene* exist in this area, with a farm at a time. Also the known bishop Johan Nordahl Brun was from a family of *Tverrafjellet*. It might be the same place as *Killestiestøl*, which is mentioned in old sources. A big snow avalanche took all the houses, by legend while they were in church, and they moved after this event." It is an approximate location.		
Source: NVE Skredatlas (2013)	Registered: NGU, Astor Furseth	

6	Type: Debris slide/-flow	Dato: approx. 1880
Location: *Furnesdalen, Herdalen*		
Description: a landslide came down *Furnesdalen* which today holds a relatively big glacial fed stream, into *Herdalen* where it dammed the river *Herdøla* which flows down to *Norddal*. When the dam collapsed, a wave of water flooded down stream and destroyed all the bridges in *Norddal*. The outermost bridge, *Rellingbrua*, was transported out into the fjord. The deposits of the landslide are still clearly visible, and today it dams up a small lake called *Måsevatnet*.		
Source: (Dale, 2012)		

7	Type: Rock fall	Date: Summer 2012
Location: "*Kvia*" by *Måsevatnet, Herdalen*		
Description: Rock outcrop has fallen down and several big boulders are deposited down by the water / river.		
Source: (Dale, 2012)		

8	**Type: Rock fall**	Date: 2008 or 09
Location: "*Hesøybakken*", close to "*Smørelva*" waterfall.		
Description: Several rock falls which closed the road. Latest in 2008 or 2009 when boulders as huge as cars were deposited in a 50 meter wide field on the road. Contact with the county geologist resulted in a conclusion saying that the whole mountain side is a possible source for rock falls.		
Source: (Dale, 2012)		

9	**Type: clay slide**	**Date: approx. 1990**
Location: *Norddal*		
Description: Clay slide by house. County geologist gave advice of how to reword the place of movement. Generally high content of clay in the terraces on both sides of the valley. Also contact with clay which easily slide out during building of small road up to a house in the same area in 1982. Wish to built a new building in the same slope where not recommended by engineers. Also several visible scars from small old clay slides in the area, as by the mentioned exit from the main road up to the houses.		
Source: (Dale, 2012)		

10	**Type: Snow avalanche**	**Date: approx. 1980**
Location: *Berg, Norddal*		
Description: Big snow avalanche after heavy snow fall in the spring. It came down the north eastern mountain side, destroying several cabins in the area and filled some houses on the opposite side of the river with snow.		
Source: (Dale, 2012), confirmed by several others during interviews		

11	Type: Rock fall / ice fall	Date:
Location: *Dale*		
Description: Patches of ice and rocks have been deposited on the upper road and the cultivated land. The fact that the area between point 10 and 11 during history have had very little settlement, indicates large probability of landslides and snow avalanches.		
Source: (Dale, 2012)		

12	Type: Rock avalanche	Date: Very old
Location: Eastern valley side south for *Kvitfjellet*.		
Description: Relict rock avalanche marked on a map. Deposits are clearly visible.		
Source: (Anda and Flemsætherhaug, 1996)	Registered:	Source 2:
13	**Type: Debris slide**	**Date: around1980**
Location: Western valley side by *Dyrdøla*		
Description: Observed debris slide scar on the northern side above the river *Dyrdøla*. The deposits blocked the river according to the source, causing a threat for flooding downwards. It did not cause any major event, but some basements may be filled with water.		
Source: Own observation, interview		

14	Type: debris slide, accident	Dato: 29th May 1934
Location: *Dunavollen, Dalhus*		
Description: "One boy, aged 16, died in a sand- and debris slide in a gravel pit at *Dunavollen*, *Dalhus*. He was working in the pit, taking out sand for the work with a new road. People discovered the slide, arrived quickly and dug him out while he was stilling showing signs of life, but he died shortly after.		
Source: NVE Skredatlas (2013)	Registered by: Astor Furseth	

15	Type: Snow avalanche	Date: 1993 or 1994
Location: *Kyrkjegrova*		
Description: The ravine by the church showed clear evidence of previous snow avalanche deposits during the first fieldtrip in May/June 2012. Later interview also cleared out that this was a fact, and that mass had been moved from the fan to secure the surrounding houses from future snow avalanche events. A report from the county council regarding the landslide hazard in the area confirms the observations of high landslide activity in the ravine, both from snow avalanches, slush avalanches and debris flows.		
Source: Observation, Anda and Flataukan (2002)		

16	Type: Rock fall	Dato: 18th February 1998
Location: *Relling, Norddal.*		
Description: Three large blocks (approx. 3 m in diameter) fell down the western mountain side above the southern settlement at Relling, and stopped approx. 100 meter above the settlement, at 60-70m.a.s.l. They started in a steep zone at approx. 225m.a.s.l. as loose blocks which started to slide at the ground surface. A similar rock fall occurred 60-70 m more south in during the 1970s, but stopped at the walking path higher up in the mountain side.		
Source: Anda and Holten (1998)		

17	Type: Debris flow	Date: 8th December 1873
Location: *Relling, Norddal.*		
Description:"Several large debris slides occured in *Geiranger* and *Norddal* the 8th December 1873. Several farms suffered from damage. At Relling, east of farm 53/25, a large debris flow caused damage on agricultural land and smallholdning. The landslide followed a small stream towards Storelva river."		
Source: NVE Skredatlas (2013)		

18	Type: Debris slide	Date: early 1990's
Location: *Hjellane, Norddal.*		
Description: Several debris slides and debris flows are determined from investigation related to a scheduled cabin site. A known debris slide from early 1990's are thought to start beneath a rock fall site called *Laushamrane* at approx. 400 m.a.s.l. and stopped around contour line 140m.a.s.l. Several other debris flow fans are determined in the area.		
Source: (Anda and Flataukan, 1998)		

19	Type: small slide, erosion	Date: 25th March 2010
Location: *Norddalsstranda*		
Description: damage on road reported		
Source: NVE Skredatlas (2013)	Registered: SVV	

Appendix E: Maximum precipitation events

Highest measured precipitation values in Norddal. Mean temperatures are from Tafjord.
Type (registered): RR: Rain (red), SS: Snow (blue), RS: Rain and Snow (green).

#	Date	Prec. [mm.w.eq.]	Type	Temp. [°C]
1	26.10.1974	71.1	RS	3.6
2	18.09.1978	70.8	RR	3.5
3	15.11.2005	69.7	RR	1.8
4	22.03.2011	69.5	RR	4.3
5	07.10.1975	68.4	RR	7.9
6	31.08.1964	67.8	RR	8.5
7	19.02.1952	67.1	RS	2.1
8	09.10.1992	65.9	RR	6
9	27.12.1975	65.5	RS	3.7
10	01.01.2002	62.2	RS	1.7
11	24.11.1994	54.3	RR	3.3
12	11.01.2001	52.5	RS	1.7
13	09.01.1957	52.4	RR	3.3
14	10.03.1945	52	RR	2
15	30.09.1969	52	RR	6.4
16	09.09.1997	51	RR	7.4
17	16.02.1999	50.7	RS	-2.5
18	31.03.1997	50.2	RR	5.4
19	17.03.2008	50.1	SS	0.1
20	30.09.1964	49.9	RR	5.6
21	13.11.2001	49.8	RS	0.8
22	09.02.1944	49.5	RS	-1.8
23	05.09.2006	49.5	RR	13.2
24	15.11.2004	49.4	RS	2.4
25	20.01.1932	49	-	4.8
26	09.09.1973	48.3	RR	8.4
27	08.09.1953	48	RR	11.6
28	08.09.1966	47.2	RR	9.7
29	27.08.1953	47.1	RR	11.8
30	14.11.1992	46.6	RS	0.8
31	15.09.1977	46.2	RR	6
32	08.10.2012	46	RR	5.9
33	06.12.1951	45.9	RR	0
34	05.11.1981	45.9	RR	3.3
35	14.12.1991	45.9	RR	5.1

#	Date	Prec. [mm.w.eq.]	Type	Temp. [°C]
36	01.12.1953	45.6	RR	3
37	22.11.2008	45.2	SS	-3.8
38	01.12.1936	45	RS	2
39	10.09.1937	45	RR	-
40	07.01.1944	45	RS	-1.3
41	22.11.1978	45	RR	3.4
42	22.07.2010	44.8	RR	11.4
43	31.01.1938	44.5	RS	1.8
44	24.09.1983	44.1	RR	7.8
45	08.11.1941	44	RR	1.8
46	17.11.1956	43.8	RR	5.5
47	28.09.1994	43.8	RR	4.3
48	27.11.2008	43.4	RR	4.2
49	14.10.1954	43.2	RR	4.1
50	09.12.1955	43	SS	-2.3
51	03.03.1949	42.7	SS	-2.2
52	06.12.1974	42.1	RR	3.2
53	12.11.2004	42.1	RR	3.7
54	18.10.1947	42	RS	1.2
55	20.10.1983	42	RR	1.9
56	25.03.1948	41.8	RR	3.1
57	10.09.1997	41.7	RR	9.4
58	03.11.2007	41.7	RR	7
59	02.04.1943	41.5	RS	2.1
60	19.02.1968	41.5	SS	-3.2
61	26.09.2003	41.5	RR	10.7
62	04.12.1986	41.4	RR	4
63	08.10.2011	41.3	RR	5.7
64	28.09.1963	41.2	RR	6
65	02.10.1971	41.1	RR	8.5
66	21.01.1983	41.1	RS	2.8
67	28.09.2008	41.1	RR	7.2
68	26.02.1976	40.6	RS	4.6
69	27.06.1976	40.5	RR	12.8
70	09.03.1983	40.5	RS	1.8

#	Date	Prec. [mm.w.eq.]	Type	Temp. [°C]
71	19.09.1982	40,4	RR	9,8
72	02.12.1999	40,3	SS	0,8
73	21.12.1936	40	RR	6,8
74	20.03.1973	39,8	SS	1,7
75	15.09.2007	39,7	RR	6,2
76	26.03.1990	39,6	RR	4,2
77	25.07.2011	39,3	RR	15,3
78	04.02.1993	39,1	RR	3
79	13.10.1934	39	RR	6,2
80	21.11.1936	39	RR	6,3
81	14.06.2000	39	RR	9
82	22.10.1931	38,5	RS	1,7
83	20.09.1943	38,5	RR	7,9
84	27.10.1955	38,5	RS	1,2
85	16.06.2004	38,5	RR	7,5
86	16.08.2003	38,3	RR	15,3
87	25.02.2004	38,3	RS	0,8
88	01.03.1945	38	RS	0,5
89	20.10.1970	38	RR	7,2
90	28.03.1955	37,9	SS	-1,9
91	05.11.1991	37,8	RR	1,3
92	13.11.1937	37,5	SS	-
93	06.11.1978	37,5	RR	7,2
94	20.10.1972	37,4	RS	1,3
95	03.11.1984	37,4	RR	4,7
96	18.11.1967	37,2	RR	6
97	15.08.2003	37,1	RR	14,4
98	19.05.1931	37	-	6,6
99	16.11.1942	37	RS	4,6
100	25.11.1957	37	RR	5,2
101	17.04.1991	36,8	RS	0
102	02.03.1997	36,6	RS	4,1
103	01.09.1936	36,5	RR	6,5
104	28.08.2007	36,3	RR	7,7
105	04.02.1949	36,2	RR	3,9
106	17.10.1936	36	RR	5,7
107	16.06.1949	36	RR	7,6
108	25.02.1963	36	RS	2,3
109	20.10.1980	36	RS	2,5

#	Date	Prec. [mm.w.eq.]	Type	Temp. [°C]
110	06.12.1981	36	SS	-4
111	14.09.1997	35.9	RR	7.4
112	27.10.1995	35.7	RR	7.3
113	04.12.1954	35.6	RR	6
114	05.10.1967	35.6	RR	8.3
115	29.09.2009	35.6	RR	4.6
116	11.09.1949	35.5	RR	12.3
117	16.07.1953	35.4	RR	14.1
118	13.08.1962	35.4	RR	10.7
119	30.01.1989	35.4	RS	2.3
120	24.09.2004	35.4	RR	10.6
121	22.10.1956	35.3	RR	7
122	03.09.1960	35.3	RR	9.1
123	11.02.1942	35.2	SS	-2.7
124	08.12.1989	35.2	RS	2.5
125	05.11.1974	35.1	SS	0.8
126	01.04.1997	35.1	RR	2.7
127	11.12.1941	35	RS	3.9
128	22.12.1941	35	RS	2.6
129	19.10.1991	35	RS	2
130	11.01.1992	35	RR	3.7
131	16.01.1981	34.8	SS	-1.5
132	29.08.1952	34.7	RR	9.5
133	13.10.1956	34.7	RR	4.3
134	24.10.1948	34.6	RS	0
135	29.12.1980	34.5	RR	5.6
136	02.03.1976	34.4	RS	0
137	18.08.1949	34.3	RR	7.4
138	23.10.1948	34.2	RS	3.2
139	04.01.2000	34.2	RR	2.3
140	19.10.1956	34.1	RR	5.1
141	25.03.1990	34.1	RS	2
142	03.10.1931	34	RR	6
143	30.09.1947	34	RS	2.8
144	05.10.1953	34	RR	7.8
145	24.03.1961	34	RS	0.4
146	17.02.2008	34	RR	2.5
147	20.10.2011	33.8	RR	2.4
148	28.07.1976	33.6	RR	10.5

#	Date	Prec. [mm.w.eq.]	Type	Temp. [°C]
149	04.10.1947	33,5	RR	6,4
150	31.01.1968	33,5	RS	0,7
151	03.01.2005	33,5	SS	1,4
152	10.01.2007	33,5	RR	1,7
153	11.06.2008	33,5	RR	6,9
154	29.04.1955	33,4	RS	8,2
155	21.01.1957	33,4	RS	0,7
156	18.12.1966	33,4	RS	3,4
157	22.12.1971	33,4	RR	1,3
158	04.10.1994	33,4	RS	1,2
159	26.01.2008	33,3	RS	0,6
160	01.12.1951	33,2	RS	0,1
161	20.02.1959	33,2	RR	-0,9
162	19.12.1963	33,1	SS	-5,9
163	13.11.2006	33,1	RS	7
164	22.02.2008	33,1	RR	0,9
165	04.03.1938	33	RR	5,9
166	18.04.1943	33	RS	3,5
167	10.10.1945	33	RR	3,3
168	07.10.1957	33	RR	9,5
169	20.10.1995	33	RR	4
170	29.10.2007	32,7	RR	8
171	06.10.2008	32,6	RR	6,9
172	02.12.1936	32,5	RS	-3,6
173	25.09.1960	32,5	RR	6,7
174	05.12.1981	32,5	RS	0
175	27.10.1983	32,5	RR	5,4
176	23.12.1988	32,4	RS	1,8
177	06.12.1955	32,3	RR	1,2
178	20.07.1988	32,3	RR	14,2
179	21.02.1932	32,2	RR	3
180	15.12.1967	32,2	RR	1,2
181	15.12.1992	32,2	RR	2,3
182	03.11.1996	32,1	RR	1,3
183	25.06.1945	32	RR	11,6
184	03.01.1954	32	RS	0,9
185	01.04.1990	32	RR	3
186	30.10.1969	31,9	RS	3,2
187	22.05.2004	31,9	RS	4,5

#	Date	Prec. [mm.w.eq.]	Type	Temp. [°C]
188	11.09.1991	31.8	RR	6.6
189	18.09.1948	31.7	RR	9.8
190	28.09.2004	31.6	RR	9.2
191	03.02.1983	31.5	SS	-1.2
192	03.10.1986	31.5	RR	2.8
193	11.11.2007	31.5	RS	0.4
194	22.02.1943	31.4	RR	3.5
195	17.12.2005	31.4	SS	0.3
196	10.11.1991	31.3	RS	0.2
197	18.04.1967	31.2	RS	-1.5
198	10.01.1968	31.2	SS	-3.4
199	18.09.1952	31.1	RR	5.4
200	22.10.1963	31.1	RR	5.8
201	14.09.1973	31.1	RR	9.7
202	07.08.1933	31	RR	12.6
203	14.09.1938	31	RR	4.7
204	30.09.1939	31	RR	4.6
205	29.03.1976	30.9	RS	4.5
206	14.11.2005	30.8	RR	6.4
207	11.04.2004	30.7	RS	2.6
208	11.04.1997	30.6	RS	1.9
209	06.02.1934	30.5	RR	1.4
210	25.08.1959	30.5	RR	13.9
211	11.11.1985	30.5	RS	2
212	13.10.1954	30.4	RR	5.3
213	19.01.1993	30.4	RS	1.9
214	29.09.2002	30.4	RR	10.4
215	21.12.1954	30.3	SS	-1.3
216	18.02.1968	30.3	SS	-3.8
217	13.11.2004	30.3	RS	2.1
218	03.12.1952	30.2	RS	1.1
219	17.03.2000	30.1	RS	2.2
220	30.12.2007	30.1	RS	1.2

Appendix F: Glossary

ENGLISH	NORWEGIAN
Bedding	Lagdeling
Bedrock	Berggrunn, fast fjell
Cliffs	Skrenter
Colluvial fan	Skredvifte (Vifteformet av usortert jord – og steinmateriale ved foten av klipper eller skråninger.)
Colluvium	Løsmateriale (Usortert jord- og steinmateriale som samler seg ved foten av skrenter eller skråninger. Massebevegelsen er forårsaket av gravitasjon eller regnvann (sheet erosion))
Conditioning factor, conditioning causes	Utløsningsårsaker, Avgjørende eller bestemmende faktor
Cosmogenic dating methods	Kosmogene dateringsmetoder
Counterscarps	Motskrenter (skrent med fall oppover fjellsiden)
Creep	Kryp
Damage	Skade
Danger, Hazard	Fare
Debris	Løsmateriale
Debris flow	Kanalisert jordskred
Debris flow, Debris flood	Flomskred
Debris slide, Debris avalanche, shallow landslide	Ikke-kanalisert jordskred, jordskred
Deglaciation	Avisning (etter en istid)
Degree of hazard	Faregrad, faresonenivå
Deposits	Avsetning
Depressions	Senkinger, innsynkninger
Detailed surveys	Detaljerte undersøkelser
Digital elevation modell (DEM)	Digital høydemodell
Disintegrate	Oppsplitting (splitte eller bryte opp i mindre fragmenter)
Events	Hendelser
Falling	Fallende
Fracture	Sprekk
Fractured bedrock	Oppsprukket berg
Frequency	Frekvens
Frontal lobes	Front lober, fronttunger
Guidelines	Retningslinjer
Guides	Veileder
Hazard map	Farekart, Faresonekart
Hazard mapping	Farekartlegging
Hazard zone	Faresone
Intensity - frequency	Intensitet - frekvens
Inventory maps	Hendelseskart
Joint	Sprekker, riss

Jointed bedrock, Fractured bedrock	Oppsprukket berggrunn
Land planning, Land use planning	Arealplanlegging
Land use map	Arealbrukskart
Landslide dam	Oppdemming, dam forårsaket av skred
Landslide database	Skreddatabase
Landslide deposit	Skredavsetninger
Landslide events	Skredhendelser
Landslide frequency	Skredfrekvens
Landslide hazard	Skredfare
Landslide hazard identification, Landslide hazard characterization	Skredfareidentifisering
Landslide identification	Skredidentifisering
Landslide inventory map	Skredhendelseskart
Landslide mapping	Skredkartlegging
Landslide path	Skredbane
Landslide prevention	Skredforebygging
Landslide processes	Skredprosessene
Landslide prone areas	Skredfarlige områder
Landslide starting area, detachment zone	Utløsningsområde,
Landslide types	Skredtyper
Landslide, Landslides	Skred
Landslides in loose soils	Løsmasseskred
Landslides in rock slopes	Skred i fjellskråninger, skred i fjellsider
Landslides in rocks	Skred i fast fjell
Lateral levée	Sidelevée
Level of mapping	Kartleggingsnivå
Mapping methodology	Kartleggingsmetodikk
Mechanism of failure	Bruddmekanisme
Mitigation	Sikring
Mitigation measures	Sikringstiltak
Monitoring	Overvåking
Natural hazards	Naturfarer
Natural threats	Naturtrusler
Outburst floods	Plutselig flom
Overhanging cliffs	Overhengende klipper, overhengende skrenter
Preparedness, Emergency	Beredskap
Probability	Sannsynlighet
Quick clays slides	Kvikkleireskred
Reach distance, runout distance, runout	Rekkevidde
Remote sensing survey	Undersøkelse med fjernsensorer
Risk and vulnerability analysis	Risiko- og sårbarhetsanalyse (ROS)
Risk map	Risikokart
Risk mapping	Risikokartlegging

Rock avalanche	Steinskred (mange blokker uavhengig av hverandre)
Rock cliff	Fjell skrent
Rock debris	Løsmasser av stein
Rock face	Fjellside (vertikal)
Rock fall	Steinsprang (få blokker, små volum)
Rock fragment	Bergartsfragment
Rock outcrop	Blotning, Blottlagt fjell
Rock slide	Fjellskred , ustabile fjellparti
Rock slope	Fjellskråning, fjellside (avhengig av størrelse – skjønnsvurdering)
Rock slope deformation	Fjellskråning- , fjellsidedeformasjon
Rock slope failures	Fjellskråning- , fjellsidekollaps
Runoff	Avrenning
Runout	Utløp
Runout area, runout zone	Utløpsområde, utløpsone
Runout distance	Utløpsrekkevidde, utløpsdistanse, utløpsavstand
Runup	Oppskyllingshøyde
Scar	Arr
Scarp area	Skrent, -klippeområde
Scree	Ur (Løsmasser: jord, grus)
Shear surface	Bruddflate
Sliding	Gliding
Slope	Skråning, side (fjell- eller dalside)
Slope deformation	Skrånings- , fjellsidedeformasjon
Snow avalanche	Snøskred
Source area	Kildeområder
Source area, Detachment, detachment zone	Kildeområdet, løsneområde
Susceptibility	Aktsomhet
Susceptibility map	Aktsomhetskart
Talus, talus slopes	Ur
Temporal distribution	Tidsfordeling
Temporal frequency	Tidsfrekvens
Terrestrial laser scanning	Terrestrisk laserovervåkning
Toppling	Velte, utvelting
Transverse ridges	Tverrgående rygger
Triggering factors	Utløsende årsaker, utløsende faktorer
Tsunamis	Flodbølge
Unstable rock slopes	Ustabile fjellparti, ustabile fjellskråninger
Vertical displacement	Vertikal forflytning
Warning	Varsling
Weathering	Forvitringsprosess